UNIVERSIDAD DE NAVARRA

Facultad de Medicina

Prognostic capacity of peripheral blood-derived biomarkers in NSCLC patients treated with PD-1/PD-L1 blockade immunotherapy

Gonzalo Fernández Hinojal
Pamplona
Julio 2021

UNIVERSIDAD DE NAVARRA

Facultad de Medicina

Prognostic capacity of peripheral blood-derived biomarkers in NSCLC patients treated with PD-1/PD-L1 blockade immunotherapy

Memoria presentada en la Facultad de Medicina de la Universidad de Navarra por Gonzalo Fernández Hinojal para obtener el grado de Doctor en Medicina

Gonzalo Fernández Hinojal

UNIVERSIDAD DE NAVARRA

Facultad de Medicina

Los doctores Don RUBÉN PÍO OSÉS, del Cima-Universidad de Navarra y Doña GRAZYNA KOCHAN, del Centro de Investigación Navarrabiomed (Fundación Miguel Servet)

CERTIFICAN:

Que el trabajo de investigación “Evaluación de la capacidad pronóstica de biomarcadores en sangre periférica en pacientes con cáncer de pulmón tratados con inmunoterapias de bloqueo de PD-1/PD-L1” del que es autor Gonzalo Fernández Hinojal, ha sido realizado bajo su dirección y se encuentra en condiciones de ser presentado para su lectura y defensa ante el tribunal correspondiente, para que su autor obtenga el grado de Doctor.

Y para que conste a todos los efectos, firman este documento en Pamplona a 1 de Julio de 2021

Fdo Dr RUBÉN PÍO OSÉS

Fdo Dra GRAZYNA KOCHAN

A Berta Hinojal,
sean estas páginas memoria y homenaje.

Agradecimientos

La realización de esta tesis doctoral ha sido posible gracias a la financiación de la ***Fundación AECC*** *(Asociación Española contra el Cáncer) a través del proyecto PROYE16001ESCO – "Efectos de la senescencia inmunológica sobre la eficacia de las inmunoterapias anti-PD-L1/anti-PD-1" (2017).*

En primer lugar, quiero dar las gracias a mis directores de tesis Grazyna Kochan y Rubén Pío por su generosidad, su paciencia y compromiso permanente y desinteresado. Desde el principio depositaron su confianza en mí y me animaron a vencer las dificultades. No tengo ninguna duda de que sin su ayuda y su optimismo no habría podido conseguirlo. Gracias.

Quisiera también agradecer a los investigadores del grupo de OncoInmunología de Navarrabiomed. En particular, a David Escors por todo lo que me ha enseñado acerca de la inmunología del cáncer, sus consejos y su buen humor. La ayuda de Ana Bocanegra con los experimentos y con el procesamiento de muestras ha sido para mí una parte fundamental de mi experiencia en esta investigación. Su disponibilidad y su optimismo han hecho mucho más fácil este camino.

El doctor Hugo Arasanz allanó mi camino para incorporarme al laboratorio y su ejemplo me ha abierto puertas a través de las que he podido ir entrando en el mundo de la investigación. Miren Zuazo también me ayudó a dar mis primeros pasos y compartimos desde el principio la inquietud por trasladar al laboratorio las preguntas que nos hacíamos desde la práctica clínica. Ester Blanco me ha enseñado mucho acerca de la biología de las células mieloides, pero también me ha animado a seguir adelante en las dificultades.

María Gato, María Ibáñez, María Jesús García-Granda, y Carlos Hernández, así como Luisa Chocarro, Leticia Fernández, Miriam Echaide, Maider Garnica y Pablo Ramos han trabajado en el laboratorio y quiero rendir un sincero agradecimiento a todos ellos, por todo lo que me han enseñado y el buen ambiente que han formado siempre.

El Servicio de Oncología Médica del Hospital de Navarra, dirigido por la doctora Ruth Vera, me ha permitido formarme como oncólogo y me ha brindado apoyo y

confianza durante esta etapa. Maite Martínez, Berta Hernández, Idoia Morilla y Lucía Teijeira, de la Unidad de Tumores Torácicos, me han transmitido su conocimiento y la pasión por cuidar y tratar a los pacientes con cáncer de pulmón. También agradecer al equipo de enfermería, en particular a Lourdes, por su ayuda con las extracciones y su disponibilidad para colaborar.

No puedo dejar de mencionar el apoyo de mi familia, en primer lugar de Carmen, de Javier y de Miguel, de mi padre y de mis hermanos, que siempre me han animado a continuar. Fue D. Antonio Viñayo quien me dio el acertado consejo "*nulla dies sine línea"* que tanto he recordado durante la escritura de esta tesis. Quiero también hacer mención a Miguel García Valdecasas por su amistad durante estos años. Y por supuesto, a la Facultad de Medicina de la Universidad de Navarra donde me formé como médico.

Finalmente, los pacientes y sus familias han dejado una huella imborrable en mi experiencia como oncólogo. Cada uno de los casos que se han incluido en este estudio encierra historias personales, y gracias a su generosidad ha sido posible la realización de este trabajo. Para mí ha sido un honor poder participar de su cuidado y quiero rendirles un sincero homenaje.

Index

Abbreviations

Alb	Albumin
ALK	Anaplastic Lymphoma Kinase
APC	Antigen Presenting Cell
ANOVA	Analysis of Variance
BL	Baseline
BTLA	B- and T-lymphocyte attenuator
CCL2	Chemokine (C-C motif) ligand 2
CD	Cluster of Differentiation
COPD	Chronic Obstructive Pulmonary Disease
CR	Complete Response
CT	Computed Tomography
CTLA-4	Cytotoxic T Lymphocyte – associated Protein 4
CX3CL1	Chemokine (C-X3-C motif) Ligand 1, Fractalkine
DC	Dendritic Cell
DCR	Disease Control Rate
DOR	Duration of Response
ECOG	Eastern Cooperative Oncology Group
EGFR	Epidermal Growth Factor Receptor
EMA	European Medicines Agency
EMR	Electronic Medical Record
FDA	Food and Drug Administration
G-MDSC	Granulocytic Myeloid-Derived Suppressor Cell
G-CSF	Granulocyte colony-stimulating factor
GM-CSF	Granulocyte-macrophage colony-stimulating factor
GRIm	Gustave Roussy Immune Score
HLA	Human Leucocyte Antigen
HP	Hyperprogression
ICB	Immune-checkpoint Blockade
IDO	Indoleamine 2,3-dioxygenase
IFN	Interferon
IL	Interleukin
IRAE	Immune-related Adverse Event
iRECIST	Immune Response Evaluation Criteria In Solid Tumors
JRC	Joint Research Centre
LAG-3	Lymphocyte-activation Gene 3
LCNEC	Large Cell Neuroendocrine Carcinoma
LDH	Lactate Dehydrogenase
LIPI	Lung Immune Prognostic Index
M-MDSC	Monocytic Myeloid-Derived Suppressor Cell
MCP1	Monocyte Chemoattractant Protein 1, see CCL2

MLR	Monocyte-to-Lymphocyte Ratio
MSI	Microsatellite Instability
n	Number of Patients
NGS	Next Generation Sequencing
NLR	Neutrophil-Lymphocyte Ratio
NonTL	Non-Target Lesion
ns	Not Significant
NSCLC	Non-Small Cell Lung Cancer
OS	Overall Survival
PBMC	Peripheral Blood Mononuclear Cell
PD	Progressive Disease
PD-1	Programmed Death 1
PD-L1	Programmed Death-1 Ligand 1
PFS	Progression-Free Survival
PLR	Platelet-Lymphocyte Ratio
PR	Partial Response
PS	Performance Status
RECIST	Response Evaluation Criteria In Solid Tumors
RT	Radiotherapy
SCC	Squamous Cell Carcinoma
SD	Stable Disease
TL	Target Lesion
TMAI	Total Auscle Area Index
Treg	Regulatory T cell
TTF-1	Thyroid Transcription Factor-1
ULN	Upper Limit of Normality
VEGF	Vascular Endothelial Growth Factor

1. Introduction

Cancer comprises a large group of diseases marked by an abnormal cell proliferation as the result of malignant transformation of somatic cells. This malignant conversion is manifested by the loss of control over cell death signals, increased proliferative signaling, deranged cell metabolism, replicative immortality, and genomic instability. As a consequence of this unregulated proliferation, malignant cells can acquire further metastatic and invasive capacities that allow them to spread to other organs and evade immune-system surveillance (Hanahan and Weinberg, 2011). This latter characteristic eventually leads to the death of the patient. The World Health Organization identified cancer as the second cause of death with an estimated number of 9.6 million deaths in 2018. Such a high cancer rate results in an increasing economic impact. Only in 2018 in Europe the cost related to cancer treatment and patient care was estimated as 119 billion € (Hofmarcher et al., 2020).

After breast tumors, lung cancer is the second most incident cancer with 2.20 million cases in 2020, but it was the most common cause of cancer death (1.79 million deaths in 2018) (Sung et al., 2021) as shown in **Figure 1**. A recently published report (July 2020) by the Joint Research Centre (JRC) of the European Commission with the European Network of Cancer Registries, together with the International Agency of Research of Cancer points to lung cancer as a large burden in morbidity and mortality in Europe. In fact, lung cancer was the most common cause of cancer-related death (20.4%) in males, and the second after breast cancer in females (Source: ECIS - European Cancer Information System, from https://ecis.jrc.ec.europa.eu, accessed on 20/01/2021).

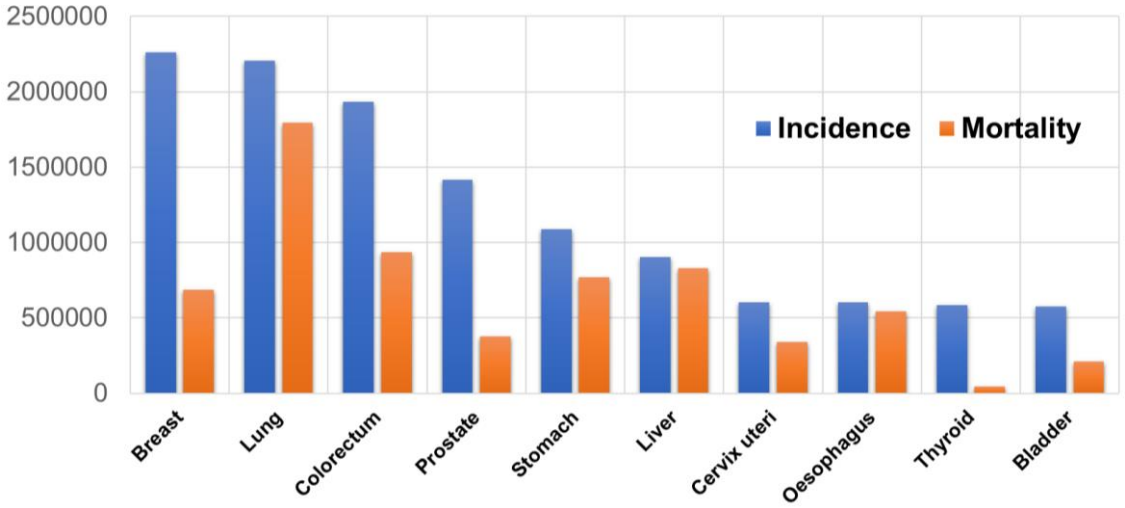

Figure 1 The ten most frequently diagnosed cancers worldwide. Lung cancer represents a significant portion in terms of incidence (2.206.771 cases, represented in blue) and mortality (1.796.441 estimated deaths, represented in orange). Non melanoma skin cancer is excluded. Colon and rectal cancer cases are combined. Source: GLOBOCAN 2020.

Risk factors for the development of cancer are related to a combination of environmental features and individual characteristics. Some factors are common for all types of cancer and can be controlled, such as diet (Anic et al., 2016), alcohol use, obesity, lack of physical activity or UV radiation. In addition to this, lung cancer is related to further factors including chronic obstructive pulmonary disease (COPD), asbestos, silica, environmental radon exposure and pollution. However, active or passive smoking should be considered the most important factor, as 80% of cases are directly associated with tobacco consumption. Indeed, smoking-related activities result in exposure to potent carcinogens such as N-nitrosamine, naphthylamine, polycyclic aromatic hydrocarbons, among more than 50 other chemicals with proven carcinogenic potential. On top of these factors, increased incidence of cases in certain families have also been described, which points to some genetic predisposition that interacts with environmental factors (Wang et al., 2017).

Lung cancer has historically been classified in two main groups, small cell lung cancer (SCLC) and non-small cell lung cancer (NSCLC), due to pathological differences that arise from their different neoplastic precursors (Travis et al., 2015). These groups have very different prognosis and protocols of treatment.

1.1 Non-small cell lung carcinoma (NSCLC)

Among all diagnosed lung cancer cases, around 80% correspond to NSCLC. The incidence varies between men (14.2%, being the second most common cancer after prostate) and women (9.1%), with a rising trend for this second group.

1.1.1 MOLECULAR PATHOGENESIS

The development and gradual implementation of screening programs with low-dose computed tomography scans in the high risk population (adults aged 55-80, with a smoking history of 30 packs/year who are active smokers or have quit within the past 15 years) has resulted in increased diagnostic rates and prolonged survival of diagnosed individuals (de Koning et al., 2020). However, lung cancer is very often diagnosed at an advanced stage based on the appearance of persistent symptoms such as cough, hemoptysis, dysphagia, dysphonia and superior vena cava syndrome. These symptoms are associated with local compression on anatomical structures. Paraneoplastic disorders and pain by metastatic disease also frequently leads to a diagnosis of lung cancer.

NSCLC can be classified in adenocarcinoma, squamous-cell lung carcinoma (SCC) and large cell carcinoma. Pathological diagnosis is based on the integration of macro- and microscopic morphological characteristics with clinical data, and immunohistochemical markers that distinguish NSCLC subtypes. Cytokeratins 5/6 and p40/p63 are diagnostic markers for SCC, while TTF-1 and napsin A are markers expressed in adenocarcinomas.

Adenocarcinoma is the most common type of NSCLC. Alveolar type II cells, exocrine mucus producing glandular cells located at the alveoli, are believed to be its precursor. These tumors can present different predominant growth patterns, namely micropapillary, solid, papillary, acinar and lepidic growths, that have different clinical behavior. These tumors harbor mutations in specific genes that confer cells their neoplastic features while promoting tumor growth (“driver mutations”). Despite the increasing knowledge on the mutational landscape

profiles of tumors, only a minority of these mutations are amenable to targeted therapies. Mutational evaluation in NSCLC has emerged during the last 15 years since the description and therapeutic targeting of EGFR mutations. Since then, genetic alterations in ALK, ROS1, RET, BRAF, HER2 or MET, have been described and proved to benefit from targeted therapy with demonstrated clinical activity (Planchard et al., 2018). Recently, it has been shown that patients with KRAS G12C mutations in cancer cells also benefit from targeted therapy (Skoulidis et al., 2021).

SCC arises as a pathogenic development of epithelial metaplasia and dysplasia, long after chronic inflammation in large bronchi. SCC is the second most common histological type in NSCLC and accounts for about one third of the cases. Unfortunately, mutations in genes amenable to therapeutic targeting are uncommon. Recurrent mutations in pathways such as CDKN2A/RB1, NFE2L2/KEAP1/CUL3, PI3K/AKT, SOX2, as well as alterations in the FGFR2 kinase family have been frequently found, relating to oxidative stress response and squamous differentiation (Cancer Genome Atlas Research, 2012), although this has not translated into clear therapeutic targets (Gandara et al., 2018). The pattern of mutations, amplifications and neoepitopes differ between adenocarcinomas and SCC. Only six genes (TP53, RB1, ARID1A, CDKN2A, PIK3CA, and NF1) have been found with significant mutation rates in both lung cancer types (Campbell et al., 2016; Campbell et al., 2018). These differential characteristics lead to differences in diagnostic procedures and targetable oncogenic drivers, as shown in **Figure 2**.

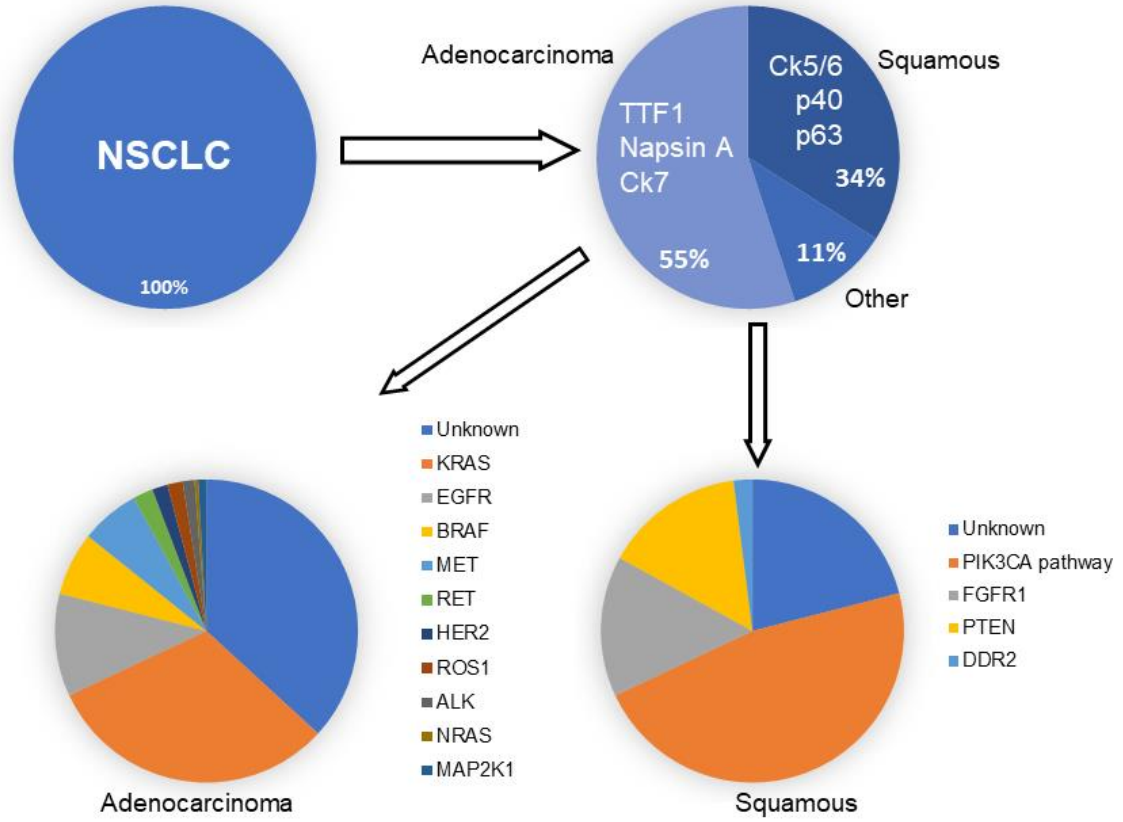

Figure 2 Histopathological and genetic differences between the most common histological types in NSCLC. The variety of oncogenic drivers identified in adenocarcinomas have led to multiple therapeutic strategies, but a deeper knowledge of the oncogenic drivers in SCC is still lacking. Source: The Cancer Genome Atlas (TCGA) (Cancer Genome Atlas Research, 2012).

The detection of mutations is essential and adds a new layer of complexity to the diagnosis of lung cancer pathology. However, definitive diagnosis can be sometimes difficult as the amount of tissue (biopsies or cytology samples obtained by fine-needle aspiration) is limited and in some cases the results from marker and histological analyses may overlap. A deeper understanding of the genetic pathogenesis and improvement of molecular diagnosis through next-generation sequencing (NGS) have increased the sensitivity of the analyses, opening the way for precision oncology strategies that are highly needed.

1.1.2 DIAGNOSIS AND STAGING

Classification of lung cancer by stage is critical for clinical decisions, and takes into account tumor size and anatomical invasion (T), lymph node extension (N) and metastatic involvement (M), to grade tumors from stage I (a solitary lesion measuring less than 4 cm without lymph node invasion) to IV (with metastatic lesions) as shown in **Table 1**.

Table 1 8th Edition of the TNM classification of lung tumors. The indicated sizes represent the largest dimension of the tumor mass (Detterbeck et al., 2017)

T	Primary Tumor
Tx	Primary tumor cannot be assessed
T0	No evidence of primary tumor
Tis	Carcinoma *in situ*, irrespective of size
T1	Tumor ≤ 3cm. No evidence of invasion beyond the lobar bronchus.
T1mi	Minimally invasive adenocarcinoma
T1a	Tumor ≤ 1cm
T1b	Tumor >1cm, but ≤ 2cm
T1c	Tumor > 2cm, but ≤ 3cm
T2	Tumor > 3cm, but ≤ 5cm. Any tumor with the following characteristics: – Invasion of main bronchus, not invading carina – Invasion of visceral pleura – Atelectasis of obstructive pneumonitis (either part or entire lung)
T2a	Tumor > 3cm, but ≤ 4cm
T2b	Tumor > 4cm, but ≤ 5cm
T3	Tumor > 5cm, but ≤ 7cm. Any tumor with the following characteristics: – Invasion of chest wall – Invasion of the phrenic nerve – Invasion of parietal pericardium – Associated separate tumor nodules in the same lobe as the primary tumor
T4	Tumor > 7cm. Any tumor with the following characteristics: – Invasion of diaphragm – Invasion of mediastinum

N	Regional Lymph Nodes
Nx	Regional lymph nodes cannot be assessed
N0	No evidence of lymph node metastasis
N1	Ipsilateral peribronchial and/or hilar nodes and ipsilateral nodes, including involvement by direct extension
N2	Ipsilateral mediastinal and/or subcarinal lymph nodes
N3	Any lymph node metastasis in the following locations: – Contralateral mediastinal – Contralateral hilar – Ipsilateral or contralateral scalene – Supraclavicular

M	Distant Metastasis
M0	No distant metastasis
M1	Distant metastasis
M1a	Associated nodules in the contralateral lung as the primary tumor, or with any of the following features: – Pleural nodules – Pericardial nodules – Malignant pleural or pericardial effusion
M1b	Single extrathoracic metastasis in a single organ or non-regional lymph node
M1c	Any lymph node metastasis in the following locations: – Contralateral mediastinal – Contralateral hilar – Ipsilateral or contralateral scalene – Supraclavicular

Staging	N0	N1	N2	N3
T1	IA	IIB	IIIA	IIIB
T2a	IB	IIB	IIIA	IIIB
T2b	IIA	IIB	IIIA	IIIB
T3	IIB	IIIA	IIIB	IIIC
T4	IIIA	IIIA	IIIB	IIIC
M1a	IVA	IVA	IVA	IVA
M1b	IVA	IVA	IVA	IVA
M1c	IVB	IVB	IVB	IVB

Although not a biomarker *per se*, tumor staging has significant prognostic information and constitutes one of the first variables to be considered at the time of diagnosis. Long-term prognosis is poor, with 5-year survival rates of less than 25%, decreasing to 5% in advanced cancer stages.

1.1.3 TREATMENT

The decision to provide a given treatment must be collegiate in an interdisciplinary environment including oncologists, pulmonologists, radiologists, pathologists, geneticists and surgeons. These decisions take into account an interplay between treatment intention, expected side effects, comorbidities and preferences. Less than one fifth of cases are diagnosed in the early stages, when are amenable to curative strategies involving surgery. Most patients present metastatic or locally advanced disease that require systemic treatment and radiotherapy. Supportive care planning and control of symptoms are essential steps in the management of lung cancer, especially for advanced disease.

Surgery

Surgery is the principal option of treatment in early stages. It requires the radical excision of tumor with safe margins, while preserving enough healthy lung tissue to ensure adequate post-surgery function. Lobectomy with lymphadenectomy is the most commonly used technique, although sublobar (atypical wedge-resections and segmentectomy), bilobectomy or pulmonectomy can be performed in some circumstances. Neoadjuvant treatment with chemotherapy can sometimes be required to down-stage tumors with confirmed mediastinal invasion, allowing a complete resection. Patients with adequate functional status can benefit from localized resection of oligometastatic disease.

Radiotherapy

Radiotherapy has proven to be an important tool for the treatment of unresectable disease concurrently with chemotherapy, and as a complementary technique to achieve palliative symptom control. The role as adjuvant therapy is currently under discussion. Recently, a phase III trial with postoperative radiation therapy

(PORT) was associated with an increase in disease free survival (DFS) in N2 disease (i.e. subcharinal and mediastinal node extension) (Le Pechoux et al., 2020), although without reaching statistical significance. Esophagitis and pneumonitis are common side effects of radiotherapy in the lung, emphasizing the importance of careful treatment planning and dosing below tissue-specific safety thresholds.

Chemotherapy

Chemotherapy doublets including platinum-based compounds have been the standard of care in the treatment of advanced lung cancer since the 1980s. It remains as first line of treatment in patients without actionable mutations, with an acceptable functional performance status (PS 0-2) and when immunotherapy is not recommended (Planchard et al., 2018). Overall, platinum doublets with third generation drugs (paclitaxel, gemcitabine, docetaxel or vinorelbine) have similar efficacy with different side-effect profiles. There are differences concerning the histological origin. Pemetrexed is the preferred agent for the treatment of non-squamous NSCLC. Chemotherapy is also indicated as adjuvant treatment in stages II and III, due to a death-risk reduction of 11% according to the LACE meta-analysis (Pignon et al., 2008).

Immunotherapy

The role that the immune system plays in the surveillance of cancer development, progression and elimination of transformed cells has been known for decades. However, the efficacious therapeutic application of stimulators of the immune system to combat cancer came into reality long after the discovery of the process. While there was abundant pre-clinical evidence on the positive effect of immunostimulatory cytokines in murine models of cancer, their approval and use for the treatment of human cancers did not meet the expectations when used as monotherapies.

The discovery of immune checkpoint molecules as key regulators of immune responses completely turned around the field of cancer immunotherapy. The development and characterization of monoclonal antibodies that could inhibit the

activity of immune checkpoint inhibitors *in vivo* radically changed all treatment strategies. There is an increasing number of different immune checkpoint molecules that have been either characterized or are under study. Nevertheless, only a small number of inhibitors targeting few immune checkpoints have been approved by regulatory agencies. **Table 1.2** shows the EMA-approved ICB antibodies in the treatment of lung cancer.

Table 2 Approved immunotherapeutic agents by the European Medicines Agency for the treatment of NSCLC as on January 2021 and their brand names. The year indicates the time of first approval. 1L: First line. 2^{+}L: At least one prior chemotherapy regimen. Except for atezolizumab, indications exclude tumors harboring sensitizing EGFR mutations or ALK translocations.

Mechanism	Drug	Approval	Clinical Scenario
Anti-PD-1			
	Nivolumab (Opdivo®)	2015	1L in combination with ipilimumab and platinum-based chemotherapy 2^{+}L in monotherapy
	Pembrolizumab (Keytruda®)	2016	1L in monotherapy: PD-L1 ≥ 50% 1L in combination with chemotherapy 2^{+}L in monotherapy: PD-L1 ≥ 1%
Anti-PD-L1			
	Atezolizumab (Tecentriq®)	2017	1L in combination with platinum-based chemotherapy and bevacizumab 2^{+}L in monotherapy
	Durvalumab (Imfinci®)	2018	Consolidation therapy after chemo-radiotherapy in locally advanced NSCLC
Anti-CTLA4			
	Ipilimumab (Yervoy®)	2020	1L in combination with nivolumab and platinum-based chemotherapy

A major problem still to be addressed is the significant number of patients intrinsically refractory to immune checkpoint blockade (ICB) strategies. Many patients either present primary resistant disease, or acquired resistance to PD-L1/PD-1 blockade. Moreover, immune related adverse events (irAE) can also be found in treated patients, even though at lower frequencies and severities than in patients treated with conventional chemotherapy. These irAE are thought to be

caused by a non-specific hyperactivation of the immune system against non-tumor tissues, leading to a loss of function of healthy organs. Thyroiditis with hypo or hyperthyroidism, pneumonitis, hypophysitis and colitis are amongst the most frequently detected adverse events in patients treated by ICB. As mentioned above, the absolute frequency is lower than with chemotherapy protocols, but its management can still be difficult. In many cases, persistence of side effects occurs despite appropriate therapy with high-dose glucocorticoids (Martins et al., 2019).

Response evaluation is a composite of clinical benefit (improvement of the symptoms present at treatment initiation), clinical examination (assessment of visible or palpable lesions), analytical interpretation and radiological control with regular CT-scans plus intravenous contrast as per clinical guidelines. An adequate antitumor immune response requires cellular infiltration after release of inflammatory cytokines. This may result in a transient increase of the target lesion size that does not represent true progression but in fact it is a consequence of effective disease control, and it is followed by target lesion reduction or stabilization for a long time. This process, known as pseudoprogression, has gained attention during the last years but has been shown to be a rare event in NSCLC (Fujimoto et al., 2019).

Another situation that oncologists may encounter in clinical practice is a worsening of the patient condition after treatment, accompanied by an acceleration of the tumor growth. This condition is known as hyperprogressive disease, or hyperprogression (HP). Whether this is a consequence of ICB or tumor evolution is still a matter of debate. Studies show its incidence to occur in about 15% of cases (Ferrara et al., 2018a; Kim et al., 2019). Several criteria to identify hyperprogressing patients have been proposed, most prominently the Gustave-Roussy radiological criteria (a tumor growth rate ratio –ΔTGR-exceeding 50%). A burst of highly-differentiated CD4 T cells in the first cycle has been correlated with tumor evolution (Arasanz et al., 2020), as well as shifts in

other populations such as type 3 innate lymphoid cells, regulatory T cells, FcyRIIb^{+} cells (Lo Russo et al., 2019; Xiong et al., 2018), and tumor related mechanisms as MDM2 and MDM4 amplifications (Forschner et al., 2020).
Targeting other immune checkpoint molecules (e.g. OX40, LAG3, TIM3) is under investigation and will probably add to the therapeutic options in many cancer types during the next years.

1.2 Major immune checkpoints in human clinical therapy

1.2.1. PROGRAMMED CELL DEATH-1 (PD-1) AND PD-1 LIGAND-1 (PD-L1)

PD-1 is a type I transmembrane receptor of the CD28 family of co-stimulatory molecules that is expressed mainly on the surface of lymphocytes. Expression by other cell types such dendritic cells has been described (Arasanz et al., 2017), and even by some cancer cells, although these latter results are still controversial (Wang et al., 2020). For PD-1 intracellular inhibitory activities, phosphatases SHP-1 and SHP-2 need to associate with their corresponding binding domains within the intracytoplasmic part of PD-1. These domains are termed ITIM and ITSM and include tyrosine residues that have to be phosphorylated so that SHP1 and SPH2 can bind to them. These phosphatases act on several targets, most prominently CD28, leading to blockade of co-stimulation upon T-cell receptor (TCR) activation (Hui et al., 2017; Kamphorst et al., 2017b). PD-1 also indirectly downregulates the PI3K-AKT and MEK/ERK pathways. These processes lead to a downregulation of the TCR and induce lower proliferative capacities of T cells. In addition, PD-1 binding to PD-L1 causes the expression in the T cell of E3 CBL ubiquitin ligases, which down-regulates components of the TCR (Karwacz et al., 2011).

PD-L1 is a type I transmembrane protein belonging to the immunoglobulin-like B7 family of co-stimulatory molecules, which presents an immunoglobulin variable-like extracellular domain, followed by a transmembrane domain and an intracellular part with signaling properties within cancer cells (Gato-Canas et al.,

2017), but also in T cells (Diskin et al., 2020). The intracellular domain is made of at least three phylogenetically conserved motifs with signaling capacities, termed RMLDVEKC, DTSSK and QFEET. These motifs possess regulatory and signal-transduction properties through mechanisms not altogether known, particularly inhibiting IFN signal transduction, and enhancing proliferation and resistance to pro-apoptotic agents. It has been suggested that mutations present in the PD-L1 gene in human carcinomas within these motifs disrupt PD-L1 anti-interferon activities, which in turn may confer resistance to anti-cancer therapies. PD-L1 can interact not only with PD-1 in *trans* and *cis*, but also with other B7 family members such as B7-1 (CD80). Posttranslational modifications (e.g. glycosylation) also play important roles in regulating their activity. PD-L1 is expressed on the surface of antigen presenting cells, myeloid cells, and a wide variety of healthy tissues to maintain immune tolerance by restricting autoreactive damage exerted by activated T cells. Not surprisingly, in many instances tumor cells overexpress PD-L1 on their surface as an escape mechanism. This overexpression helps cancer cells to grow faster, counteract pro-apoptotic stimuli and inhibit cytotoxic activities by tumor-reactive T cells. Therefore, PD-L1 up-regulation is used to induce T cell anergy and exhaustion through PD-1 binding in the tumor microenvironment.

1.2.2 CLINICAL APPLICATION OF PD-1/PD-L1 BLOCKADE IN NSCLC

The promising results of phase 1 trials with PD-1 blockade led to the development of phase 2 and phase 3 clinical trials to evaluate the safety and efficacy of monoclonal antibodies targeting PD-L1/PD-1 binding compared to standard therapies. Specifically, in metastatic NSCLC several PD-L1/PD-1 blockade immunotherapies have demonstrated consistent and durable clinical benefit, including the use of blocking agents pembrolizumab, nivolumab with or without ipilimumab, durvalumab and atezolizumab.

In the phase III CheckMate 017 (Brahmer et al., 2015) and CheckMate 057 (Borghaei et al., 2015) clinical trials, the administration of 3 mg/kg nivolumab (an

anti-PD-1 antibody) was compared to docetaxel after progression to platinum-based chemotherapy, which was the first line standard of care at the time. Four-year overall survival (OS) was 14% in a pooled cohort of four pivotal studies with nivolumab (Antonia et al., 2019), including phase II Checkmate 063 (Rizvi et al., 2015) and phase I Checkmate 003 (Gettinger et al., 2015).

The positive results of the KEYNOTE-010 phase II/III trial led to the approval of pembrolizumab, a humanized IgG4 anti-PD-1 antibody, by the EMA in 2016 (Herbst et al., 2016) for the treatment of stage IV NSCLC after progression to chemotherapy. In this trial, median OS was 10.4 months for 2 mg/kg pembrolizumab, 12.7 months for 10 mg/kg pembrolizumab, and 8.5 months for docetaxel at a dose of 75 mg/m^2. All treatment arms were administered once every three weeks.

PD-L1 blockade with atezolizumab has also demonstrated clinical benefit in patients with advanced NSCLC. The OAK (phase III) and POPLAR (phase II) trials (Rittmeyer et al., 2017) showed an improvement in OS. The 4-year OS rates in POPLAR were 14.8% (8.7–20.8) and 8.1% (3.2–13.0) and those in OAK were 15.5% (12.4–18.7) and 8.7% (6.2–11.3) for atezolizumab and docetaxel, respectively. Moreover, a majority of the long-term survivors in the chemotherapy arm received ICB after progression (Mazieres et al., 2021). The benefit in OS in these trials is represented in **Figure 3**.

The results in previously treated patients led to the incorporation of immunotherapy into the first-line treatment of advanced NSCLC, either in monotherapy with pembrolizumab (KEYNOTE-024) or in combination with chemotherapy (KEYNOTE-189 and KEYNOTE-407 trials) depending of PD-L1 expression in the tumor. Consolidation treatment after definitive chemo-radiotherapy with Durvalumab (an antiPD-L1 antibody) is now considered a standard-of-care after the OS and PFS benefit seen in the PACIFIC trial (Antonia et al., 2017). More options of ICB will probably be incorporated into the neoadjuvant and adjuvant setting in the near future.

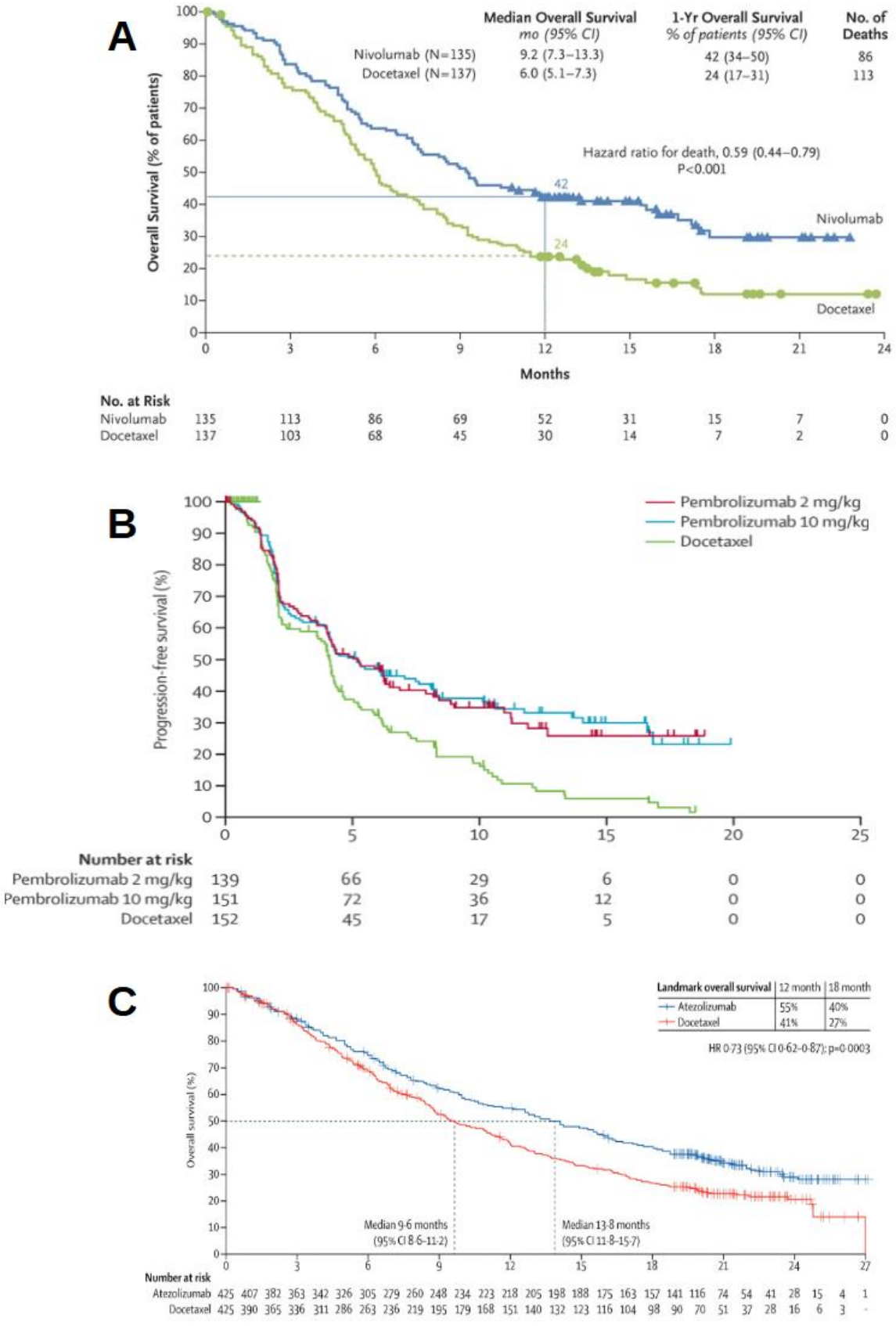

Figure 3 A consistent benefit for OS was observed in phase III trials in second and following lines of treatment with PD-1 and PD-L1 blockade. **A**: Checkmate 017 trial with nivolumab (Brahmer et al., 2015). **B**: KEYNOTE-010 trial with pembrolizumab (Herbst et al., 2016). **C:** OAK trial with atezolizumab (Rittmeyer et al., 2017).

1.2.3 CYTOTOXIC T LYMPHOCYTE ASSOCIATED PROTEIN-4 (CTLA-4)

It is worth to mention the first immune checkpoint to be targeted in human therapy, the co-inhibitory molecule CTLA-4, which is expressed on the surface of *in vitro* activated T cells, and in human regulatory T cells (Fife and Bluestone, 2008; Leach et al., 1996). CTLA-4 also binds to B7 and induces T cell unresponsiveness. The first immunotherapies blocking CTLA-4/CD80 interactions in humans showed a significant benefit compared to standard treatments in human melanoma. Although with worse toxicity profiles than PD-L1/PD-1 blocking antibodies, the CTLA-4-targeted antibody ipilimumab has also emerged as an option when used in combination with PD-1 blockade for the management of treatment-naïve NSCLC, as demonstrated in the Checkmate-9LA and Checkmate-227 clinical trials.

1.3 Biomarkers of response to anti-PD-1 and anti-PD-L1 immunotherapy

Without any doubt, immunotherapy strategies targeting immune checkpoints have significantly advanced the standard of treatment for many cancer types. However, these strategies entail high costs that increase the financial burden of the healthcare systems globally. In high-income countries, the annual per-patient cost of ICB drugs is in the order of thousands of euros € ($70000 in the USA). The lack of prognostic and predictive molecular biomarkers to guide treatment decisions with the notable exception of the widely used PD-L1 expression in tumor biopsies, worsens the problem (Nesline et al., 2020). Fixed dosing and prolonged treatments in responders can also influence the final cost that includes outpatient visits, cost of hospitalizations, emergency department visits and management of adverse events (Legoupil et al., 2020). This situation is even more complex in low-income countries and the scarcity of medical resources that the COVID-19 or other pandemics may bring in the future.

Strategies such as the ESMO Magnitude of Clinical Benefit Scale (ESMO-MCBS Evaluation) in Europe, NCCN Evidence Blocks in the USA or the VALTERMED information system in Spain have been proposed as tools to evaluate the combination of clinical benefit and associated costs of new therapies.

The identification of appropriate biomarkers of response to immune checkpoint therapies would also enable the identification of patients with high probability of benefit from these therapies, or with low probability of developing unwanted irAE. Predictive and prognostic biomarkers could be monitored before the administration of immunotherapies, but could also be monitored during treatment to follow responses.

So far, a large collection of biomarkers has been studied in the context of different cancer immunotherapies for many years since their introduction, which mainly include quantification of peripheral blood immune cells, cytokine/chemokine plasma levels and the degree of tumor infiltration with T cells as quantified by immunohistochemistry from tumor biopsies. These “classical” immune biomarkers have also been studied in the context of immune checkpoint inhibitor therapies, but several others have also been specifically developed for ICB. Amongst these, the most studied are PD-L1 expression in tumor cells and in immune cell infiltrates, mutational burden, quantification of tumor-infiltrating immune cells, characterization of specific gene mutations, human leucocyte antigen (HLA) heterogeneity, immune cell populations and gut microbiota profiling. All these potential biomarkers have been chosen because they have been found to affect responses to immunotherapy treatment by several mechanisms (Chen DS, Nature 2017).

1.3.1 PD-L1 EXPRESSION IN TUMOR CELLS

Quantification of PD-L1 expression in tumor cells was one of the first biomarkers of response to PD-L1/PD-1 blockade immunotherapies to be evaluated. This is a logical choice as PD-L1 corresponds to one of the partner targets of these immunotherapies. Indeed, PD-L1 expression on the surface of tumor cells could

be considered as an adaptive mechanism for tumors to escape from the attack of the immune system. PD-L1 is up-regulated by pro-inflammatory stimuli such as IFNs, TNF-α or IL1-β, possibly as a response to dampen autoreactive damage in “physiological“ immune responses (Escors et al., 2018). PD-L1 expression in cancer cells also stimulates cell proliferation, and protects them against the pro-apoptotic properties of type I and type II interferons (Gato-Canas et al., 2017). The importance of PD-L1 as a tumor escape mechanism is also highlighted by its constitutive expression in many cancer cells driven by oncogenes. PD-L1 directly inhibits T cell cytotoxic activities by engaging with PD-1 expressed on the surface of activated T cells.

It is well accepted that high PD-L1 expression by tumor cells is associated with objective responses to PD-L1/PD-1 blockade therapies. Thus, the percentage of PD-L1-positive cancer cells is associated with response rates that reach up to 37% in the case of high tumor PD-L1 expression levels in NSCLC (Garon E et al ESMO 2014). When used in combination with other immune biomarkers, such as the abundance of highly-differentiated CD4 memory cells, it can discriminate a subset of patients with up to 70% of objective responders (Zuazo et al., 2019). Most clinical trials addressing PD-L1/PD-1 blockade strategies included quantification of PD-L1 expression in cancer cells, immune cell infiltrates or a combination of both by immunohistochemistry assays. Hence, there is not current standardization of anti-PD-L1 antibodies for quantification. Each clinical trial uses different antibodies with varying sensitivities and specificities, thresholds and positivity criteria. For instance, OAK trial stratified patients according to their PD-L1 expression in tumor cells (TC1/2/3) or immune cells (IC1/2/3). Another complication is that PD-L1 expression is heterogeneous and dynamic over time. For example, PD-L1 can be strongly up-regulated by interferons following PD-L1/PD-1 blockade. In this way, patients with tumors that were apparently PD-L1-negative show benefit from therapy. Therefore, results from the use of PD-L1 tumor expression as a biomarker do differ between studies.

1.3.2 TUMOR-INFILTRATING LYMPHOCYTES AS PROGNOSTIC BIOMARKERS OF RESPONSE

The degree of tumor infiltration with immune cells, especially CD8 T cells, has been a well-known prognostic maker for many anti-cancer therapies before the application of ICB therapies in human patients. Therefore, it is not surprising that tumor infiltration with immune cells has also been studied as a prognostic marker for CTLA-4 and PD-L1/PD-1 blockade, amongst other types of immunotherapies. It is evident that any significant antitumor cellular response requires an infiltration of cytotoxic immune cells within the tumor microenvironment, both for antigen recognition and tumor cell killing. Currently, tumors can be classified according to the type and degree of immune cell infiltration. This subject is covered in detail elsewhere (Teng et al., 2015). Briefly, tumors can be classified as immunogenic or “hot” when they present a high *in situ* immune infiltrate, as a contrast with “cold” tumors that present little immune infiltration. These tumors have been associated with better response to treatments, including ICB therapies. The degree and localization patterns of tumor infiltration by T cells and macrophages are currently used to derive the so-called “immunoscore”, widely used as a prognostic marker mainly for the treatment of colorectal cancer (Galon et al., 2014). Overall, accumulating studies indicate that patients with highly infiltrated “hot” tumors respond significantly better to immunotherapy treatment (Duan et al., 2020)

1.3.3. TUMOR MUTATIONAL BURDEN

Cancer immunotherapy relies on the activation of T cells reactive towards tumor antigens, including neoantigens. Tumors consist of a collection of cell variants that have non-synonymous single nucleotide mutations in their genomic DNA, which can be related to abnormal protein expression and production of novel antigens (neoantigens) not present in the original germinal protein repertoire. This phenomenon occurs across different tumors, and it is especially evident in cancers with a high frequency of loss of genetic repair mechanisms (MMR deficiency), with microsatellite instability (MSI) or with POLE mutations. Smoking

history has been correlated with increased mutational burden, which interestingly may single out these patients more likely to respond to ICB. This is particularly true in most lung cancer patients, as many mutations in lung cancer are caused by carcinogens present in tobacco. A high mutational burden in cancer cells seems to correlate with better responses in ICB therapies. Pembrolizumab use was therefore granted approval by the FDA for the treatment of TMB^{high} (defined as tumors that present ≥ 10 mut/Mb) advanced lung cancer independently of histological classification (Le et al., 2015). A later study showed that the impact of mutational burden does not correlate with response in all cancer types, restricting its predictive value to melanoma, lung and urothelial carcinomas (McGrail et al., 2021b).

Nevertheless, it has to be taken into account that neoantigens can be produced by heteroclonal tumors, leaving a proportion of tumor cells that lack their expression. As a consequence of this tumor heterogeneity, prolonged responses to drugs such as pembrolizumab may be impaired with the selection of poorly immunogenic variants in a process of acquired resistance (McGranahan et al., 2016). Moreover, mutational burden should be complemented with information on tumor purity and the presence of certain mutational signatures, that can improve our predictive capabilities (Anagnostou et al., 2020).

1.3.4 HUMAN LEUKOCYTE ANTIGEN (HLA) AND MUTATIONS IN SPECIFIC GENES

HLA is a key structural element of antigen presentation. Hence, its genetic variation is relevant to the antitumor performance of ICB. Both HLA homozygosity and B*44 supertype have been associated with durable responses to immunotherapy, although these findings have not been replicated in NSCLC-specific cohort studies (Chowell et al., 2018; Negrao et al., 2019).

Inactivating mutations in certain genes have been linked to a lack of response to immunotherapy. Alterations in STK11, or LKB1, appear in a 25% of KRAS-mutated lung adenocarcinomas, and virtually none of the patients with this

molecular feature responds to ICB despite high PD-L1 expression and high mutational burden (Skoulidis et al., 2018). A similar phenomenon occurs with KEAP1 mutations. Moreover, combination of these mutations results in a more aggressive phenotype (Arbour et al., 2018). Interestingly, loss of STK11 in tumors with KRAS mutations induces a genetic program of trans-differentiation into squamous or adenosquamous histologies, and a lack of tumor inflammatory microenvironment.

1.3.5 MICROBIOTA AND ANTIBIOTIC USE

Although mostly described in melanoma patients, the relative abundance of certain bacterial species in the gut has been related to immunotherapy responses in NSCLC (Routy et al., 2018). Moreover, although it still is a matter of debate, the use of antibiotics prior to ICB start might impair an antitumoral response and it is associated with unfavorable outcomes (Pinato et al., 2019).

1.3.6 QUANTIFICATION OF BLOOD CELL TYPES IN ROUTINE CLINICAL ANALYSES

Peripheral blood analyses are extensively used to monitor the overall health status of a patient. Any deviation of cell counts or concentrations of certain metabolites from normality uncovers a wide variety of pathological events, including cancer. Therefore, the first biomarkers to be tested derived from standard clinical analyses of peripheral blood. As an example, neutrophilia and thrombocytosis are well-established factors in patients with advanced cancer. As routine analysis for quantification in peripheral blood is readily accessible and its assessment is a key element of daily practice in clinical oncology, it is logical to assume that it could be used to derive prognostic and potentially predictive parameters.

The ratio between neutrophil and lymphocyte absolute counts in peripheral blood is an indirect marker of the balance between myeloid and lymphoid cell compartments, the overall inflammatory status of the patient and the coordinated

response of adaptive immunity. High rates of neutrophil-to-lymphocyte ratios (NLR) represent a state of systemic inflammation and stress, and it can be calculated by different methods. The most commonly used is the derivation of the ratio between neutrophil/lymphocyte absolute counts. Nevertheless, there are more refined methods to obtain derived parameters with enhanced prognostic capacities. This is the case of the derived NLR, which is calculated by dividing the difference between white blood cell counts and lymphocyte counts, instead of only using lymphocyte counts. The dNLR could in principle be a less restrictive prognostic parameter because it includes for its calculation myeloid populations such as eosinophils and basophils in the analysis.

NLR has been found to be related to many clinical scenarios and not only in oncology, ranging from preoperative rate of complications, myocardial infarction, pulmonary embolism and viral infections. The inflammatory status of the subject can play a very important role in the development and pathophysiology of many diseases. This status influences the generation of different immune populations that can be studied at a systemic level in peripheral blood.

Howard et al (2019) analyzed the prognostic value of NLR in a large cohort of cancer patients (n=5636). The authors of the study identified age, disease stage, race, gender and cancer type as significant factors contributing to the calculated baseline NLR in melanoma, breast, colorectal, esophageal, hepatocellular, prostate, ovarian and pancreatic cancers (Howard et al., 2019).

NLR can be either interpreted as a continuous or a dichotomous variable. Establishing a minimum threshold offers the advantage of better classification of patients that may respond to treatments differently. NLR must be interpreted as a dynamic ratio, with changes over time in relation to the development of cancer. In the context of lung cancer screening, Sanchez-Salcedo P *et al* (Sanchez-Salcedo et al., 2016) found that NLR and platelet-lymphocyte ratio (PLR) were related to a higher incidence of lung cancer, with an implication of other concomitant diseases such as chronic obstructive pulmonary disease (COPD). NLR increases significantly with tumor progression due to the systemic

expansion of neutrophils. Nakamura et al retrospectively found an incremental relationship between a NLR cut-off point of 9.21 and death probability within one month (Nakamura et al., 2016).

NLR has also been studied as a predictor of responses to immunotherapy. A meta-analysis published in 2020 showed a significant trend for high NLR values to correlate with worse OS and PFS in patients with lung cancer treated with immunotherapy. However, the authors of the study acknowledged a high degree of heterogeneity in the analysis (Jin et al., 2020). The dynamic increase of this ratio after treatment initiation is also related to worse prognosis and treatment failure. This was described in early drug-development trials of immunotherapy and later confirmed in later observational studies (Ameratunga et al., 2018; Simonaggio et al., 2020).

PLR has also been studied as a surrogate of response, although the specific threshold is highly variable across studies and ranges from 198.5 to 262 with variable degrees of sensitivity and specificity (Diem et al., 2017; Kos et al., 2016).

1.3.7 DYNAMICS OF IMMUNE BLOOD POPULATIONS AS INDICATORS OF RESPONSE

As an alternative to the study of the cytotoxic lymphocyte activity at the tumor microenvironment, the status of immune cells in the bloodstream has recently gained attention. An advantage of this strategy is the easy access and homogeneity of the results, since peripheral blood is obtained by venipuncture and does not require the use of invasive procedures to obtain biopsies. The use of techniques such as high dimensional flow cytometry and CYTOF allows a heightened degree of accuracy in the identification of cell types and also activation subsets. In addition, the dynamic fluctuations of specific blood populations provide another degree of detail for biomarker studies, but also the biology of anti-tumor systemic immune responses. Indeed, CD8 PD-1+ T cells were found to be increased in NSCLC patients treated with anti-PD-1 ICB and were associated with increased objective responses. This elevation was tumor-

specific and depended on the expression of costimulatory molecules (particularly CD28) that could be detected by flow cytometry (Kamphorst et al., 2017a; Kamphorst et al., 2017b). Another study utilizing CYTOF from frozen PBMC samples identified a relative increase in monocytic populations in peripheral blood from responder patients before starting immunotherapies (Gubin et al., 2018). Zuazo et al identified a subset of highly-differentiated $CD27^{neg}$ $CD28^{neg}$ memory CD4 T cells that was significantly increased in peripheral blood from responder patients before starting immunotherapies. In this study, a threshold of 40% was found to separate responders from non-responders, below which clinical responses to ICB were not observed (Zuazo et al., 2020; Zuazo et al., 2019). The group distribution below or above this threshold allowed patient classification in 2 groups according to their phenotype, namely G2 and G1 patient cohorts. This study highlighted the importance of a functional CD4 immunity. Similar results were obtained independently by Kagamu et al in a Japanese NSCLC cohort (Kagamu et al., 2020) by CYTOF analysis, using a different set of markers to identify circulating CD4 memory T cells.

Myeloid derived suppressor cells (MDSCs) consist of heterogeneous populations of myeloid cells with strong immunosuppressive activities. These cell subsets arise from early myeloid precursors in the bone marrow that in healthy individuals mature into dendritic cells (DCs), monocytes/macrophages or granulocytic precursors. These populations, although difficult to identify in the absence of commonly accepted markers, develop in the context of inflammatory conditions as obesity, pregnancy, autoimmune diseases, or bacterial infections. However during cancer development and progression their expansion is uncontrolled (Veglia et al., 2018). Granulocytic (G-MDSCs) and monocytic (M-MDSCs) subtypes are known to induce T-cell immunosuppression at the tumor microenvironment (TME). This suppression can be exerted also systemically using different suppressive mechanisms such as consumption of aminoacids that are essential for lymphocyte activity (by production of arginase and Indoleamine 2,3-dioxygenase), induction of oxidative stress (iNOS and reactive oxygen

species) and production of anti-inflammatory cytokines (IL-10 and TGF-beta), (Ibañez-Vea et al., 2018).

1.3.8 SERUM AND PLASMA PROTEINS WITH BIOMARKER POTENTIAL

Immune responses are physiologically regulated by multiple soluble factors such as hormones, cytokines, chemokines and soluble checkpoint molecules. These proteins regulate and alter the functions and dynamics of immune cell populations. This is also the case for anti-cancer immune responses. In addition to physiological responses, tumor cells express high levels of cytokines and chemokines that end up systemically in the blood stream. These cytokines usually exert their activity in autocrine, paracrine and endocrine fashions, so determination of their concentrations and dynamics in the bloodstream, not only provides an overall view of the potential mechanisms implicated in anti-tumor immunity but also in tumor progression.

A key cytokine shown to impair the anti-tumor responses is IL-8, which is produced by the tumor cells and possesses chemoattractant properties for neutrophils, which in turn induce an immunosuppressive environment. In a study by Sanmamed et al, high IL-8 levels were associated with poor response to ICB in NSCLC. Interestingly, IL-8 quantification could identify pseudoprogressive disease from disease progression (Sanmamed et al., 2017; Teijeira et al., 2021). Moreover, high IL-6 levels before treatment were shown to be associated with worsened OS and PFS in patients with NSCLC. Other circulating factors that have been proposed as predictors of response are granzyme B and indoleamine 2,3-dyoxogenase (IDO) (Botticelli et al., 2018; Costantini et al., 2018; Kang et al., 2020).

The evolution of circulating markers could also be used for the early detection of toxicity induced by a hyperactivation of the immune response. For example, after transplantation of CAR-T cells in acute leukemia, increased soluble IFN-γ, gp130, IL-6 and its receptor are associated with the incidence of cytokine-release syndrome, as found in a study by Teachey et al. (Teachey et al., 2016). IL-18, IL-

8, IP10, MCP1, MIG and MIP1B were also detected in more severe forms in this study. Interestingly, the standard of treatment for this clinical adverse event is the use of IL-6 blockade with antibodies such as siltuximab or tocilizumab.

Many factors contribute to anti-tumor immune responses, including the requirement of a functional systemic immunity that interacts with the tumor at its microenvironment (Spitzer et al., 2017). Therefore, it is likely that a combination of biomarkers could accurately predict responses. To implement a feasible model in clinical practice, this combination should be as simple and accessible as possible, so that it can improved personalized immuno-oncology therapeutic strategies.

2. Hypothesis and Objectives

HYPOTHESIS:

There is an unmet clinical need for tools that anticipate treatment responses to immunotherapy in lung cancer. Aiming to improve patient selection and avoid treatment futility, the profile and dynamics of systemic blood cell populations and soluble factors can be used as prediction markers in NSCLC patients treated with immunotherapy.

OBJECTIVES:

1. Evaluation of body composition and nutritional status as factors affecting the response to PD-1/PD-L1 blockade immunotherapy in NSCLC patients.
2. Derivation and validation of classical prognostic variables derived from routine clinical analyses as predictive/prognostic markers of response to PD-1/PD-L1 blockade immunotherapy.
3. Quantification of baseline numbers and dynamic changes of immune myeloid cell populations by flow cytometry in peripheral blood, and their evaluation as predictive/prognostic biomarkers of response to PD-1/PD-L1 blockade immunotherapy.
4. Quantification of baseline concentrations of soluble immune checkpoints and chemokines, and their changes in plasma from advanced NSCLC patients. Evaluation of their predictive/prognostic power in PD-1/PD-L1 blockade immunotherapy.
5. Characterization of anti-tumor immune responses in patients stratified according to histopathological characteristics of the primary tumor, and treated with PD-1/PD-L1 blockade immunotherapy.

3. Materials and Methods

3.1 Study design

A prospective observational study was carried out with a cohort of 87 patients treated with PD-L1/PD-1 blockade immunotherapies. Patients were treated with anti-PD-1 (pembrolizumab 2 mg/kg every 21 days, nivolumab 3 mg/kg every 14 days) or anti-PD-L1 (a fixed dose of 1200 mg atezolizumab every 21 days) following current clinical guidelines. The inclusion criteria for eligibility were confirmed stage IV non-small cell lung carcinoma (NSCLC), age >18 years and confirmed progression on at least one prior line of systemic treatment. Exclusion criteria were one or more from the following: refusal to participate in the study after informed consent; coexistence of a different neoplastic disease; concomitant administration of chemotherapy and prior administration of other immune-checkpoint blocking antibodies. Age-matched healthy individuals were recruited as a control cohort. The study protocol strictly complied with the principles of the WMA Declaration of Helsinki and the Department of Health and Human Services Belmont Report Good Clinical Practice guidelines. The study was approved by the Ethics Committee at the Complejo Hospitalario de Navarra (Pamplona, Spain, http://www.navarra.es/home_es/Temas/Portal+de+la+Salud/Profesionales/Investigacion/CEIC/Comite+de+Etica+de+la+Investigacion+con+medicamentos+CEIm.htm, approval reference Pyto 2017/4). Following a careful and detailed exposition of the study, its objectives and procedures, written informed consent was obtained from all patients and healthy participants.

3.2 Clinical data

Clinical data composed of medical records, tumor stage, analytical laboratory results and date of diagnosis were collected. All patient data were obtained, treated and stored following applicable legislation (Organic Law 03/2018, on Protection of Personal Data). Any data that linked clinical to personal information

and could lead to patient identification was codified and anonymized to ensure confidentiality.

Data from standard analytical blood analyses were used to calculate absolute neutrophil, lymphoid and monocyte counts, and platelet content. All the standard relative ratios (NLR, MLR, PLR) with potential prognostic value as shown in previous reports were calculated from these data. Briefly, standard analytical clinical blood testing was based on an automatic classification of physical characteristics such as electric impedance, angle light scattering, cell volume or granularity in a flow cytometer. CD45 was used as a marker for validation. Luminex technology was used for quantification of biochemical parameters. Biochemical parameters with potential prognostic value (cholesterol, albumin, lactate dehydrogenase) were also analyzed.

Radiological responses were evaluated from computed tomography (CT) scans according to RECIST v1.1 and iRECIST criteria using RAIMViewer v2.5.0.517 software (Hospital Universitari Parc Tauli, Sabadell) measuring the sum of the largest diameter of lesions. Complete response (CR) was defined as the disappearance of all target lesions (TLs) and absence of new non-target lesions (nonTLs) in the first radiological evaluation. Partial response (PR) was defined as a decrease of the sum of TLs ≥ 30%. Progressive disease (PD) was defined as an increase of the sum of TLs ≥ 20% or the appearance of new nonTLs. Disease was defined as stable (SD) if the criteria of CR or PR were not met and objective evidence for tumor progression was absent.

Overall survival (OS) was defined as the time in days from immunotherapy treatment start to the date of death from any cause. Progression-free survival (PFS) was considered as the time from immunotherapy treatment start to the date of the first documented tumor progression or death from any cause. Patients who had not progressed or died were censored on the date of their last radiological evaluation (de Castro et al., 2015). Disease control rate (DCR) was considered the sum of patients with complete response (CR), partial response (PR) and stable disease (SD). If a patient died without a confirmed radiological progression,

the date of their death was considered as their progression date. Per iRECIST criteria, any radiological progression required confirmation in a second radiological evaluation if available, to exclude pseudoprogression phenomena.

3.3 Collection of blood samples

Blood samples were collected before the start of the first immunotherapy cycle and prior to every cycle up to the first radiological evaluation. Sample collection was also stopped following clinical progression that contraindicated immunotherapy, or after death of the patient.

Briefly, collected blood was transferred into 15 ml Falcon tubes and centrifuged at 1,000 rpm, 4ºC, for 10min (Survall Legend XFR centrifuge with a TX-750 rotor, ThermoFisher Scientific). The plasma fractions were collected, transferred into Eppendorf tubes and additionally centrifuged at 10,000 rpm for 1 min at 4ºC in a bench refrigerated microcentrifuge (1730R model with a GRF-M-m2.0-24 fixed-angle rotor, Gyrozen) to remove residual cells. Plasma samples were aliquoted into new labeled sterile tubes and stored at -80ºC either in the laboratory when further analyses were required, or at the Blood and Tissue Bank of Navarre, Health Department of Navarre, Spain, for prolonged storage (National Biobank Registry Number B.0000735). Cells in Falcon tubes were diluted with PBS (1:1), loaded onto 14 mL Ficoll-Plaque (Cytiva, former GE) and centrifuged at 800 g for 20 min at room temperature (RT). Rotor brakes were removed during the deceleration stage to avoid disruption of the peripheral blood mononuclear cell (PBMC) fraction.

After centrifugation, PBMC rings were transferred into new Falcon tubes and diluted with PBS. Cells were spin down at 300 g RT for 10 min. Contaminating red blood cells (RBC) were burst by an osmotic shock by incubation with 500 µL of red blood lysis buffer (Gibco ACK Lysing Buffer, Thermo Fisher Scientific) for 5 min at RT. Immediately after this incubation, cells were washed twice with PBS and centrifuged at 300 g RT for 10 min. Cells were resuspended in PBS and stained for flow cytometry analyses.

3.4 Flow cytometry

Cells were stained with a combination of specific fluorochrome-conjugated antibodies to label specific lineage and activation markers for the cell types under study. To avoid nonspecific antibody binding, all Fc-binding receptor sites present on the cell surface were blocked by incubation with an anti-Fc receptor antibody in the blocking buffer (PBS, 20% fetal calf serum (FCS), Fc-blocking reagent, Miltenyi Biotec) for 15 min on ice. Following the blocking step, cells were labeled with the antibodies listed in **Table 3** organized in 8 staining groups for each sample. All the antibodies were used at 1:50 dilution unless indicated otherwise. Samples were then analyzed by flow cytometry in a BD FACS Canto II (BD Biosciences). Sample data were acquired with DIVA software and downloaded for detailed analyses by FlowJo software (FlowJo LLC, Ashland). A maximum of 9 parameters can be obtained for each staining using FACS Canto II (side-scatter, forward-scatter and 7 additional fluorochromes).

Table 3 Staining combinations and fluorochromes used in the flow cytometry assay. All the antibodies were used at a 1:50 dilution unless indicated otherwise next to the marker. APC: Allophycocyanin. Cy: Cyanin. FITC: Fluorescein isothiocyanate. PE: Phycoerythrin. PerCP: Peridinin-chlorophyll-protein.

Staining number	Target	Fluorochrome	Provider
ST1	CD11b (1:300)	PerCP-Cy5	TONBO
	CD14	Pacific Blue	TONBO
	CD163	PE	Miltenyi
	CD124	APC	Biolegend
	CD39	APC-Cy7	Miltenyi
ST2	CD11b (1:300)	PerCP-Cy5	TONBO
	CD14	Pacific Blue	TONBO
	TIM-3	FITC	Miltenyi
	LAG-3	PE	Biolegend
	CD33	PE-Cy7	Miltenyi
	VEGFR1	APC	Miltenyi
	CD38	APC-Cy7	Biolegend
ST3	CD11b (1:300)	PerCP-Cy5	TONBO
	CD14	Pacific Blue	TONBO
	CD69	FITC	Biolegend
	CD115	PE	Biolegend
	CD16	PE-Cy7	Miltenyi
	PD-L1	APC	Biolegend
ST4	CD11b (1:300)	PerCP-Cy5	TONBO
	CD14	Pacific Blue	TONBO
	PD-1	FITC	Biolegend
	CD86	PE	TONBO
	CD62L	APC	Miltenyi
	CD10	APC-Cy7	Miltenyi
ST5	CD11b (1:300)	PerCP-Cy5	TONBO
	CD14	Pacific Blue	TONBO
	C3aR (1:200)	PE	Biolegend
	C5aR	PE-Cy7	Miltenyi
	CD64 (1:100)	APC	Biolegend
	CD66b	APC-Cy7	Miltenyi
ST6	CD11b (1:300)	PerCP-Cy5	TONBO
	CD14	Pacific Blue	TONBO
	HLA-DR (1;25)	FITC	TONBO
	CCR2	PE	Miltenyi
	CD32 (1:500)	PE-Cy7	Biolegend
	CCR7	APC	Biolegend
	CD36 (1:500)	APC-Cy7	Miltenyi
ST7	CD11b (1:300)	PerCP-Cy5	TONBO
	CD14	Pacific Blue	TONBO
	CD206	FITC	Biolegend
	CD19	PE	TONBO
	CD56	PE-Cy7	Miltenyi
	CD116	APC	Miltenyi
	CD66b	APC-Cy7	Miltenyi
ST8	CD11b (1:300)	PerCP-Cy5	TONBO
	CD14	Pacific Blue	TONBO
	CD4	FITC	Biolegend
	CD27	PE	TONBO
	CD28	PE-Cy7	TONBO
	CD3	APC	Miltenyi
	CD8	APC-Cy7	Biolegend

3.5 Analysis of soluble factors in plasma

A selection of soluble factors that could be implicated in systemic immune responses was carried out. The concentration in plasma of these selected proteins was quantified by Luminex technology (Milliplex MAP bead-based assay, reading with MAGPIX Instrument, Luminex), which is schematically represented in **Figure 4**. Briefly, plasma samples were incubated with a set of antibodies specific for the factors of interest (**Table 4**) labeled with dyed polystyrene microspheres . Microspheres were then immobilized with magnetic beads to prevent removal during washing steps.

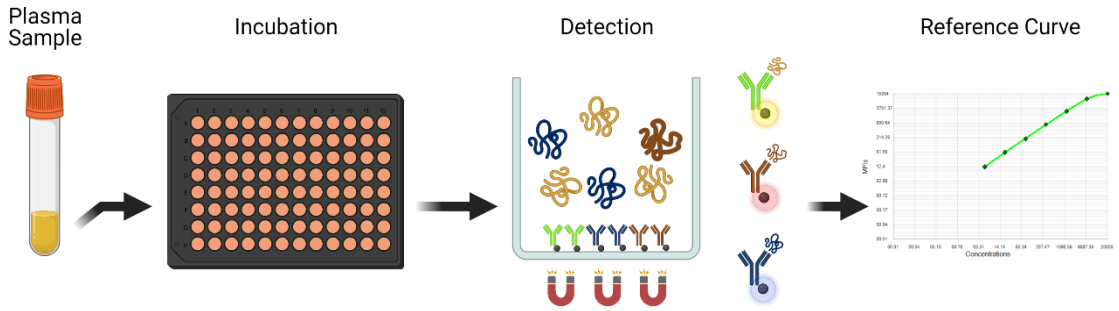

Figure 4 Luminex assay principles and procedure. Samples were incubated in 96-well plates with a set of pre-specified antibodies labelled with dyed polystyrene microspheres with magnetic properties to avoid removal during washing.

After an overnight incubation at 4ºC, samples were analyzed in a Luminex instrument and mean fluorescent intensities (MFIs) were quantified for each factor. Background fluorescence (matrix diluent) was removed and the net MFI was calculated by comparison with standards of known concentrations with the xPonent software algorithm. Data from the standards were used to construct a regression equation, and molecule concentrations in pg/mL were calculated for each of the factors of interest. Protein concentrations below the range of detection were not considered for further analyses.

Table 4 Protein panels used in the Multiplex immunoassays

Milliplex Human Immuno-Oncology Checkpoint Protein Panel 1	Milliplex MAP – Human Cytokine / Chemokine Panel
CD40 LAG-3 PD-1 CTLA-4 CD80 / B7:1 CD86 / B7:2 PD-L1 ICOS BTLA CD27 CD28 TIM-3 HVEM GITR GITRL TLR-2	FGF-2 Eotaxin G-CSF GM-CSF Fraktalkine sCD40-L IFN-α2 IL-10 MCP-3 IL-12p70 IL-15 IIL-1Ra L-9 IL-3 IL-6 IL-7 IL-8 IP-10 MCP-1 MIP-1a MIP-1b VEGF

3.6 Statistics

Data were analyzed by Student's t-test or ANOVA if normally distributed, or by Mann–Whitney U test or Kruskal–Wallis test for data not normally distributed or with intrinsic variability. Friedman non-parametric test was performed for repeated measures across multiple groups. Log-rank test and Cox-proportional hazards models were used in OS and PFS analyses. Survival results according to patient groups were represented in Kaplan-Meier plots.

4. Results

4.1 Characteristics of the study cohort

The patients included in the study had received a first line of chemotherapy for metastatic lung disease before progression, for which immunotherapy was started. The detailed characteristics of the cohort before the start of immune checkpoint blockade (ICB) treatments are shown in **Table 5**. The cohort includes non-small cell lung cancer (NSCLC) patients, with a predominance of male (72.9%) subjects with a prior history of heavy smoking. Overall, the cohort of patients did not include those with tumors containing targetable driver mutations, with the exception of two subjects, one carrying an EGFR mutation and another patient with a ROS1 rearrangement. These patients had been previously pretreated with targeted therapies and did not respond to these treatments. Another patient had a BRAF-mutation in the tumor that initially responded to treatment with ICB but was lost to follow-up after disease progression. Approximately two-fifths of the patients had received prior radiotherapy, either in combination with chemotherapy (platinum-based compounds plus vinorelbine) for the treatment of their unresectable primary tumor, or only radiotherapy for management of metastatic lesions.

Table 5. Characteristics of the cohort of patients with the distribution of descriptive variables of clinical interest, including immune-related adverse events.

Patient characteristic	N = 87, (%)
Sex	
Male	64 (73.6)
Female	23 (26.4)
Age (years)	
18-40	1 (1.1)
41-50	4 (4.6)
51-60	19 (21.8)
61-70	42 (48.3)
71-80	18 (20.7)
≥ 80	3 (3.4)
Performance Status (ECOG)	
0-1	71 (81.6)
2-4	16 (18.4)
Smoking History	80 (92.0)

Prior Radiotherapy	41 (47.2)
Prior Lines of Systemic Therapy	
1 Line	69 (79.3)
≥ 2 Lines	18 (20.7)
Histology	
Squamous	25 (28.7)
Adenocarcinoma	60 (71.3)
LCNEC	1 (1.1)
Sarcomatoid	1 (1.1)
No. of Metastatic Locations	
< 3	24 (27.6)
≥ 3	63 (72.6)
Liver Metastasis	27 (31.0)
Therapeutic Driver Mutation	
EGFR	1 (1.1)
ROS1	1 (1.1)
BRAF	1 (1.1)
None	84 (96.6)
Tumor PD-L1 Expression	
0%	31 (35.6)
1-4%	10 (11.5)
5-49%	19 (21.8)
≥ 50%	12 (13.8)
Unknown	15 (17.2)
Drug	
Nivolumab (AntiPD-1)	41 (47.1)
Pembrolizumab (AntiPD-1)	10 (11.5)
Atezolizumab (AntiPD-L1)	36 (41.4)
Gustave Roussy Immune (GRIm) Score	
0-1	35 (40.2)
2-3	12 (13.8)
Not available	40 (46.0)
Lung Immune Prognostic Index (LIPI)	
Good	9 (10.3)
Intermediate	21 (24.1)
Poor	18 (20.7)
Not Available	39 (44.8)
Radiological Response	
PR	20 (23.0)
SD	7 (8.0)
PD	51 (58.6)
Not evaluable	9 (10.3)
Disease Control Rate (DCR) at 6 months	
Yes	24 (27.6)
No	63 (72.4)
Immune-related adverse events (IRAEs)	
G1-2	19 (22.1)
G3-4	1 (1.2)
None	66 (76.7)

The median progression-free survival (PFS) and overall survival (OS) of the cohort were 65 days (range, 8-1136 days) and 269 days (range, 11-1169 days), respectively. As expected, radiological progression was related to the subsequent death of the patients, with a median post-progression disease (post-PD) survival of 116 days. iRECIST criteria, an adaptation of the previous RECIST1.1criteria (Eisenhauer et al., 2009; Seymour et al., 2017), were used to classify radiological responses. Partial response (PR) was defined as a decrease of at least 30% of the sum of the target lesion (TL) diameters. Stable disease (SD) was defined as changes in the sum of the TL diameters between an increase of 20% and a decrease of 30% without the appearance of new lesions. Hence, disease control rate (DCR) was considered the sum of PR and SD patients. Of note, iRECIST criteria consider disease progression as a confirmed target lesion increase in a second radiological evaluation: before this re-evaluation is performed, patients are classified as unconfirmed PD (iUPD). However, in our cohort this was the case of only one patient with a transient target lesion increase that was compatible with pseudoprogression. A schematic representation of the study design and overall outcomes is presented in **Figure 5.**

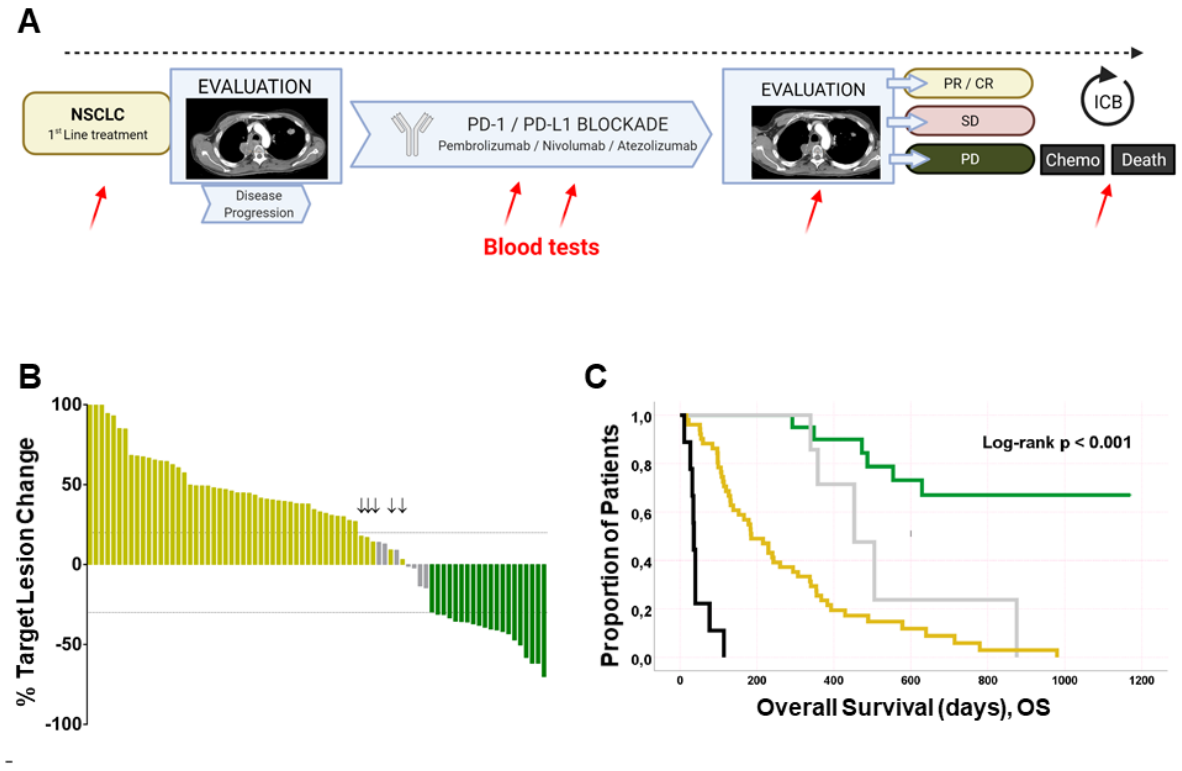

Figure 5. Study design and overall outcomes (**A**) An overview of the study is schematically presented. Each step of the study is shown within boxes together with flow arrows. All patients included in the study had received platinum-based chemotherapy as a first line treatment for their metastatic disease. Quantification of blood cell populations were recorded from the electronic medical record (EMR) at several time-points: disease diagnosis, ICB start, after the first two immunotherapy cycles, at CT evaluation and prior to death (in case of progression). (**B**) Waterfall plot presenting radiological response distribution across the cohort according to RECIST1.1 criteria. Green, patients classified as objective responders; Ochre, patients classified as progressors; Gray, patients classified as having stable disease. Patients indicated with an arrow are patients whose target lesion change did not meet PD criteria but presented new non-target lesions. (**C**) Kaplan-Meyer survival plot for the indicated response groups of patients according to radiological evaluation. PD, progressive disease in orange; SD, stable disease in grey; PR, partial response in green. Non evaluable patients show the worse prognosis and are represented in black.

Thus, 20 patients (23.0%) met the criteria for partial response (PR) in the first radiological evaluation, 7 patients were classified as having stable disease (SD, 8.0%), and progressive disease (PD) was observed in 51 patients (58.6%). Disease control as defined by the sum of PR and SD was observed in 27 patients following immunotherapy. Finally, 9 patients were classified as radiologically non-evaluable due to non-measurable disease or the absence of radiological control. Non-evaluable patients conferred the worst prognosis in our cohort since this

group includes patients that died before radiological assessment could be performed.

Safety assessment was also an important concern in the study. Asthenia was the most significant side-effect, which occurred in 5 patients, followed by thyroiditis (4), pneumonitis (3) and colitis (2). Immune-related toxicity in the form of G3 colitis led to interruption of ICB in one patient and initiation of corticosteroid treatment. Other less-frequent IRAEs such as pericarditis, nephritis, hepatitis and arthritis were observed in individual cases. An association between IRAE diagnosis and treatment response was not found ($p = 0.175$), but survival was improved in patients with irAEs (median OS 429 vs 240 days, log-rank test $p = 0.042$).

Due to the incomplete availability of lactate dehydrogenase (LDH) baseline results in our cohort, the Lung Immune Prognostic Index [LIPI] (Mezquita et al., 2018) could only be calculated in 48 patients. This index is based on the detection of increased LDH and derived neutrophil to lymphocyte ratio (dNLR) above 6, to classify patients between good, intermediate or poor prognostic groups according to the presence or none, one or two factors. Among these, 18.8% had a good prognosis, 43.8% were included in the intermediate prognosis group, while 37.5% of the patients had poor prognosis. We also calculated the Gustave Roussy Immune (GRIm) score in 47 patients (Bigot et al., 2017). The difference lies in the introduction of low serum albumin (<3.5g/dL) prior to anti-PD-1/PD-L1 treatment. Most of the patients (74.5%) had none or one factor, while a quarter of those evaluable patients presented 2 or 3 factors.

Univariant analysis of the LIPI score was not a predictor of survival, since in our cohort patients presenting 1 factor (intermediate prognosis) had significantly shorter survival, in comparison with the presence of none or 2 factors. However, patients in the good prognostic group presented the longest PFS (median PFS 186 days vs 44 and 76 in the intermediate and poor prognostic groups, log-rank test $p = 0.038$). These results might be influenced by the burden of prior chemotherapy lines. We observed that patients with GRIm scores above 2

presented a shortened survival although not statistically significant (median OS 112 vs 358 days, log-rank test p = 0.665).

4.2 Clinical determinants of response

4.2.1 ABSOLUTE COUNTS OF SYSTEMIC BLOOD IMMUNE CELL POPULATIONS AND DISEASE EVOLUTION

The total counts of systemic immune cell blood populations and their deviation from normality have been previously used as indicator biomarkers of different clinical responses to chemotherapy and radiotherapy. Increased numbers of selected immune cell populations have been previously used as a predictive factor in lung, prostate, and colon cancer patients (Sylman et al., 2018). One study showed that absolute monocyte counts above 450/µL were an independent negative predictive factor correlating with shorter OS (Lin et al., 2014). Correspondingly, decreased absolute numbers of lymphocytes from normality have been also correlated with shortened OS (Zhao et al., 2020).

Based on all the previous evidence, quantification of immune cell blood populations retrieved from the electronic medical record (EMR) were used to find out if these values had prognostic or predictive value for OS and PFS in our ICB-treated cohort. EMR data were collected at different time points during treatment, starting at disease diagnosis and before the start of ICB therapies, during the first two immunotherapy treatment cycles, at re-evaluation by CT scan and prior to the death of the patient whenever these data were available.

Results are summarized in **Figure 6**, with the focus on the main cell lineages identified by routine blood analyses, with previous evidence of correlation with prognosis. In our cohort, we observed increased absolute neutrophil counts in progressors with a notable increase in the last EMR, suggestive of a sudden increase of neutrophils before *exitus*. These results suggested that increased neutrophil counts could be associated with disease progression. It has been previously published that administration of corticosteroids may cause neutrophilia

by induction of myelopoiesis, inhibition of neutrophil apoptosis and detachment from the endothelial surface (Ronchetti et al., 2018). To find out whether neutrophil count increase was in fact related to disease progression, or whether it it constituted instead an artifact from corticosteroid treatments, we evaluated neutrophil increase in corticosteroid-treated *versus* non-treated patients. There were no significant differences between the two groups (mean 12811 neutrophils/µL in the corticosteroid-receiving group vs 12276 neutrophils/µL, Student's t test p = 0.792). Therefore, we concluded that increase in neutrophil counts could not be justified by corticosteroid treatment in our cohort of patients. No significant changes in monocyte or platelets counts were observed using data from routine clinical blood analyses (**Figure 6**).

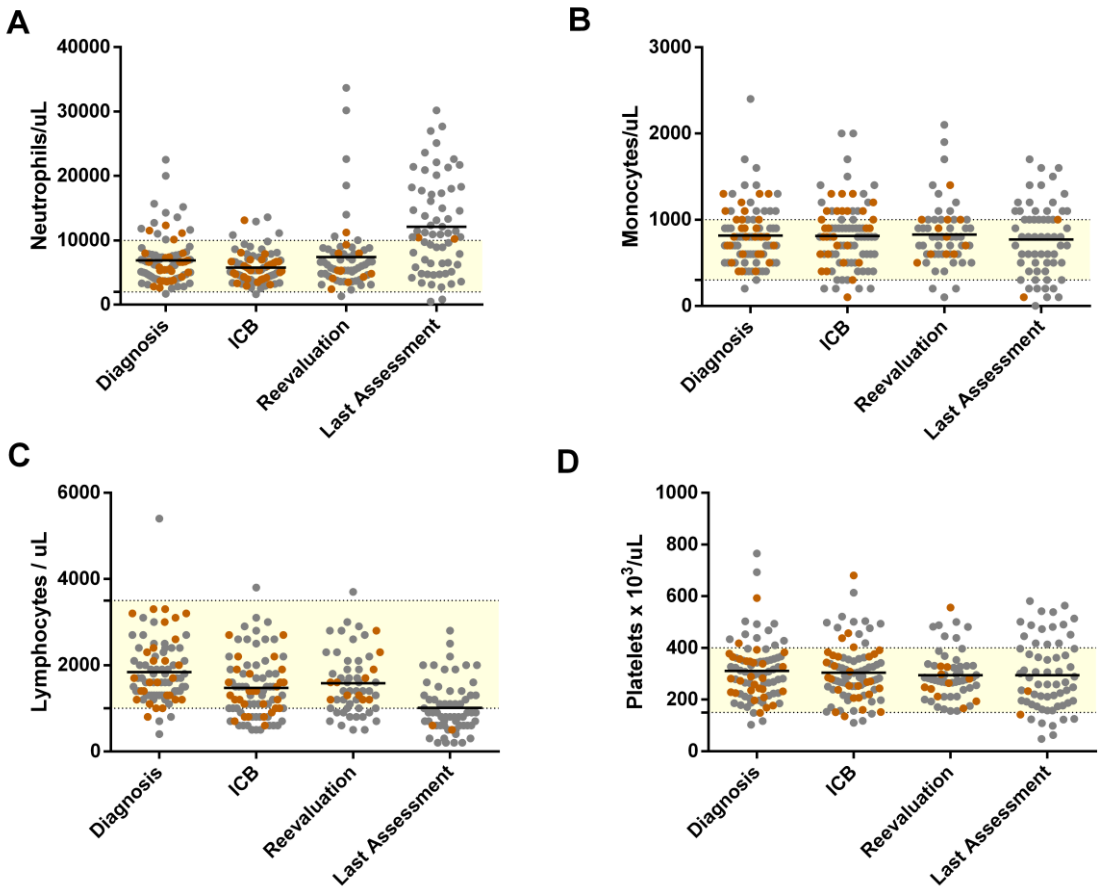

Figure 6 Quantification of major immune cell lineages in peripheral blood populations along disease evolution in NSCLC as per EMR data. Absolute cell counts are shown for (**A**) neutrophils, **(B)** monocytes, **(C)** lymphocytes and **(D)** platelets. The points of analyses are indicated in the graphs: diagnosis, ICB (before ICB start), re-evaluation (first CT after ICB administration), and last available assessment before death. Brown dots, data from patients classified as objective responders at the first CT evaluation. Gray, data from patients classified as non-objective responders or progressors after an initial response. Yellow shading represents the upper-lower limits of reference normal values in healthy population.

Interestingly, there was a trend for progressive lymphopenia along disease span that was accelerated in patients with progressive disease shortly before death. This might be influenced by the administration of further lines of chemotherapy, given after progression to immunotherapies and that were administered to 41 patients (47.1%). The most commonly administered chemotherapy drug was docetaxel (28 patients). However, in our cohort there were no statistically significant differences in mean lymphocyte count when comparing post-progression chemotherapy groups (925 lymphocytes/µL in the chemotherapy-receiving group *vs* 1110 in patients who did not receive further lines of treatment after ICB termination, Student's t test p = 0.222).

Analyses from EMR data did not uncover any significant differences in monocyte and platelet numbers between responders and progressors. Of note, some patients died at home or in palliative care institutions. Therefore, the data prior to their decease were not available for analysis. A patient with basal lymphocytosis due to chronic lymphocytic leukemia was also excluded from the analyses.

4.2.2 DYNAMIC CHANGES OF SYSTEMIC IMMUNE CELL BLOOD POPULATIONS AND ASSOCIATION WITH RESPONSE

To determine whether longitudinal data from the EMR along the treatment could be used as indicators of responses, quantification of the main immune cell lineages in peripheral blood was plotted separately for responders and progressors, as identified by radiological response (**Figure 7)**.

Neutrophil counts at disease diagnosis were increased in progressors compared to ICB-responding patients but without reaching statistical significance (mean 7194 *vs* 6246 neutrophils/µL, Student's t test p = 0.384). The analysis over the course of the disease (at disease diagnosis, at ICB start, at re-evaluation and prior to death) revealed a statistically significant difference between re-evaluation and the last available neutrophil concentration result (ANOVA test for repeated measures with Tukey's pairwise comparison p < 0.001), but without reaching

statistical significance at the early stages of the disease. This is shown in **Figure 7A, B**.

No statistical or clinically significant differences were observed in dynamic changes in monocyte or platelet numbers between progressors and responders from disease diagnosis to treatment initiation, as assessed by the data obtained from the EMR (**Figure 7C, D, E, F**).

Interestingly, there were differences in absolute lymphocyte counts between diagnosis and ICB start, since responders showed elevated numbers at the time of diagnosis without reaching statistical significance (mean 1805 lymphocytes/µL in progressors *vs* 2436 in responders Student t test p = 0.107). Again, longitudinal data along disease evolution showed a marked decrease in patients at the start of ICB therapies (1476 and 1490 lymphocytes/ µL in progressors and responders, respectively) that was maintained prior to patient's death but without statistical significance (1748 lymphocytes/ µL in progressors, 1645 in responders, Tukey's pairwise test after ANOVA for repeated measures between diagnosis and ICB, p = 0.871) (**Figure 7G, H**).

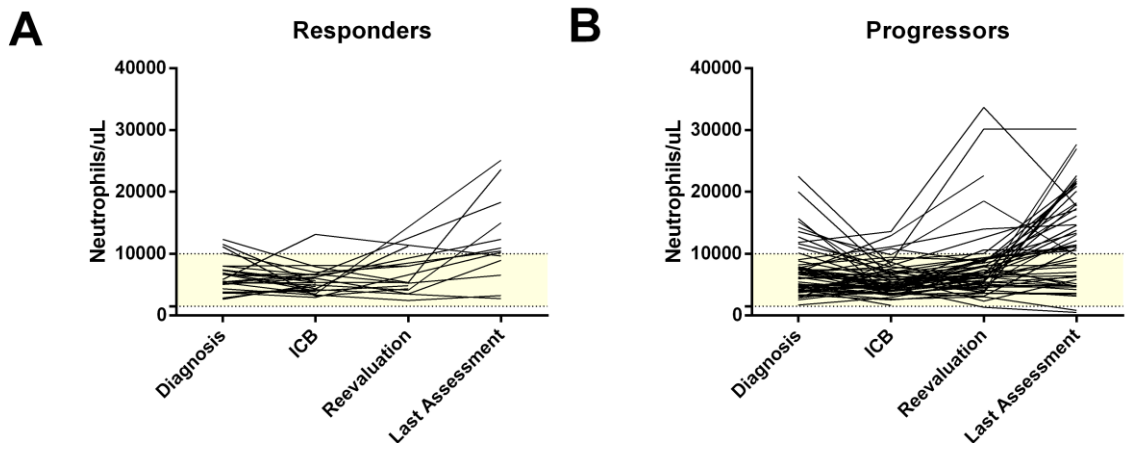

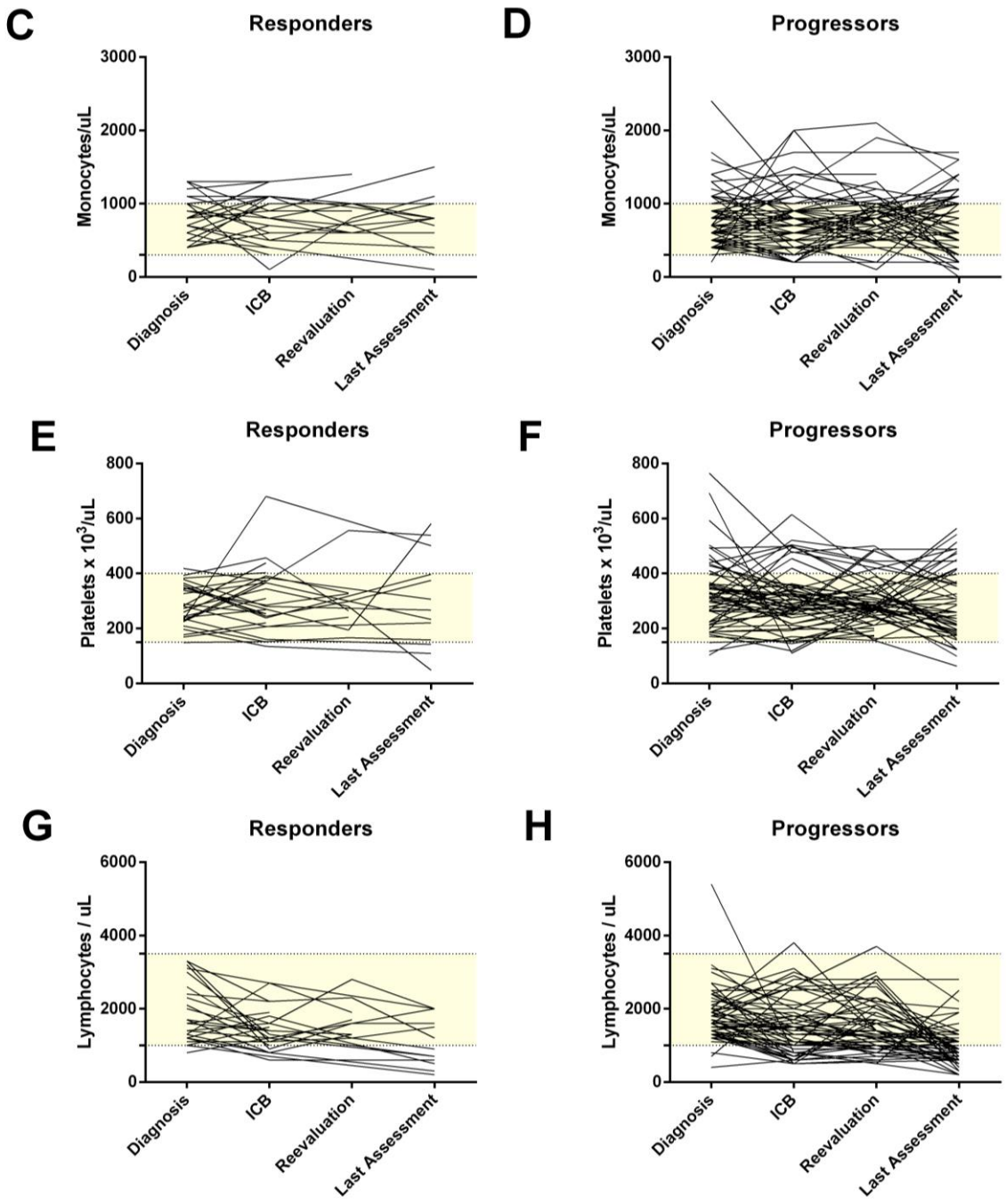

Figure 7 Dynamic changes of the indicated immune cell populations in peripheral blood. Data are shown as absolute counts per μL, within the indicated groups as identified according to radiological response. Data were obtained at four different time points, as indicated. **(A)**, **(B)** neutrophils in responders and progressors. **(C)**, **(D)** monocytes in responders and progressors. **(E)**, **(F)** lymphocytes in responders and progressors. **(G)**, **(H)** platelets in responders and progressors. Each line corresponds to each individual patient. Reference values in healthy population are shaded in yellow.

4.2.3 CORRELATION OF RELATIVE INDICATORS OF IMMUNE CELL BLOOD POPULATIONS WITH CLINICAL RESPONSES: NLR, MLR, PLR

Numerous studies have correlated neutrophil-to-lymphocyte (NLR), monocyte-to-lymphocyte (MLR) and platelet-to-lymphocyte ratios (PLR) to response to different anti-cancer treatments (Liu et al., 2019). An elevated number of neutrophils as quantified by NLR was correlated with shortened survival in lung cancer patients in several published meta-analyses with hazard ratios (HR) for OS) ranging from 1.43 to 1.70 (Gu et al., 2015; Peng et al., 2015; Yang et al., 2016; Yin et al., 2015; Zhao et al., 2015). This phenomenon has not only been addressed in lung cancer but in other oncologic malignancies as well (Templeton et al., 2014). As some of the counts from immune cell blood populations in our study cohort showed subtle changes along disease evolution, which could correlate with clinical responses, we further analyzed the relative ratios of these populations at the start and during the first 2 treatment cycles. We hypothesized that specific dynamics of these relative indicators across subgroups could show better correlates with response to treatment.

However, only small differences between response groups for either MLR or PLR were observed, without reaching statistical significance (data not shown). In contrast, there were significant differences in neutrophil counts between responders and non-responders, in agreement to previous studies, with an non-significant trend for NLR increase in non-responders. Indeed, there was a significant worsening in OS in patients that presented an NLR increase above 50% between treatment initiation and the first cycle of therapy **(Figure 8)**.

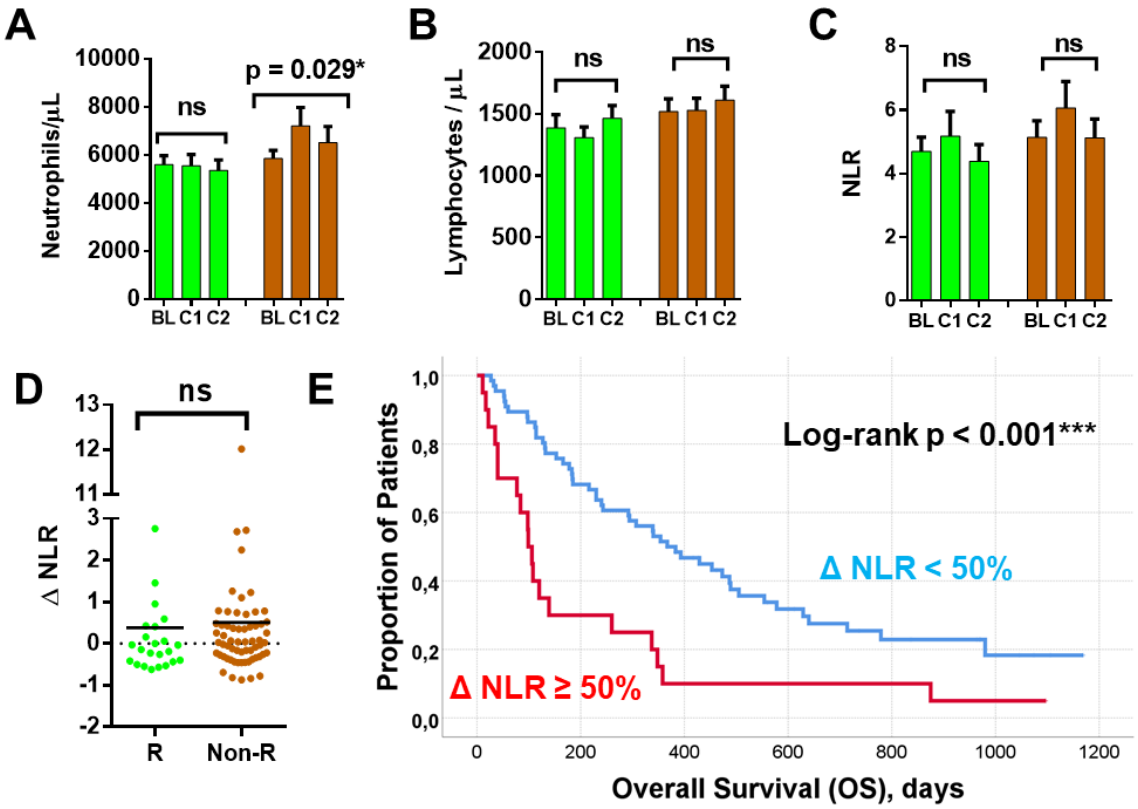

Figure 8. Neutrophil **(A)** and lymphocyte **(B)** counts in responders and non-responders to ICB**.** (**C**) Neutrophil-to-lymphocyte ratio. Non-responders are shown in brown, and responders in green; Baseline ("BL") indicates the sample collected before ICB; "C1" shows data obtained before the 2nd cycle of ICB; "C2" shows data obtained before the 3rd cycle of ICB. (**D**) Relative differences in NLR from baseline to C2 (ΔNLR) in responders (R) and non-responders (Non-R). (**E)** Kaplan-Meyer plot of OS stratifying patients according to neutrophil-to-lymphocyte ratio (NLR) increase between cycles 1 and 2. Increase ≥ 50% red; increase < 50% blue. Statistical differences were evaluated by two-way ANOVA and log rank tests.

4.2.4 NUTRITIONAL STATUS AND CLINICAL RESPONSES TO ICB

Poor nutritional status is a multifactorial state that includes poor caloric intake or inadequate dietary patterns. Total cholesterol and albumin values can be used as indirect markers of nutritional status (Cabrerizo et al., 2015; Keller, 2019). Some studies suggest that serum cholesterol concentrations have prognostic value in lung cancer (Zwickl et al., 2020). Indeed, hypocholesterolemia has previously been related to risk of death in chronic conditions (Iseki et al., 2002). Serum albumin concentration has been related to malnutrition, cachexia and a poor overall well-being (Trestini et al., 2020).

To find out whether cholesterol or albumin values were associated with clinical responses to ICB treatment, cholesterol and albumin concentrations were quantified prior to the start of ICB therapies whenever data were available. No significant differences were found between responders and non-responders (**Figure 9**). The mean total cholesterol in responders was 189 mg/dL *vs* 187 mg/dL in non-responders (p = 0.383). Mean serum albumin concentration was 38.6 g/L in both groups (p = 0.952).

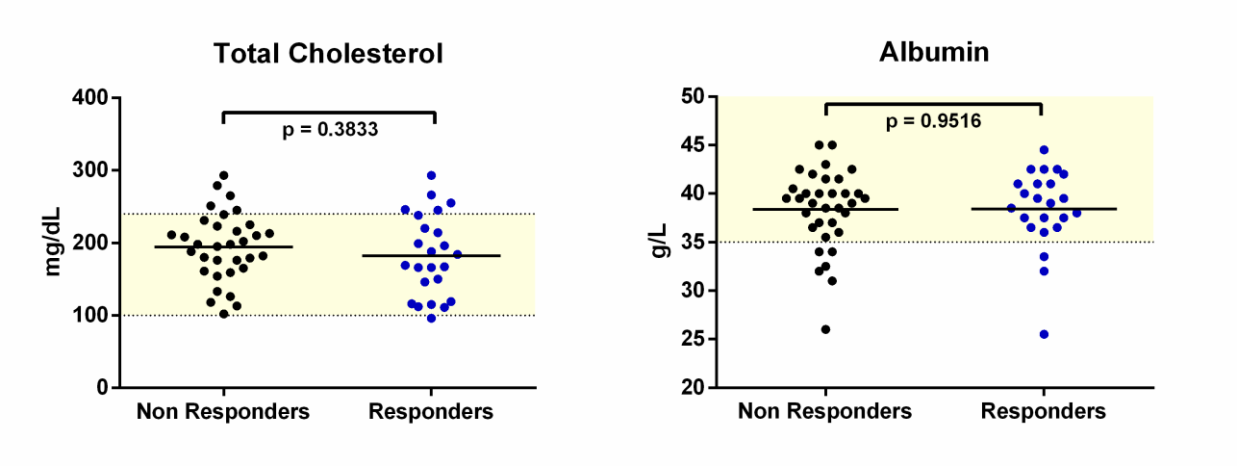

Figure 9 Cholesterol and albumin serum concentrations in responders and non-responders. The left dot-plot shows cholesterol concentrations in non-responders and responders, as indicated. The right dot plot shows albumin concentrations in non-responders and responders, as indicated. Reference values in healthy population are shaded in yellow. Statistical comparisons were carried out by unpaired t tests.

Obesity has been recently reported to favor an immunosuppressive tumor microenvironment (Ringel et al., 2020). In our cohort, differences in body mass index were also studied, without finding any significant difference between response groups. However, patients with similar anthropometric measures can have different body compositions in terms of relative lean (i.e. muscle) mass. Hence, we also studied whether body composition and relative quantities of lean body mass in patients could be related to ICB responses. The surface occupied by muscle was measured in a cross-sectional image at the L3 lumbar vertebra and this value was divided by patient height as an indication of sarcopenia, which is an independent negative prognostic factor in the preoperative management of early-stage NSCLC (Shoji et al., 2017). Furthermore, in a recent study the authors

found the median OS to be only 3.1 months if skeletal muscle mass was classified as low in a cohort of 23 patients treated with nivolumab, but without reaching statistical significance. In this study, a threshold of 41 cm^2/m^2 was used in women, 42 cm^2/m^2 in men with BMI < 25, and 53 cm^2/m^2 in men with BMI ≥ 25 (Cortellini et al., 2019).

In our cohort no differences were found in the total muscle area index (TMAI) between responding (mean TMAI = 42.9 cm^2/m^2) and non-responding patients (41.1 cm^2/m^2, p = 0.267) using these thresholds (**Figure 10**). Although the threshold to define sarcopenia is gender-specific, no differences were found in survival according to the presence of sarcopenia, which affected 64 patients (73.6%).

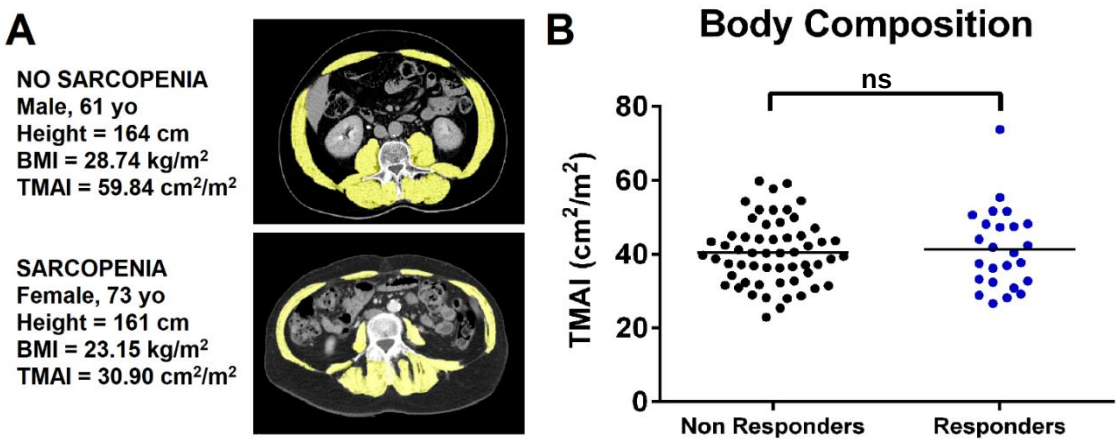

Figure 10 Assessment of body composition in our cohort and association with clinical responses. (**A**) An illustrative example of muscle surface in two patients measured by a coronal CT-scan image at the L3 vertebra, for identification of sarcopenia. (**B**) The dot plot represents total muscle area index (TMAI) (cm^2/m^2) in 81 patients classified according to their radiological response into non-responders or responders as indicated in the graph. Data from each individual patient is represented by a dot. The differences were not statistically significant (unpaired t test).

4.3 Analysis of systemic immune cell blood populations using high-dimensional flow cytometry

EMR data provide quantification of main immune cell lineages in peripheral blood, but they do not provide sufficiently detailed information on the heterogeneity of immune cell subsets according to lineage, differentiation status and activation

phenotypes. Therefore, we hypothesized that high-dimensional flow cytometry applied to the identification of peripheral blood immune cells would provide sufficient resolution to quantify diversity of immune cell types and activation status. These experiments were carried out using multiple panels consisting of combinations of marker-specific antibodies by flow cytometry. This procedure allows the simultaneous use of multiple makers to precisely identify the cell populations of interest (**Table 6**). The procedure and the list of antibodies used are shown in materials and methods.

4.3.1. ASSOCIATION OF MYELOID CELL POPULATIONS QUANTIFIED BY HIGH-DIMENSIONAL FLOW CYTOMETRY WITH CLINICAL RESPONSES TO ICB THERAPIES

Although not exclusively present in the myeloid lineage, the CD11b marker is predominantly expressed by myeloid cells. Therefore, all cell quantifications were first calculated within CD11b+ cells. High-dimensional flow cytometry also allowed the proper identification of monocytic and granulocytic myeloid-derived suppressor cells (M-MDSC, G-MDSC), which are not discriminated by standard clinical blood analyses.

Table 6 Surface markers used in immunophenotyping of myeloid populations in PBMCs.

Cell	Markers
Monocytes	$CD11b^{+}$ $CD14^{+}$ HLA-DR^{+} $CD36^{hi}$ $CD33^{+}$ $CSF1R^{+}$
Neutrophils	$CD11b^{+}$ $CD14^{+}$ $CD66b^{+}$ HLA-DR^{+} $CD33^{+}$ $CSF1R^{+}$
M-MDSC	$CD11b^{+}$ $CD14^{+}$ HLA-$DR^{-/lo}$ $CD36^{lo}$ $CD33^{+}$ $CSF1R^{+}$
G-MDSC	$CD11b^{+}$ $CD14^{-}$ $CD66B^{+}$ HLA-DR^{-} $CD33^{low}$ $CSF1R^{-}$

The relative percentage of the main myeloid populations as defined in **Table 6** was calculated in peripheral blood samples for all patients before the start of ICB immunotherapies. Percentages of myeloid subsets were then plotted as a

function of change in tumor volume by radiological assessment (**Figure 11**) and of survival (**Figure 12**).

We evaluated the impact of neutrophilic $CD66b^+$ cells, which included both classical neutrophils and granulocytic MDSCs. Increases in these populations have been previously correlated with poor prognosis in cancer (de Goeje et al., 2015; Wang et al., 2018a). Overall, patients that responded to ICB therapies showed low percentages of neutrophils within $CD11b^+$ cells. In our cohort, there were only two responders with relative quantities above 25% (**Figure 11**). Hence, we calculated the impact of neutrophil values over survival using 25% as a threshold to stratify patients (**Figure 12**). Although statistical significance in survival was not reached by a log-rank test, the difference was close to significance ($p = 0.053$). In agreement with this result, we observed clinically meaningful differences within the neutrophil-high group (median survival 184 days) *vs* the neutrophil-low population (median survival 339 days).

Responding patients had elevated percentages of monocytes compared to non-responders (49 vs 26%, Student's t test $p = 0.004$, **Figure 11**). In particular, all progressing patients but one had monocyte levels below 60%. A threshold value above 25% of relative abundance of monocytes prior to the start of ICB therapies was established to stratify patients. This stratification clearly identified prognostic groups as assessed by Kaplan-Meier survival plots. Patients with monocyte percentages above 25% had a median survival of 609 days while patients with values below this threshold had a median survival of only 230 days. This difference was statistically significant (log-rank test $p<0.001$, **Figure 12**).

Then, the influence of granulocytic MDSCs was studied. It has to be noted that standard clinical blood analyses cannot discriminate neutrophils from G-MDSCs. Interestingly, patients that showed rapid increments in tumor volume during immunotherapy were those that had elevated proportions of G-MDSCs before the start of immunotherapies (**Figure 11**). Nevertheless, there were exceptions, with one patient with stable disease who had over 90% G-MDSCs and maintained this clinical response. However, disease was stable for over a short period of time in

this particular case. Only one partial response was observed in patients with G-MDSCs above 25%. However, the percentage of G-MDSCs before the start of immunotherapies did not seem to influence prognosis, as differences in survival were non-significant between groups stratified according to the selected threshold (median OS was 339 days with G-MDSC > 25%, while patients stratified as G-MDSC < 25% had a median survival of 240 days).

Another major immunosuppressive myeloid population that negatively correlates with responses corresponds to monocytic MDSCs. However, M-MDSCs cannot be discriminated from classical monocytes by standard clinical blood analyses. Therefore, the relative abundance of M-MDSCs within $CD11b^+$ cells identified by high-dimensional flow cytometry was evaluated over clinical responses to ICB immunotherapies. No significant differences in survival were found in patients stratified according to 25% of M-MDSCs before the start of immunotherapies (median OS 337 vs 294 days, p = 0.794).

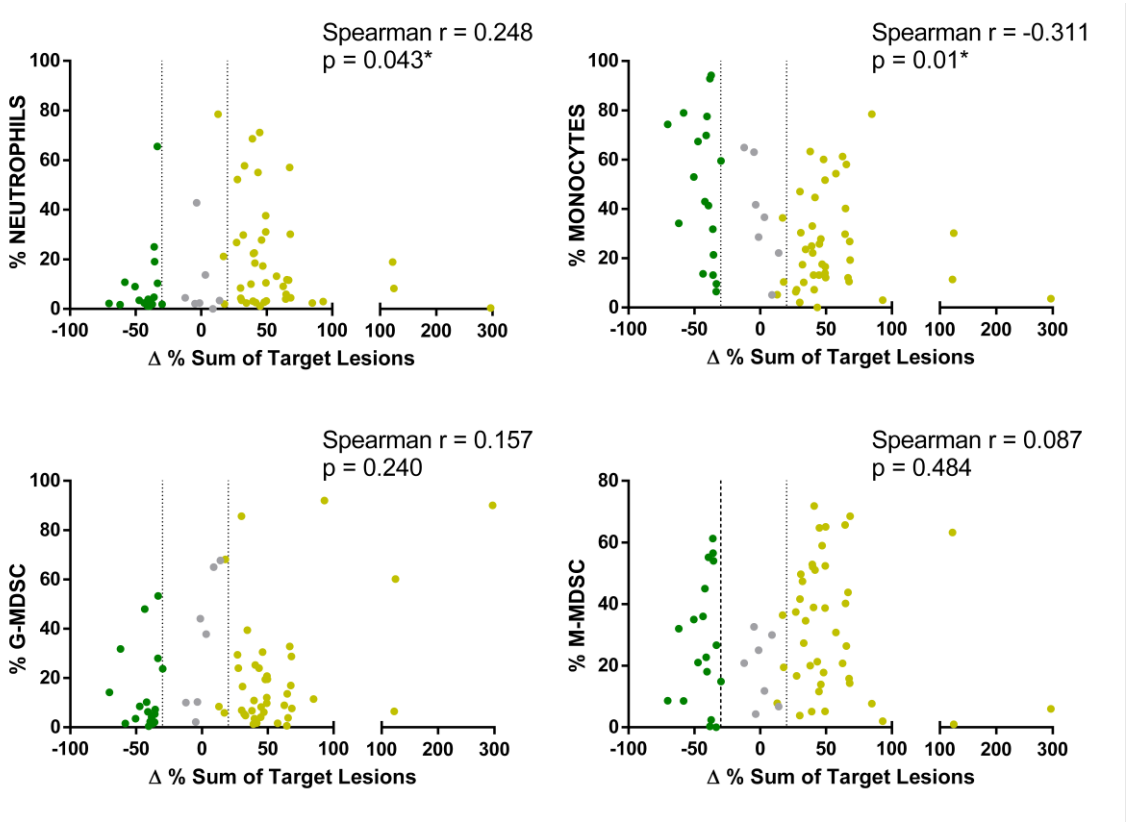

Figure 11. Correlation of the relative percentage of main myeloid cell populations with tumor progression**.** The dot plots show for each patient the percentage of the indicated myeloid cell subset and the changes in the sum of target lesions. Patients are classified as responders (green), stable disease (grey) and progressors (ocher). Of note, patients without a radiological evaluation are not represented in the figure since the differences in lesion diameter could not be assessed.

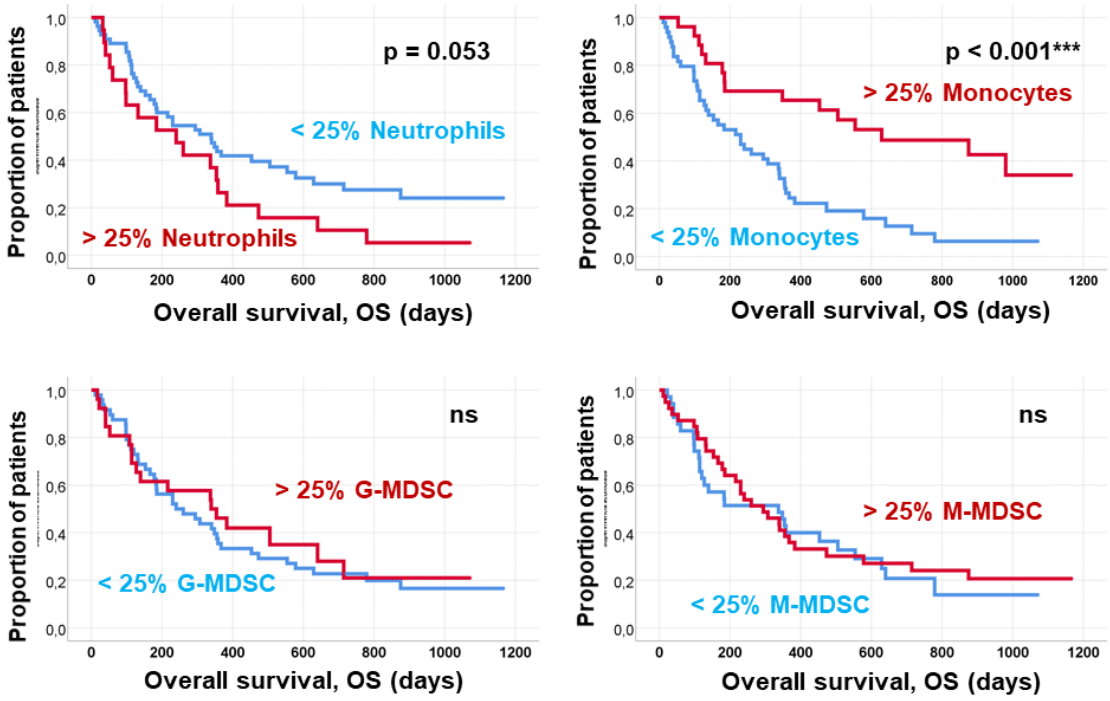

Figure 12 Overall survival in patient cohorts stratified by the percentage of myeloid cell populations before the start of ICB therapies. Kaplan-Meier survival plots of patients stratified by the indicated myeloid cell population using the threshold values of percentage shown within the figure. Monocyte predominance above 25% shows statistically significant differences between the two groups as a positive factor. Log-rank tests were carried out to compare groups. Red, patients with percentages above the selected threshold; Blue, patients with percentages below the selected threshold.

Next, we considered the relative contribution of the four myeloid cell subsets as defined in **Table 6** by calculating the relative percentage between them (% monocytes + % neutrophils + % M-MDSC + % G-MDSC = 100). The relative percentages of the four main myeloid subsets as defined in **Table 6** were plotted (**Figure 13**). The myeloid cell compartment of responders was generally dominated by elevated quantities of monocytes and M-MDSCs, while progressors showed more heterogeneous compositions but with a clear overall abundance of neutrophils and G-MDSCs. Patients with disease classified as stable had intermediate compositions of myeloid cell subsets, usually with an expansion of the MDSC compartment in detriment of monocytes.

The mean relative proportion of monocytes in patients achieving a partial response was 49%, while it was lower in patients with SD (37%), and non-responders (25%). One-way ANOVA followed by Tukey post-hoc comparisons

showed that this difference was statistically significant in partial responders as compared with non-responders (p = 0.002) but not with stable disease patients. The subgroup of patients without a radiological evaluation had a mean value of only 13%. We performed the same analysis using the proportion of the other populations without achieving statistical significance, although non responding patients had twice as many neutrophils as responders (20.7 vs 9.3%, p = 0.199). These results confirmed that an elevation of the monocytic compartment within all myeloid subsets was a defining profile of responders before the start of ICB immunotherapies.

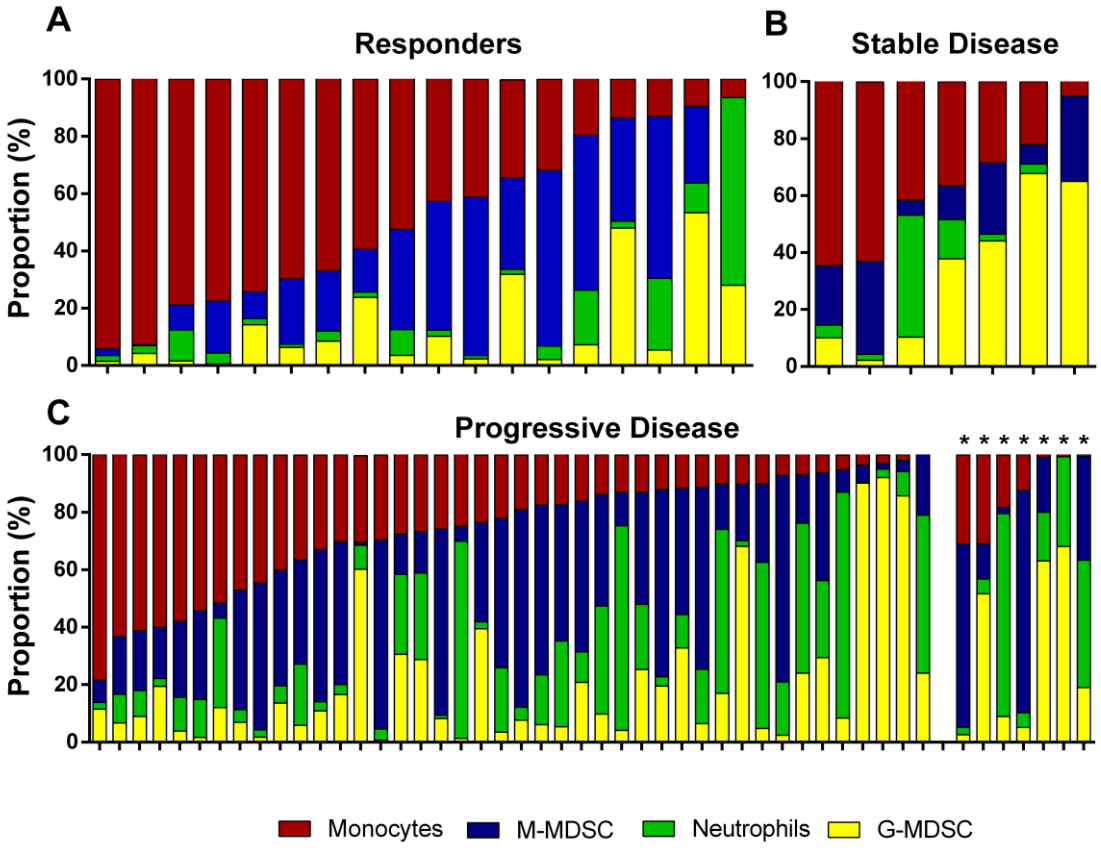

Figure 13 Relative compositions of the myeloid compartment in patients before the start of immunotherapies (n = 74). **(A)** The bar graph represents the relative proportion of the main indicated myeloid populations (red, monocytes; blue, M-MDSC; green, neutrophils; yellow, G-MDSC) within the four major myeloid subsets in responder patients. Each bar represents an individual patient. **(B)** Relative proportions in patients classified as SD. **(C)** Relative proportions in patients classified as progressors. Patients represented with an asterisk (*) are patients that could not be radiologically re-evaluated with RECIST 1.1 due to early death.

4.3.2 PD-L1 EXPRESSION IN MYELOID CELLS AS A POTENTIAL BIOMARKER OF RESPONSE

PD-L1/PD-1 interactions constitute the signalling axis targeted by ICB in our patient cohort. PD-L1 expression within the tumor constitutes the most widely validated biomarker for patient selection. Nevertheless, it has been demonstrated that some patients with PD-L1-negative tumors before starting immunotherapies can also benefit from ICB therapies. It is well-known that PD-L1 is expressed by myeloid cells, and it is especially up-regulated after activation (Karwacz et al., 2011).

To evaluate if PD-L1 expression in myeloid populations could be contributing to clinical responses to immunotherapy in our cohort, we quantified PD-L1 expression in the different myeloid subsets within $CD11b^+$ cells. Using part of this cohort, we have previously published that the percentage of $PD\text{-}L1^+$ myeloid cells have prognostic value for response to ICB immunotherapies (Bocanegra et al., 2019). In this thesis we present the results of a validation cohort of 25 patients, in which we observed a small increment in the PD-L1 expression in the $CD11b^+$ and the $CD11b^+CD14^+$ subsets in responder patients, without reaching statistical significance. In this particular subgroup, PD-L1 expression followed a bimodal distribution (**Figure 14**).

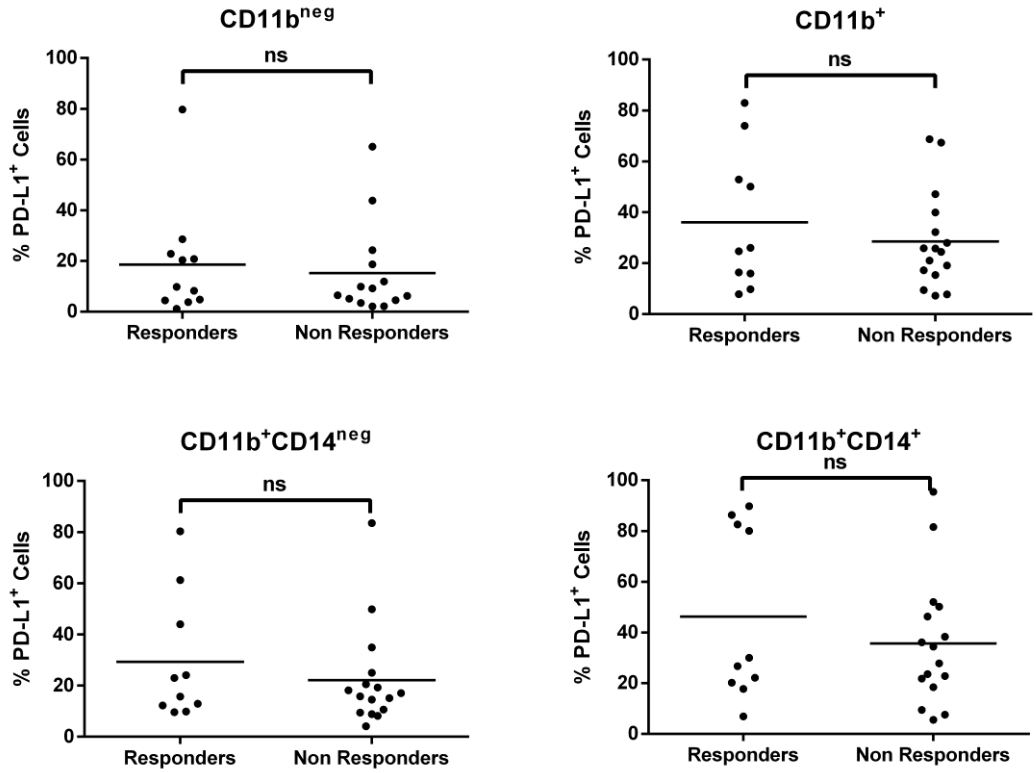

Figure 14 PD-L1 expression within myeloid cells and association with responses**.** The dot plots represent the relative abundance in percentage of PD-L1$^+$ cells in compartments of immune cells and their association with responses as indicated in each graph. Horizontal lines represent the mean percentage in each group. PD-L1 expression was evaluated over (**A**): CD11b$^-$ cells. (**B**): CD11b$^+$ cells. (**C**): CD11b$^+$ CD14$^-$ cells. (**D**): CD11b$^+$ CD14$^+$ cells. ns, non-significant differences. Statistical comparisons were carried out by unpaired t tests.

4.4 Soluble factors in plasma

It has been previously shown that patients with cancer have soluble variants of immune checkpoint molecules circulating in plasma, including PD-1, PD-L1, LAG-3 and others (Dong et al., 2020; Gu et al., 2018). The distinct profiles of myeloid cell subsets observed in our cohort of patients according to their response to ICB therapies suggested that these patients could have different systemic factors that were affecting systemic myeloid profiles. To test this hypothesis, plasma samples were analyzed for the evaluation of the concentration of 40 selected analytes (see materials and methods). These proteins were classified in two groups: soluble immune checkpoints and chemokines. An initial analysis of the concentration of each soluble molecule

showed that the distribution was asymmetric and leptokurtic, suggesting that most of the values in the cohort of patients were held between thin ranges, with some outlier values far above from the reference interval. The distribution of granulocyte colony-stimulating factor (G-CSF) is shown in **Figure 15** as an illustrative example.

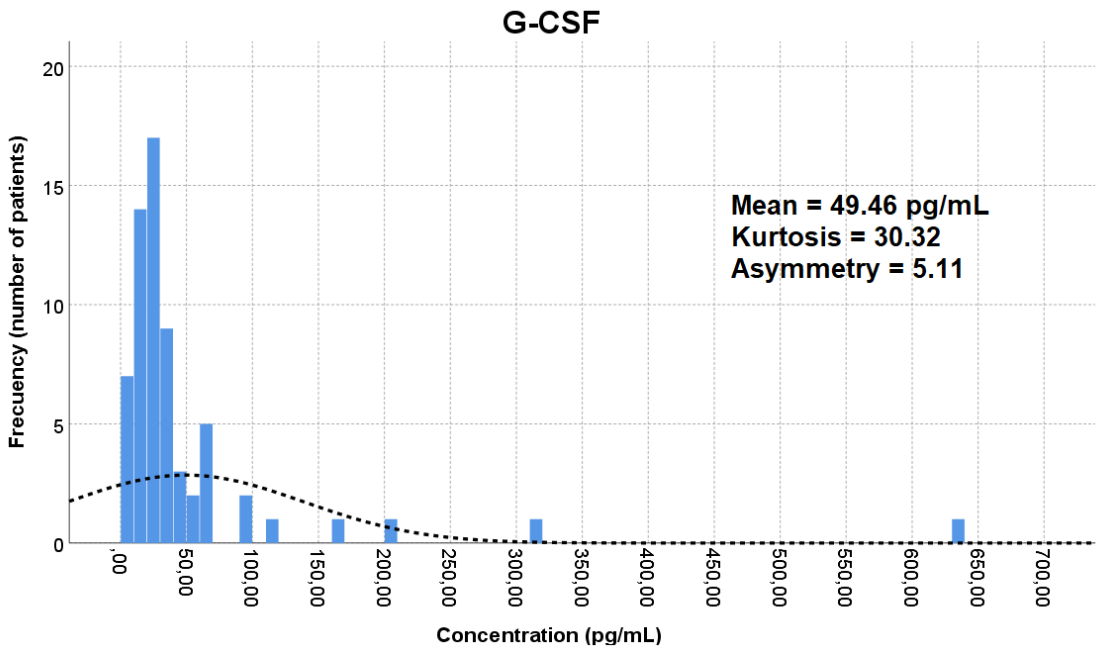

Figure 15. Distribution of the concentration of soluble molecules in plasma samples from patients. Histogram representing the frequency distribution of soluble granulocyte colony stimulating factor (G-CSF), as a representative example of the 40 soluble molecules evaluated in plasma from the cohort of patients. Most patients presented basal values within thin ranges, with some outliers that gave the cohort its leptokurtic and positively asymmetric distribution. The discontinuous line represents values according a normal distribution.

4.4.1 SOLUBLE IMMUNE CHECKPOINT MOLECULES

We quantified the mean concentrations of the soluble immune checkpoint molecules at different time points in responder and non-responder patients (**Figure 16**). This latter group included patients not achieving disease control and with non-evaluable disease due to early death.

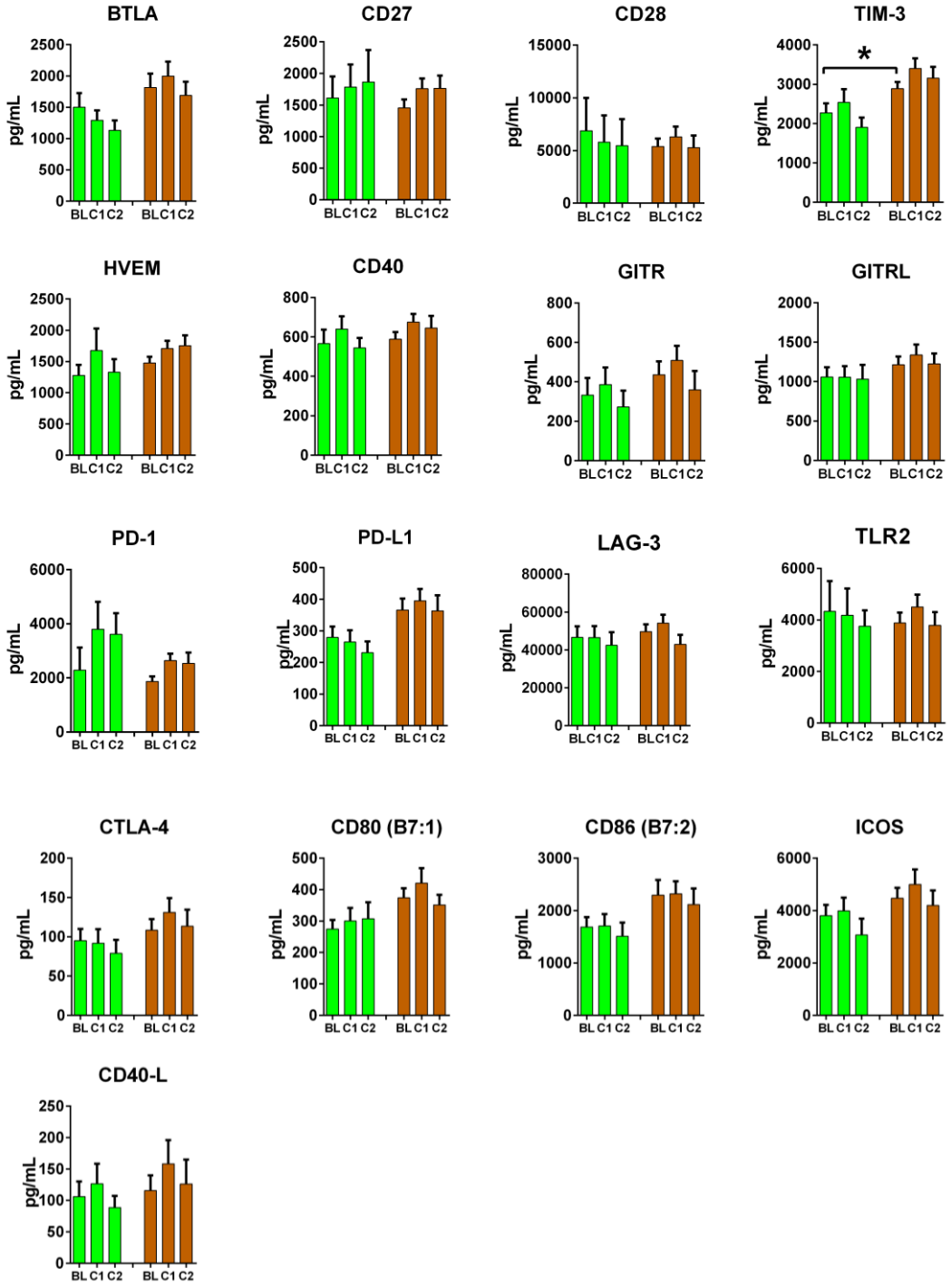

Figure 16 Plasma concentrations of soluble immune-checkpoint molecules**.** Bar graphs show mean concentrations of the indicated soluble immune-checkpoint molecules according to response to ICB (green, responders; brown, non-responders). Data are shown as mean and standard error of the mean (n=64). Relevant statistical comparisons are shown within the graphs using Mann-Whitney U test. BL, C1 and C2 represent baseline, cycle 1 and cycle 2, denoting the cycles of treatment at which the samples were retrieved just before their application.

Overall, significant differences were observed between responders and non-responders in values of T-cell immunoglobulin and mucin-domain containing-3 (TIM-3) concentration. Responders had significantly lower plasma concentrations. To test if concentrations of soluble immune checkpoint molecules could be associated with survival, patients were stratified into two groups; patients with values above or below the mean concentration for each molecule (**Figure 17**). OS in patients with decreased TIM-3 plasma concentrations was significantly improved (median survival 473 vs 183 days, log-rank p = 0.036), in agreement with the differences that had been observed in plasma samples between responders and non-responders. Median PFS was similar in both groups (81 vs 64 days, log-rank p = 0.230).

Although HVEM did not show differences in concentration at the beginning of ICB, we detected prognostic differences in the univariate survival analysis. Median OS in patients with HVEM above the mean was 178 days, vs 473 days in patients below the mean (log-rank test p = 0.012). Again, median PFS was similar in both groups and did not reach statistical significance.

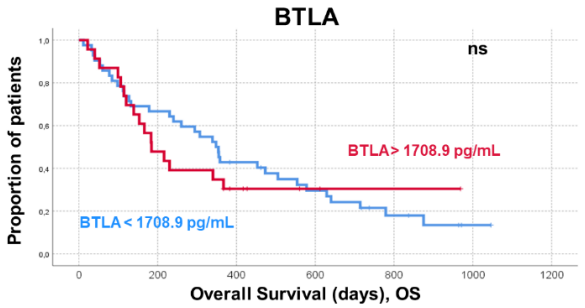
BTLA
ns
BTLA> 1708.9 pg/mL
BTLA < 1708.9 pg/mL
Proportion of patients
Overall Survival (days), OS

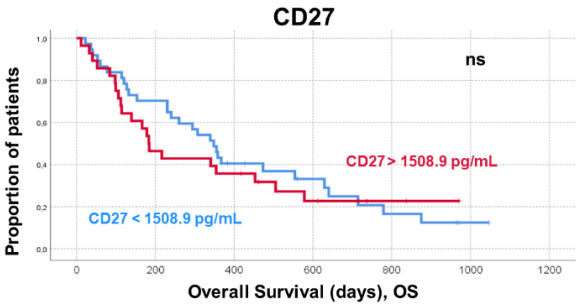
CD27
ns
CD27> 1508.9 pg/mL
CD27 < 1508.9 pg/mL
Proportion of patients
Overall Survival (days), OS

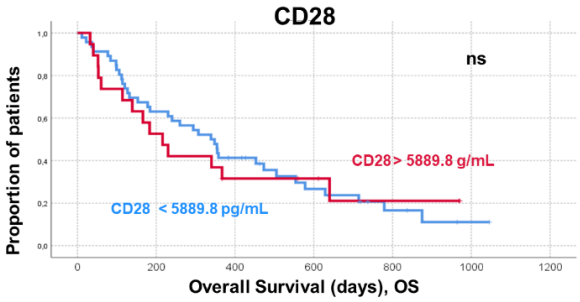
CD28
ns
CD28> 5889.8 g/mL
CD28 < 5889.8 pg/mL
Proportion of patients
Overall Survival (days), OS

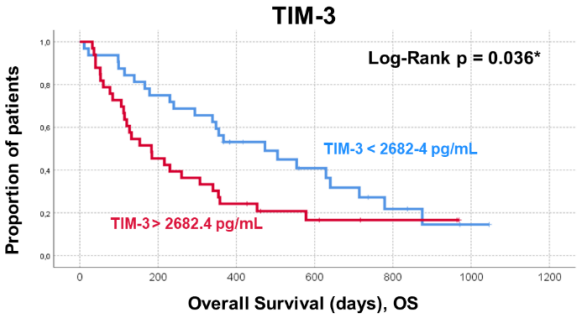
TIM-3
Log-Rank p = 0.036*
TIM-3 < 2682-4 pg/mL
TIM-3> 2682.4 pg/mL
Proportion of patients
Overall Survival (days), OS

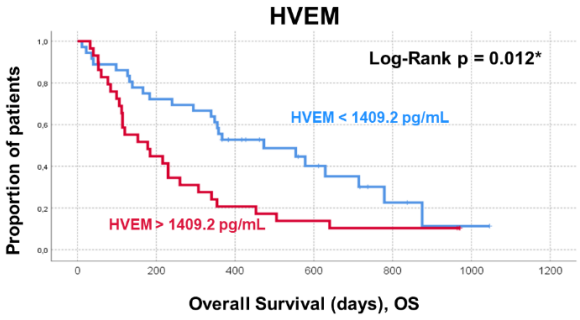
HVEM
Log-Rank p = 0.012*
HVEM < 1409.2 pg/mL
HVEM > 1409.2 pg/mL
Proportion of patients
Overall Survival (days), OS

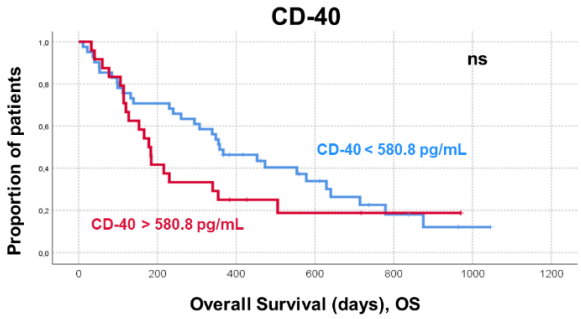
CD-40
ns
CD-40 < 580.8 pg/mL
CD-40 > 580.8 pg/mL
Proportion of patients
Overall Survival (days), OS

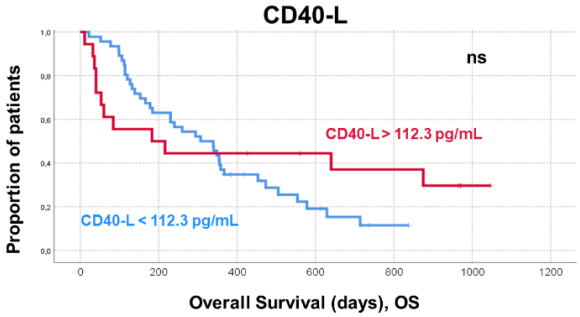
CD40-L
ns
CD40-L> 112.3 pg/mL
CD40-L < 112.3 pg/mL
Proportion of patients
Overall Survival (days), OS

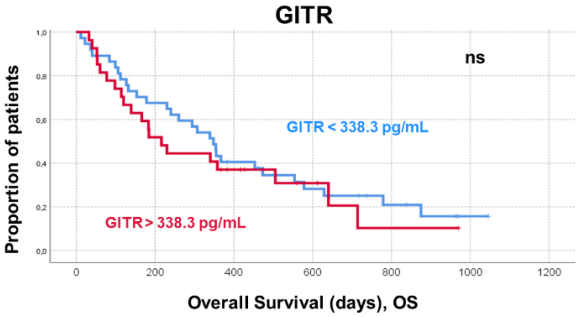
GITR
ns
GITR < 338.3 pg/mL
GITR> 338.3 pg/mL
Proportion of patients
Overall Survival (days), OS

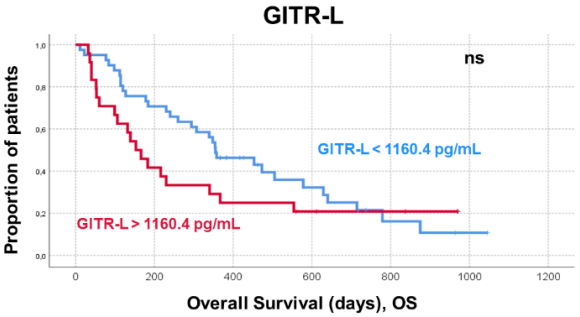
GITR-L
ns
GITR-L < 1160.4 pg/mL
GITR-L > 1160.4 pg/mL
Proportion of patients
Overall Survival (days), OS

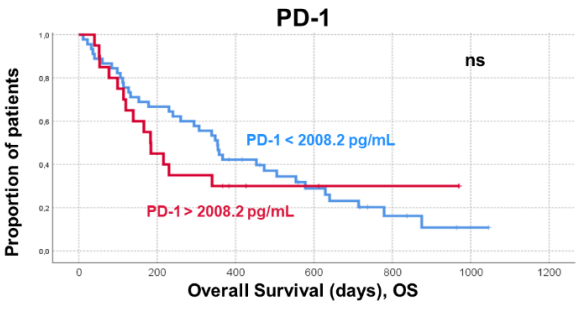
PD-1
ns
PD-1 < 2008.2 pg/mL
PD-1 > 2008.2 pg/mL
Proportion of patients
Overall Survival (days), OS

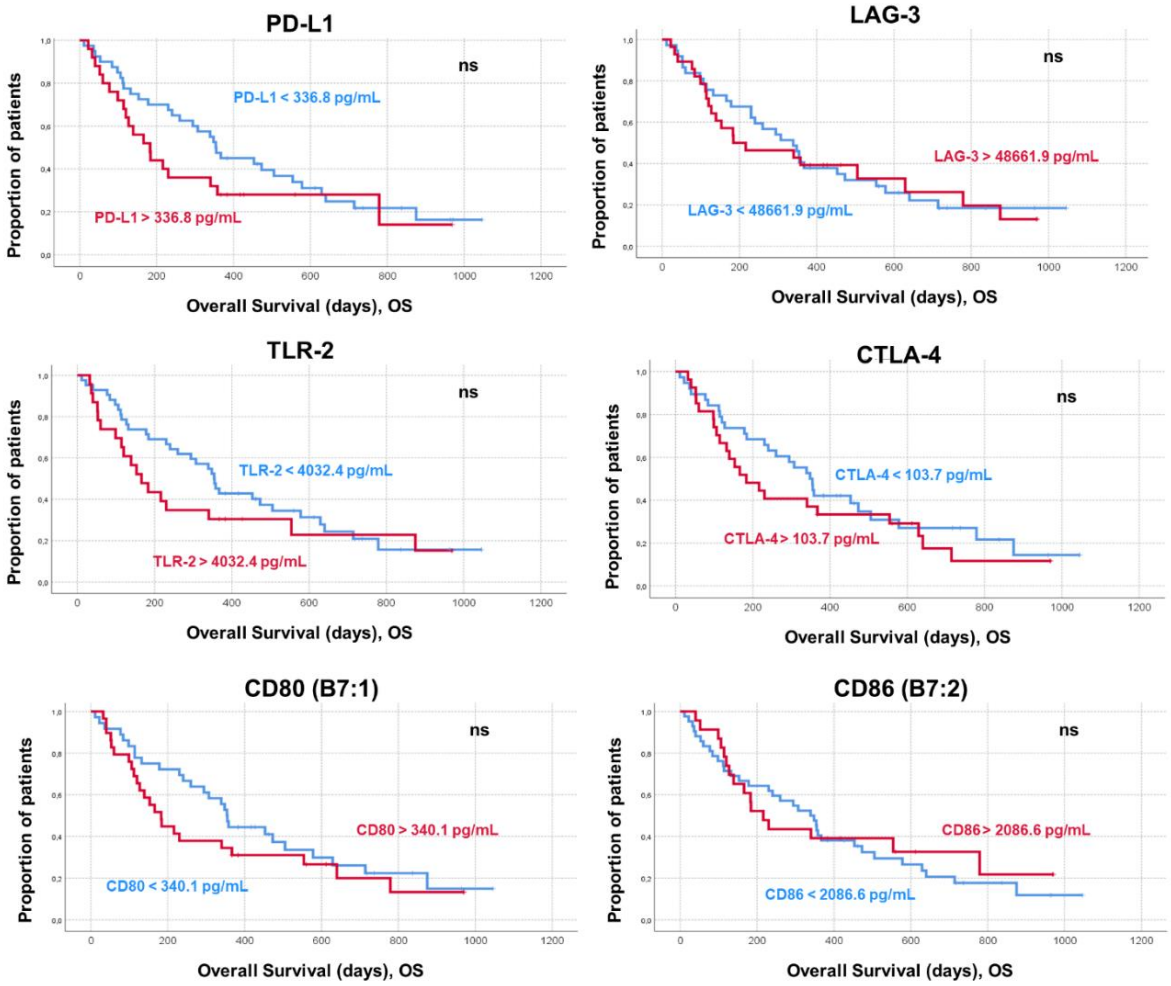

Figure 17 OS according to plasma mean concentrations of soluble immune checkpoints. The Kaplan-Meier plots represent survival of the indicated patient cohorts classified according to plasma values above (red) or below (blue) the mean values of the overall cohort for the indicated molecules. Log-rank tests were used to evaluate if differences in survival were statistically significant. P-values are provided within the graphs when relevant. ns indicates non-significant differences ($p > 0.05$).

4.4.2 CHEMOKINES AND CYTOKINES

A selection of cytokines and chemokines with diverse immunological functions were also included in the analysis panel, as many cytokines are known to regulate myelopoiesis and immune responses. From all the tested detectable molecules in the plasma of responders and non-responders, only two proteins showed relevant differences in their concentration between the two groups of patients before the start of immunotherapies: fractalkine (CX3CL1) and chemokine (C-C motif) ligand 2 (CCL2), also known as MCP1 (**Figure 18**).

Fractalkine (CX3CL1) is a membrane-bound chemokine with roles in T cell regulation and inflammatory diseases (Conroy and Lysaght, 2020). The soluble form is generated by the activity of metalloproteases ADAM10 and ADAM17. In our cohort, fractalkine plasma concentrations were increased in responders (mean 72.7 pg/mL) compared to non-responder patients (39.1 pg/mL), achieving statistical significance (p=0.015; Mann-Whitney's U test). Patients were then stratified into two groups according to fractalkine concentrations using its mean value over the whole cohort as a threshold (46.5 pg/mL). Patients with fractalkine values above the mean showed significantly improved survival (median OS 578 vs 216 days, p= 0.001) (**Figure 19**). This result indicated that fractalkine plasma concentrations could be a positive prognostic biomarker that could be evaluated before starting PD-L1/PD-1 blockade immunotherapies.

In contrast, CCL2 (MCP1) plasma concentrations were decreased in responder patients before the start of immunotherapies (**Figure 18**) approaching statistical significance (289.8 vs 429.5 pg/mL, p=0.073, Mann Whitney's U test). This result suggested that CCL2 plasma concentrations could constitute a negative prognostic biomarker. Patients were also stratified according to CCL2 plasma concentrations into two groups. Patients above and below the mean of the cohort (398.9 pg/mL). In agreement with the previous results, patients with CCL2 plasma concentrations above the threshold had a significantly shortened survival (**Figure 19**, median OS 132 vs 355 days, p = 0.014). This protein has chemotactic properties for monocytes in sites of local inflammation, and has a dual role in the activity of tumor-associated macrophages depending on their predominant phenotype (Yoshimura, 2018).

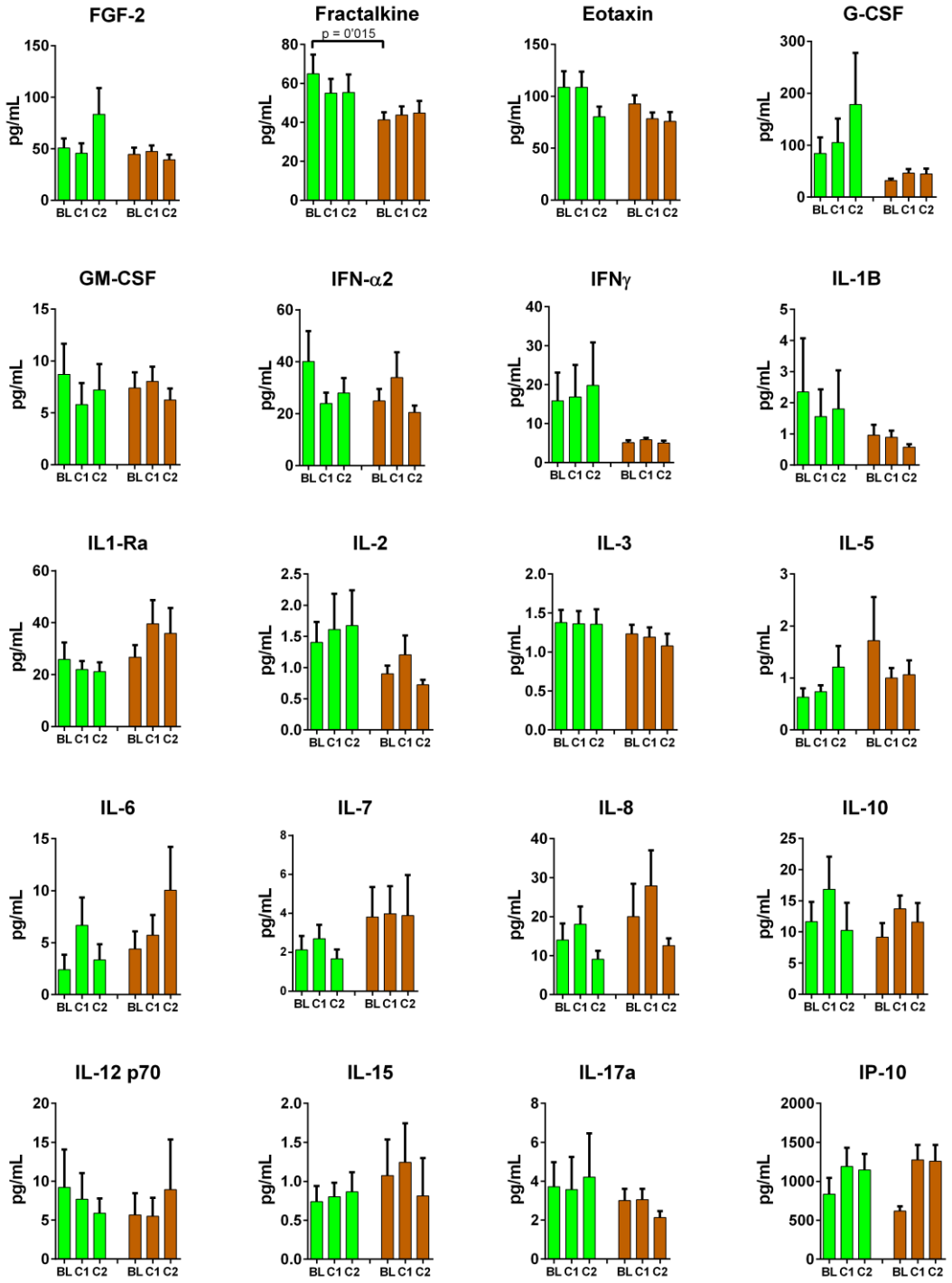
FGF-2
Fractalkine
p = 0'015
Eotaxin
G-CSF
GM-CSF
IFN-α2
IFNγ
IL-1B
IL1-Ra
IL-2
IL-3
IL-5
IL-6
IL-7
IL-8
IL-10
IL-12 p70
IL-15
IL-17a
IP-10
pg/mL
BL C1 C2 BL C1 C2

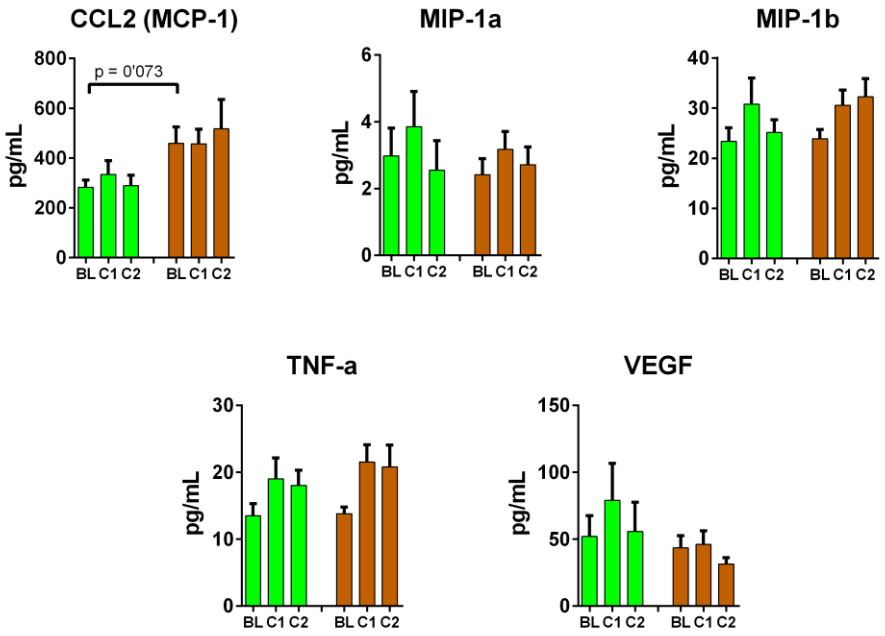

Figure 18 Plasma concentrations of soluble cytokines and chemokines. Bar graphs show mean concentrations of the indicated soluble cytokines and chemokines according to response to ICB (green, responders; brown, non-responders). Data are shown as mean and standard error of the mean (n=64). Relevant statistical comparisons are shown within the graphs using Mann-Whitney's U test. BL, C1 and C2 represent baseline, cycle 1 and cycle 2, denoting the cycles of treatment at which the samples were retrieved just before their application.

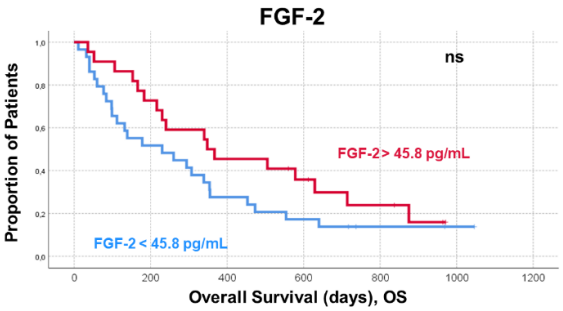
FGF-2
ns
FGF-2> 45.8 pg/mL
FGF-2 < 45.8 pg/mL
Proportion of Patients
Overall Survival (days), OS

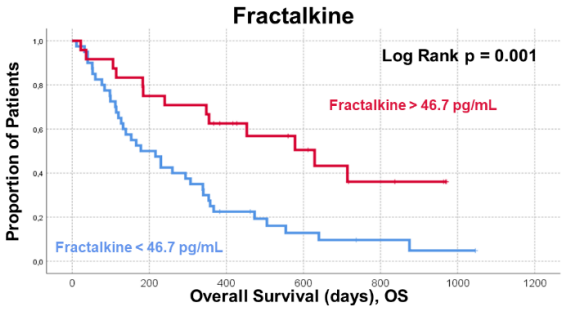
Fractalkine
Log Rank p = 0.001
Fractalkine > 46.7 pg/mL
Fractalkine < 46.7 pg/mL
Proportion of Patients
Overall Survival (days), OS

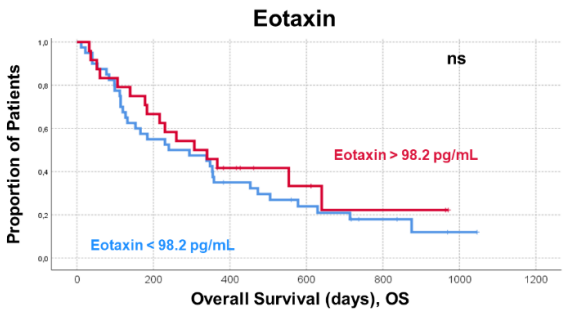
Eotaxin
ns
Eotaxin > 98.2 pg/mL
Eotaxin < 98.2 pg/mL
Proportion of Patients
Overall Survival (days), OS

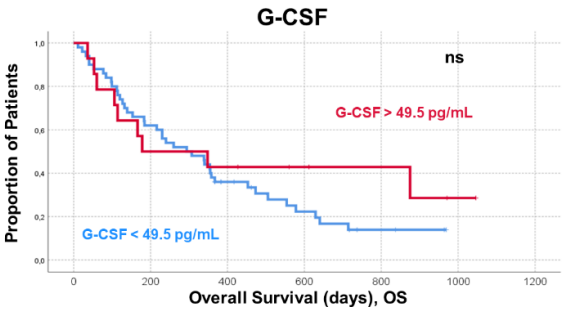
G-CSF
ns
G-CSF > 49.5 pg/mL
G-CSF < 49.5 pg/mL
Proportion of Patients
Overall Survival (days), OS

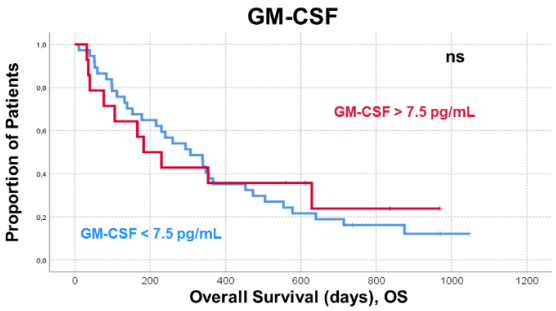
GM-CSF
ns
GM-CSF > 7.5 pg/mL
GM-CSF < 7.5 pg/mL
Proportion of Patients
Overall Survival (days), OS

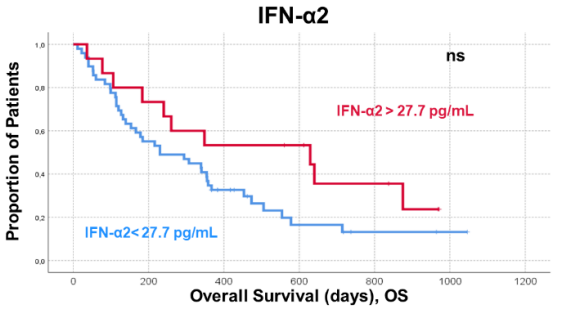
IFN-α2
ns
IFN-α2 > 27.7 pg/mL
IFN-α2< 27.7 pg/mL
Proportion of Patients
Overall Survival (days), OS

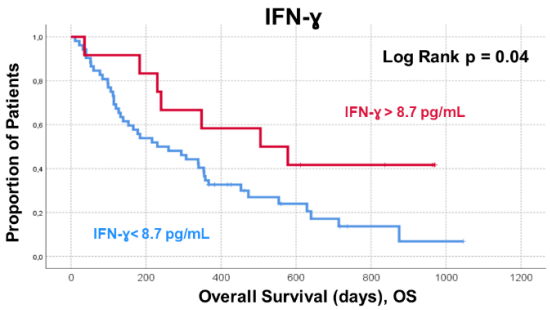
IFN-γ
Log Rank p = 0.04
IFN-γ > 8.7 pg/mL
IFN-γ< 8.7 pg/mL
Proportion of Patients
Overall Survival (days), OS

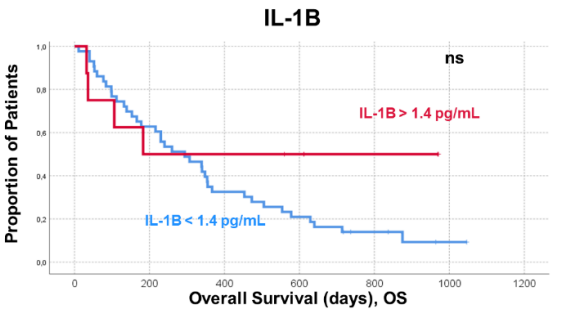
IL-1B
ns
IL-1B > 1.4 pg/mL
IL-1B < 1.4 pg/mL
Proportion of Patients
Overall Survival (days), OS

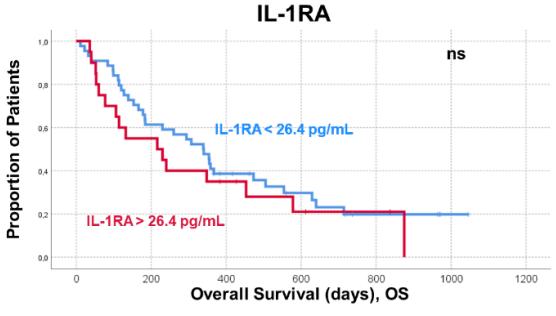
IL-1RA
ns
IL-1RA < 26.4 pg/mL
IL-1RA > 26.4 pg/mL
Proportion of Patients
Overall Survival (days), OS

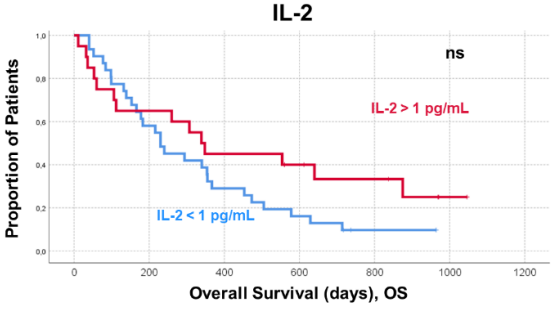
IL-2
ns
IL-2 > 1 pg/mL
IL-2 < 1 pg/mL
Proportion of Patients
Overall Survival (days), OS

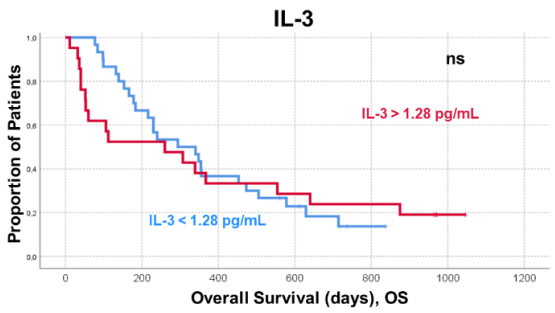
IL-3
ns
IL-3 > 1.28 pg/mL
IL-3 < 1.28 pg/mL
Proportion of Patients
Overall Survival (days), OS

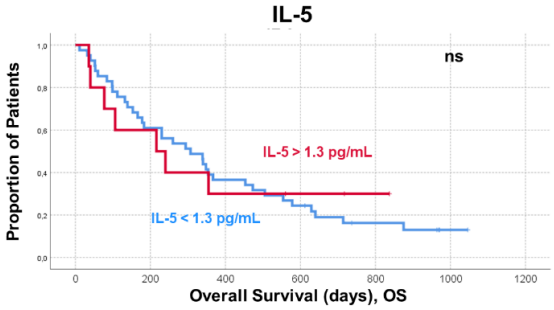
IL-5
ns
IL-5 > 1.3 pg/mL
IL-5 < 1.3 pg/mL
Proportion of Patients
Overall Survival (days), OS

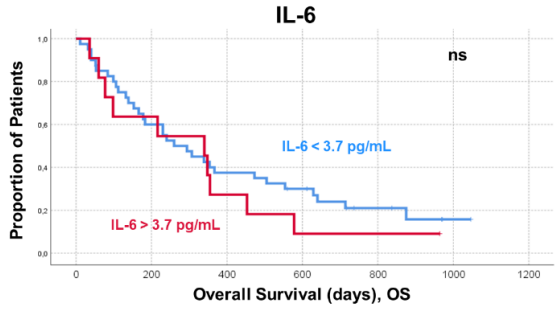
IL-6
ns
IL-6 < 3.7 pg/mL
IL-6 > 3.7 pg/mL
Proportion of Patients
Overall Survival (days), OS

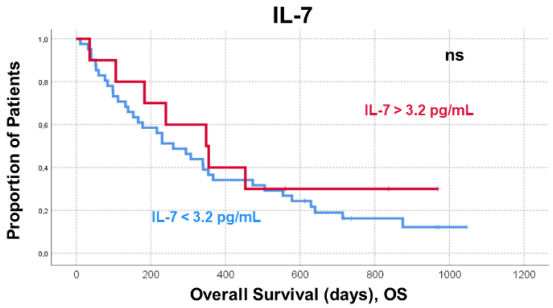
IL-7
ns
IL-7 > 3.2 pg/mL
IL-7 < 3.2 pg/mL
Proportion of Patients
Overall Survival (days), OS

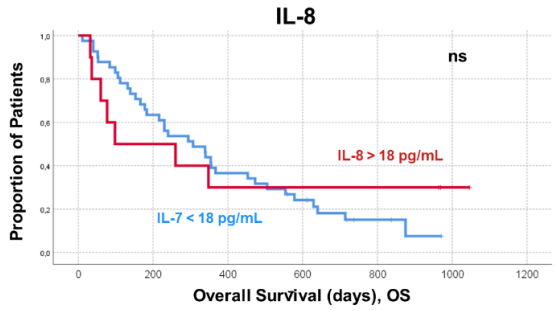
IL-8
ns
IL-8 > 18 pg/mL
IL-7 < 18 pg/mL
Proportion of Patients
Overall Survival (days), OS

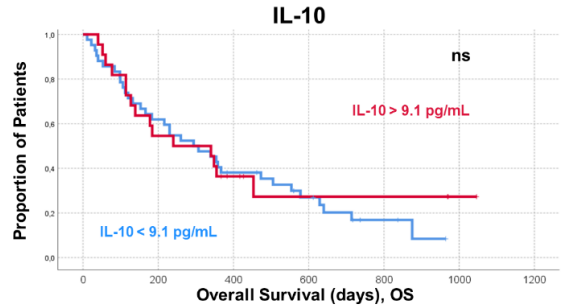
IL-10
ns
IL-10 > 9.1 pg/mL
IL-10 < 9,1 pg/mL
Proportion of Patients
Overall Survival (days), OS

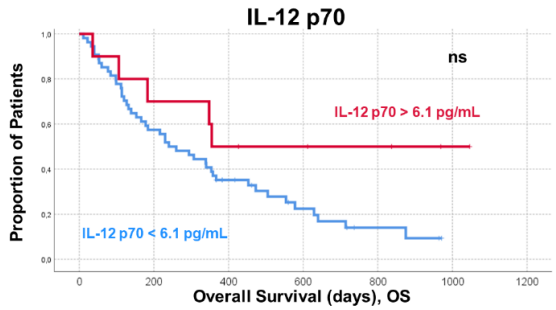
IL-12 p70
ns
IL-12 p70 > 6.1 pg/mL
IL-12 p70 < 6.1 pg/mL
Proportion of Patients
Overall Survival (days), OS

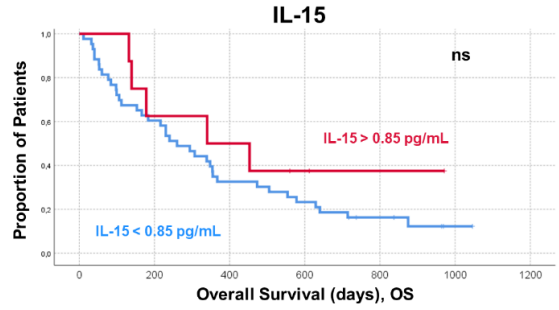
IL-15
ns
IL-15 > 0,85 pg/mL
IL-15 < 0,85 pg/mL
Proportion of Patients
Overall Survival (days), OS

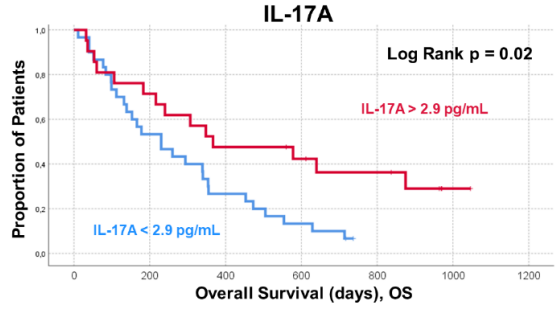
IL-17A
Log Rank p = 0.02
IL-17A > 2.9 pg/mL
IL-17A < 2.9 pg/mL
Proportion of Patients
Overall Survival (days), OS

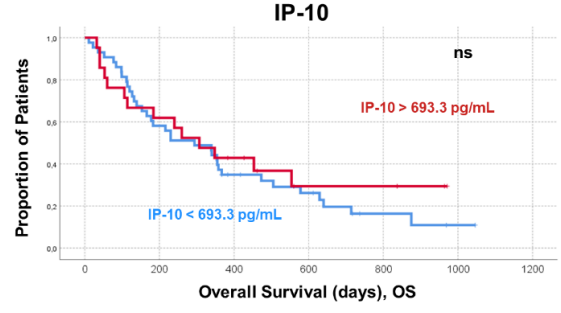
IP-10
ns
IP-10 > 693.3 pg/mL
IP-10 < 693.3 pg/mL
Proportion of Patients
Overall Survival (days), OS

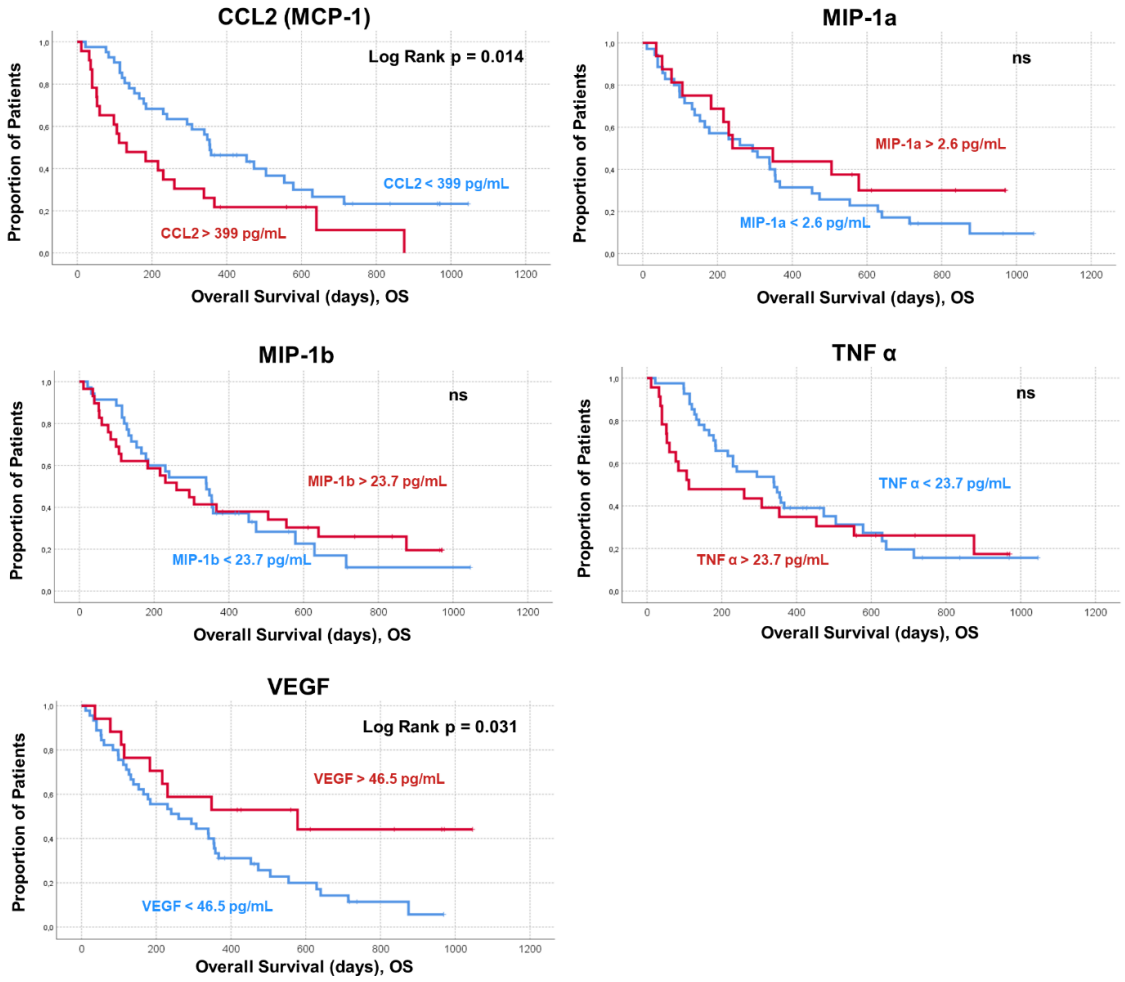

Figure 19 OS according to plasma mean concentrations of soluble chemokines and cytokines. The Kaplan-Meier plots represent survival of the indicated patient cohorts classified according to plasma values above (red) or below (blue) the mean values of the overall cohort for the indicated molecules. Log-rank tests were used to evaluate if differences in survival were statistically significant. P values are provided within the graphs when relevant. ns indicates non-significant differences ($p > 0.05$).

4.5 Immunological profiling of lung cancer patients according to histological classification

NSCLC comprises a group of heterogeneous subtypes of lung cancers with variable ontologies, leading to different pathological behaviour, distinct prognosis and different therapeutic approaches. NSCLC can be further classified into two most frequent subtypes according to histological classification: Adenocarcinomas and squamous cell carcinomas (SCC). Non-squamous lung carcinomas often

include other subtypes such as large-cell neuroendocrine carcinomas (LCNEC) or sarcomatoid lung cancer, although these subtypes also have unique features. We hypothesized in this thesis that subtype classification into non-squamous cell carcinomas (non-SCC) and SCC could introduce another stratifying factor that, combined with the biomarkers evaluated in this study, could contribute to more fine-tuned prognostic markers. Hence, patients were stratified according to clinical response and histological classification of tumors, and some of the biomarkers studied in this PhD thesis were re-evaluated in these subgroups.

4.5.1 NLR ACCORDING TO HISTOLOGY AND CLINICAL RESPONSES

NLR was evaluated as a classical prognostic variable. Patients with SCC (n = 25) presented higher baseline NLR in non-responders than in responders (5.29 vs 4.93, p = 0.069). Furthermore, the increases in NLR following the first cycle of therapy and its negative prognostic significance were restricted to SCC patients. **Figure 20** shows the absolute neutrophil and lymphocyte counts, as well as their ratio, in responding and non-responding patients across different histologies. We quantified the differences in neutrophils from ICB start to C2 through independent analyses of responding and non-responding patients by Friedman non-parametric test.

For responding patients with squamous histologies we did not find any significant difference, and the mean neutrophil concentration stayed stable after ICB start. In non-responding patients, however, an increment was observed after treatment initiation that was statistically significant (p = 0.041). Patients responding to immunotherapy had a mean NLR elevation of 77% following the first cycle of treatment, while non-responding patients had a mean elevation of 185% (Friedman test, p = 0.044 for NLR in non-responders).

These differences were not observed for patients with non-SCC histologies, with a mean baseline NLR of 5.15 in non-responders *vs* 4.93 in responder patients without statistically significant changes in the distribution after ICB start (Friedman test p = 0.250 for NLR in non-responders).

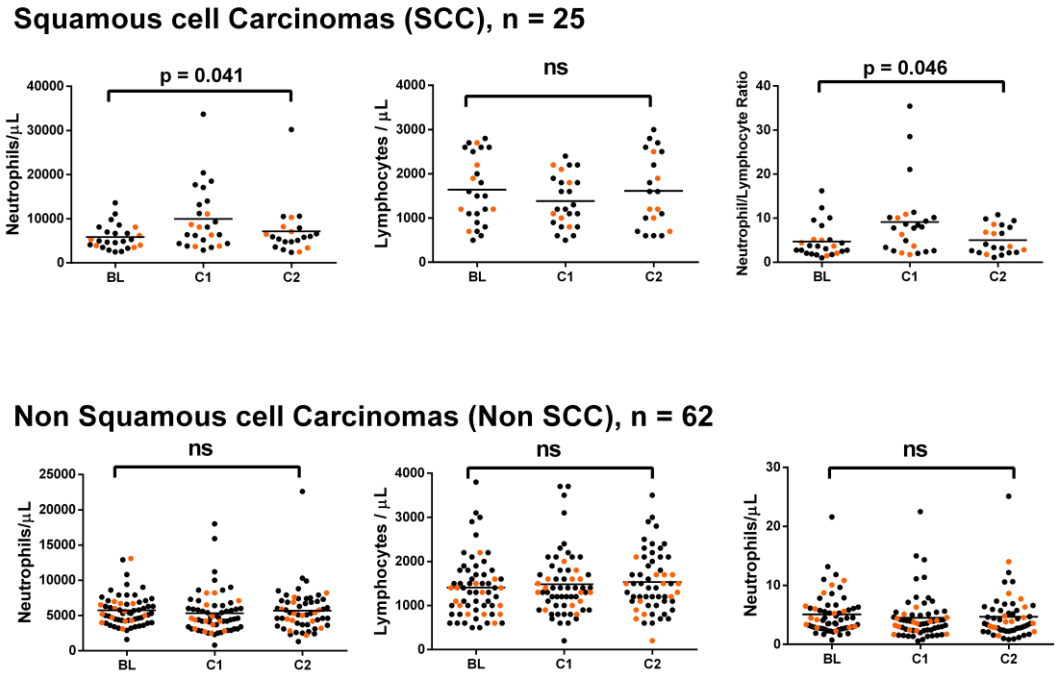

Figure 20 Neutrophil and lymphocyte quantification as per EMR data, in squamous and non-squamous cell carcinomas**.** The upper dot plots show neutrophil and lymphocyte absolute numbers in squamous cell carcinomas at baseline, before the application of the first cycle of therapy (cycle 1) and before the application of the second cycle of therapy (cycle 2). Data from individual patients are represented in the graph. Brown dots represent data from responder patients and black dots from non-responders. The lower dot plots represent the same variables as shown in the upper plots, but in patients with non-SCC. Relevant statistical comparisons are indicated with the graphs using the Friedman non-parametric test for repeated measures. ns indicates non-significant differences.

4.5.2 PLASMA CONCENTRATIONS OF SOLUBLE IMMUNE-CHECKPOINT MOLECULES.

To obtain a general overview on the immunological plasma profile of lung cancer patients distributed according to histological classification, patients were grouped and plasma concentrations of soluble immune checkpoints were analysed by a heatmap (**Figure 21**). In our cohort, patients with radiological response in squamous cell carcinomas presented reduced plasma concentrations of soluble immune checkpoints prior to the start of ICB. In contrast, elevated values were associated with low response-rates and a shortened survival. Interestingly, this was not the case for patients diagnosed with non-SCC. Among this group of patients, those that developed a significant response exhibited a much wider distribution of plasma concentrations of immune checkpoint molecules (**Figure**

21). The cohort under study contained a limited number of patients with SCC who achieved a significant response after ICB. In these patients, plasma concentrations of immune checkpoints were consistently decreased following immunotherapy.

From these analyses a pattern emerged suggesting that patients presented concordant distributions in molecules implicated in shared immunological mechanisms. All these data could be translated to patient survival (**Figure 22)**.

SCC-patients with increased soluble PD-1, for example, had a median OS of only 77 days, vs 355 days in patients with decreased soluble PD-1 (log-rank p = 0.005). This pattern was not followed by non-SCC patients and indeed PD-1 seemed to identify a subgroup of long-term responders (**Figure 22A**). This pattern was common in most of the soluble immune checkpoints, except for LAG-3 and CD40 in our cohort, suggesting a role for immunosuppression and ICB-resistance in squamous cell carcinomas that can be detected through detection of a “fingerprint” of circulating plasmatic factors. In our previous analyses, TIM-3 and HVEM plasma concentrations were associated with differential responses to immunotherapy, according to their roles as regulators of immunosuppression (Wolf et al., 2020). This worse clinical evolution with shortened survival was found to be independent of the tumor subtype in these proteins. These results suggested that TIM-3 and HVEM could be implicated in a mechanism of resistance that could overcome PD-1/PD-L1 blockade independently of the tumor subgroup (**Figure 22B,C**).

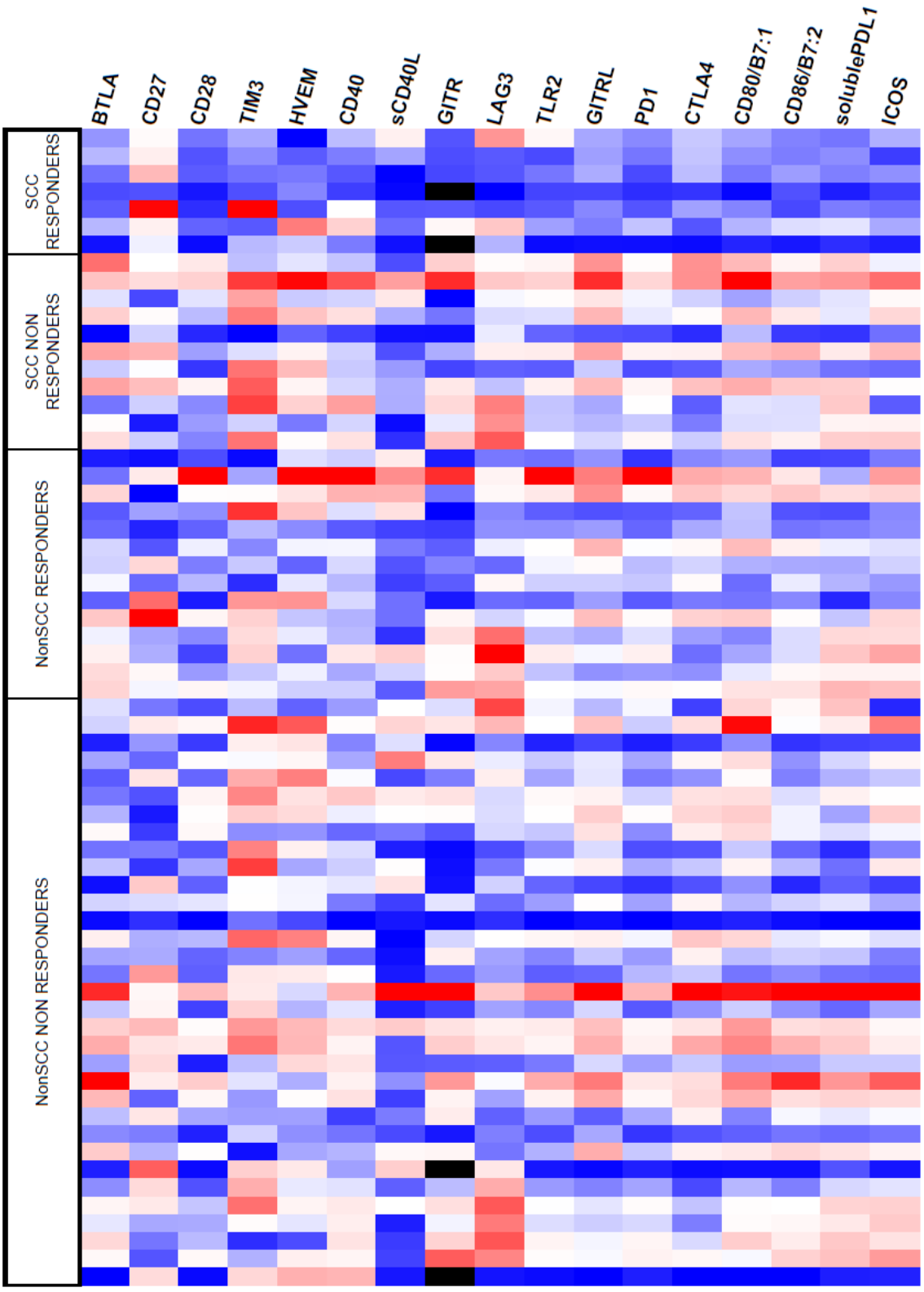

Figure 21 Heatmap representing the distribution of plasma concentrations of immune-checkpoint molecules grouped according to radiological response and tumor histology. Each patient is represented in a row while columns show the individual results. Color intensity represents deviations from the mean, which is shown in white. Red and blue represent increased and decreased levels, respectively.

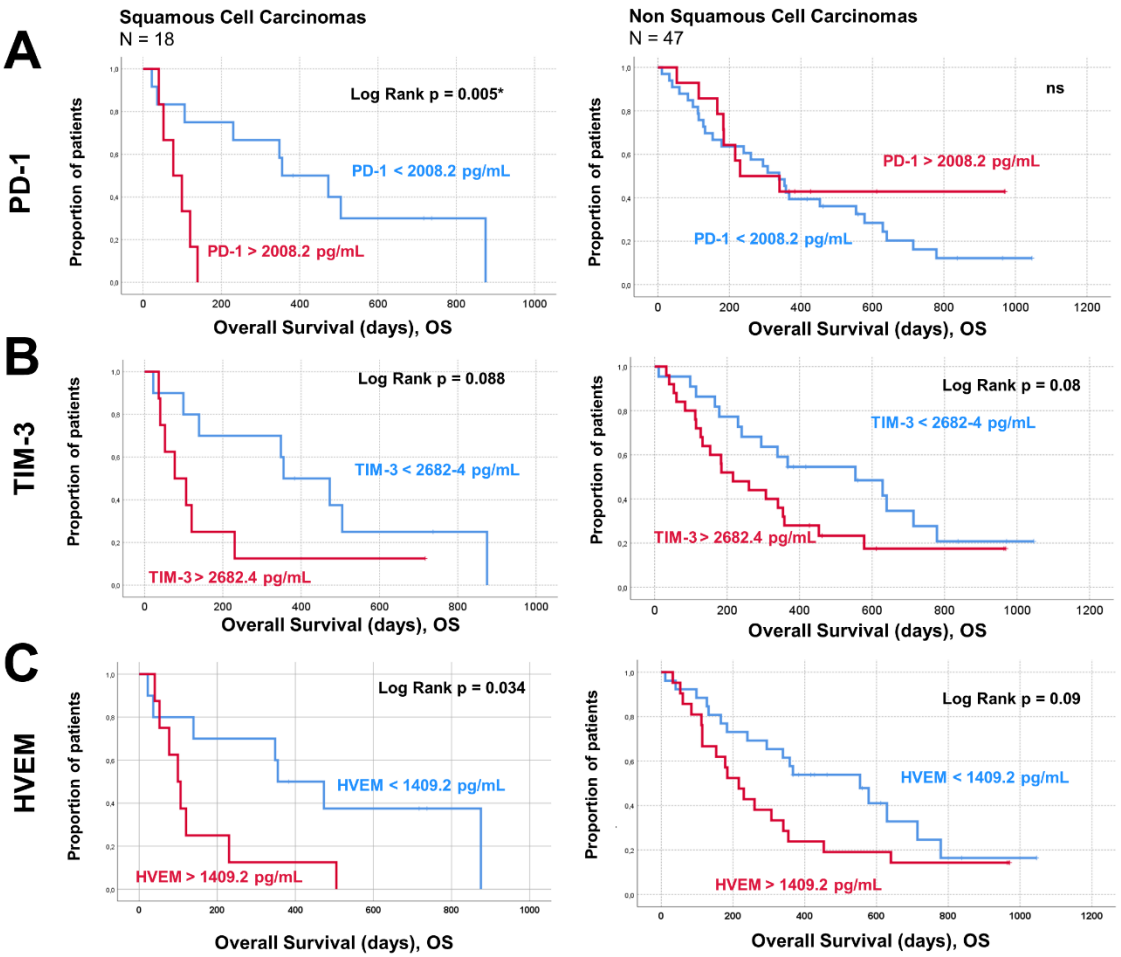

Figure 22. OS according to baseline mean plasma concentrations of selected immune checkpoints**.** As an illustrative example, Kaplan-Meier plots for PD-1, TIM-3 and HVEM plasma concentrations are shown. Elevated PD-1 plasma concentration conferred a significant poor prognosis in SCC tumors (median survival in the high PD-1 group was 77 days [CI 95% 21-133] vs 355 days in the low PD-1 group [CI 95% 162-547]). In contrast, patients with non-SCC did not show statistical differences, with 3 long-term responders with elevated PD-1 plasma levels at baseline. In contrast, TIM-3 plasma concentrations were associated with poor prognosis, with a concordant behaviour across tumor histologies. A similar phenomenon occured with soluble HVEM. Statistical comparisons were performed with log-rank test. Probabilities are shown within the graph when relevant. ns indicates non-significant differences ($p > 0.05$).

4.5.2 PLASMA CONCENTRATIONS OF SOLUBLE CHEMOKINES AND CYTOKINES

Then, the association between plasma concentrations of soluble chemokines and cytokines with responses was re-evaluated in patients further stratified according to histological tumor classification. First, a heatmap analysis was performed with all quantified values (**Figure 23**). Overall, a tendency for elevated baseline plasma concentrations of soluble chemokines and cytokines was observed for non-SCC patients responding to immunotherapies, while they were decreased in progressors. The pattern observed for patients with tumors classified as SCC was found to be more heterogeneous.

Elevated concentrations of fractalkine in plasma of patients with non-SCC were clearly a very significant predictor of response and improved survival (**Figure 24**). Indeed, patients with elevated values presented an overall response rate at the first radiological evaluation of 47%, while the overall response rate of patients with decreased values was only 6.9%. In contrast, no significant prognostic value for fractalkine was detected in patients with SCC.

Interestingly, plasma concentrations of vascular endothelial growth factor (VEGF) had opposite prognostic value depending on the histological classification of lung cancer tumors. In the cohort under study, baseline VEGF plasma concentrations were clearly elevated in non-SCC patients that responded to immunotherapy. In contrast, VEGF elevation conferred a worse prognosis in patients with SCC lung cancer, although without reaching statistical significance (**Figure 24**).

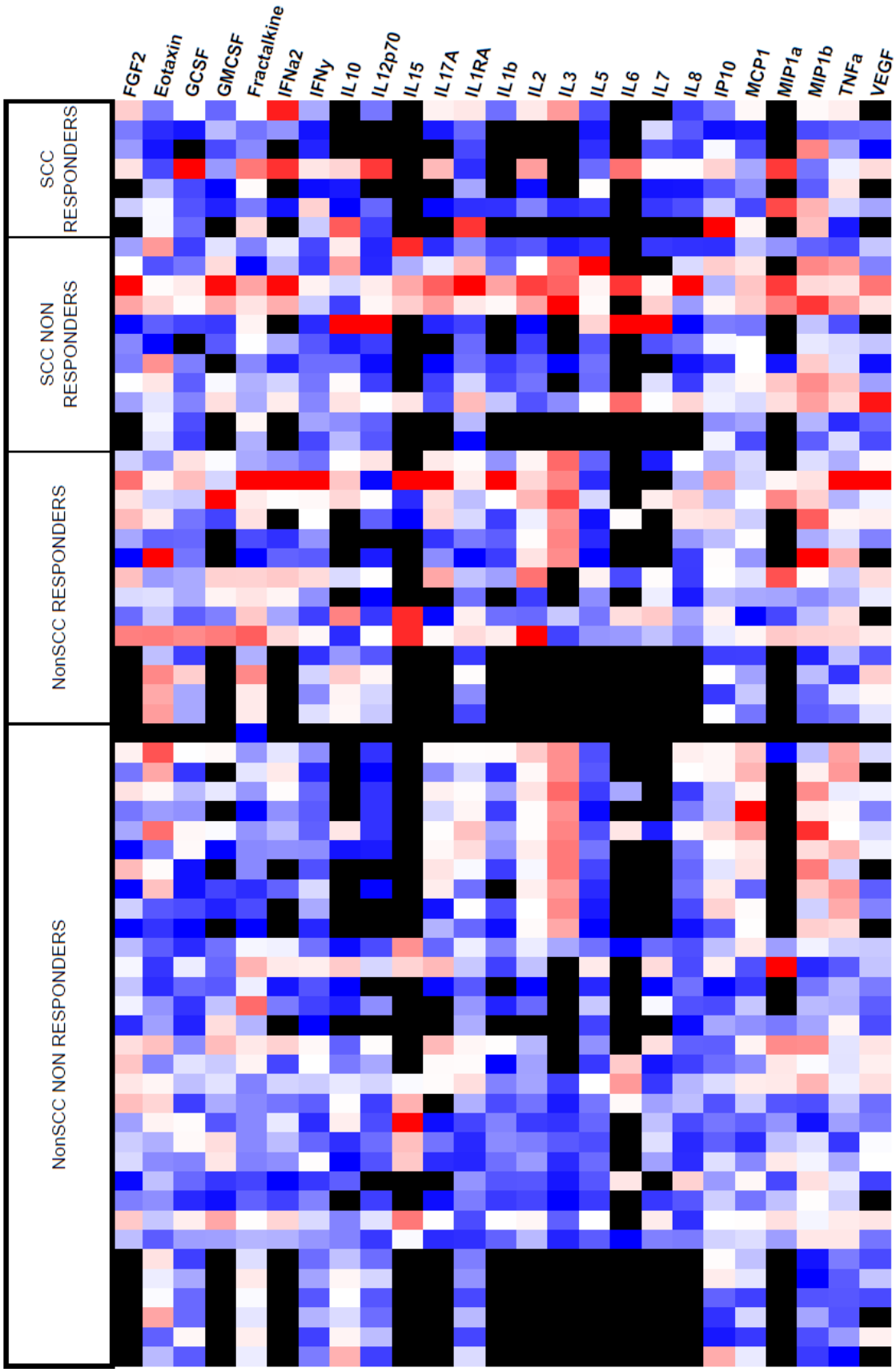

Figure 23 Heatmap representing the distribution of cytokine/chemokine plasma concentrations according to radiological response and tumor histology**.** Each patient is represented in a row across all factors distributed in columns. Color intensity represents deviations from the mean, which is shown in white. Red and blue represent increased and decreased levels, respectively.

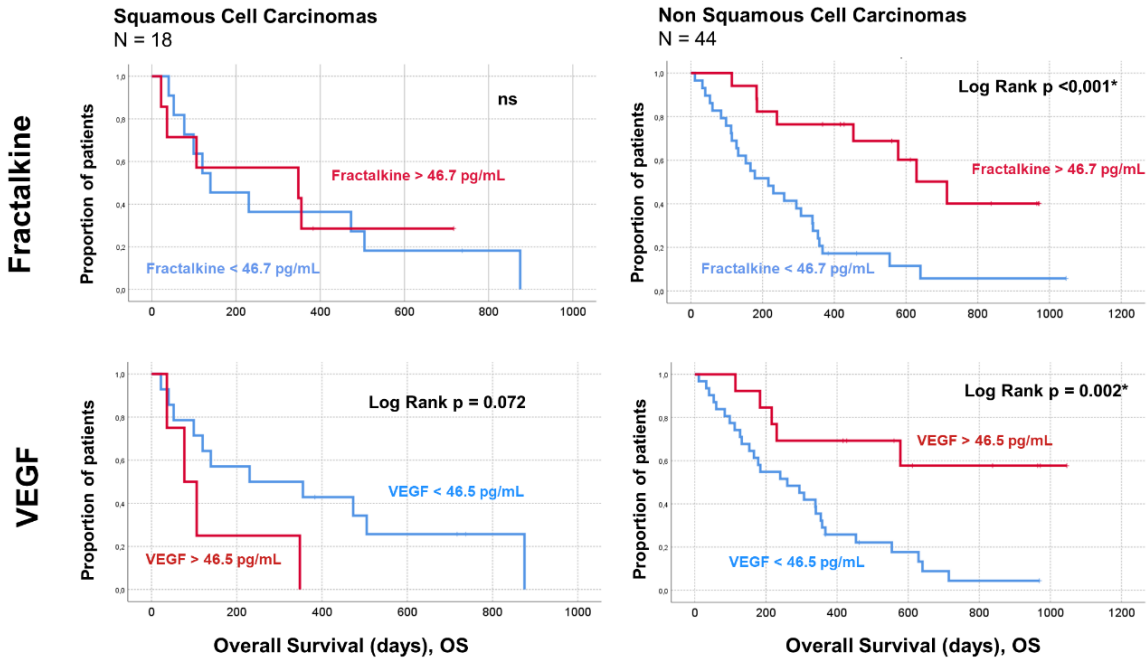

Figure 24 OS according to the baseline mean plasma concentration of fractalkine and VEGF in patients with distinct primary tumor histology**.** Kaplan-Meier plots showing fractalkine and VEGF plasma concentrations. In red, patients with plasma concentrations above the mean, and in blue, patients with plasma concentrations below the mean. Statistical comparisons were performed with log-rank test. Probabilities are shown within the graph when relevant. ns indicates non-significant differences ($p > 0.05$).

The value for plasma concentrations of other cytokines/chemokines such as IL-12 p70 or IFNγ exhibited a pronounced leptokurtic distribution. Stablishing the stratification threshold in the mean of the whole cohort only identified a small group of 5 patients in the non-SCC group, all of which had prolonged survival (beyond 400 days).

4.6 Multivariate analysis of overall survival

In an initial approach, each of these factors was studied by univariate analyses, identifying several clinical and immunological variables that could influence clinical outcomes. Then, multivariate Cox-regression analyses were performed to identify which one of these factors independently influence overall survival (OS) (**Table 7**).

Multivariate analyses showed that several factors had independent prognostic value on shortened survival: More than 2 previous lines of chemotherapy, worsened ECOG, liver metastatic dissemination, more than 2 metastatic locations, increased proportion of neutrophils in the myeloid compartment and levels of circulating CCL2 and IL-17a.

Table 7 Multivariate analysis of predictive variables of OS in our study cohort. HR: Hazard Ratio.

Variable	HR (95% CI)	p value
Age > 70 years	1.29 (0.48-3.50)	0.612
Female	1.08 (0.41-2.85)	0.878
Non-squamous cell lung carcinoma	1.39 (0.52-3.77)	0.512
Tumor PD-L1 ≥ 1%	0.55 (0.22-1.36)	0.195
> 2 Lines of treatment	0.23 (0.09-0.59)	**0.002****
ECOG ≥ 2	13.19 (2.93-59.37)	**< 0.001*****
> 2 Metastatic locations	0.24 (0.07-0.79)	**0.019***
Liver M1	5.13 (1.65-15.85)	**0.005****
Δ NLR ≥ 50% after C1	0.80 (0.27-2.35)	0.693
≥ 25% Neutrophils	4.45 (1.43-13.79)	**0.010***
Soluble TIM 3 > 2682.4 pg/mL	0.61 (0.21-1.74)	0.358
Soluble HVEM > 1409.2 pg/mL	1.37 (0.48-3.88)	0.553
Soluble fractalkine > 46.7 pg/mL	1.15 (0.36-3.66)	0.800
Soluble CCL2 (MCP1) > 399 pg/mL	5.95 (2.08-17.03)	**< 0.001*****
Soluble VEGF > 46.5 pg/mL	1.58 (0.42-5.84)	0.497
Soluble IL-17a > 2.9 pg/mL	0.13 (0.04-0.42)	**< 0.001*****

5. Discussion

NSCLC is the first cause of cancer-related death worldwide. The treatment of the disease has radically changed since the introduction of immunotherapies over the last decade. Yet, resistance to immunotherapies and disease progression are still major problems in thoracic oncology. Moreover, the cost of immunotherapies is rather high, and this reinforces the necessity to identify patients who will respond to these treatments. Additionally, some of the patients are intrinsically refractory to immunotherapies and some of them can even develop hyperprogressive disease.

Considering all these factors, numerous efforts are currently being made to categorize biomarkers that can identify potential responders to treatment. Measuring the benefit of these drugs by assessing biomarker-based outcomes would also improve the regulatory procedures leading to drug approval by agencies and optimize resources in oncology research. So far, tumor expression of PD-L1 has been approved as a biomarker for the application of pembrolizumab, although its utility is often questioned.

A previous study carried out by our group identified a profile of memory CD4 T cells that identified patients who would either respond or fail to PD-L1/PD-1 blockade therapies (Zuazo et al., 2019). Nevertheless, among the potential responders identified by this T cell profile, around 50% were progressors after receiving immunotherapy.

Based on published studies about the participation of different factors on the outcome to ICB treatments, a collection of these factors were evaluated in this thesis. We studied how their values influenced tumor evolution in response to immune checkpoint blockade (ICB) in 87 NSCLC patients who had previously progressed to chemotherapy.

It is widely accepted that a detailed immunological profile, including the relative proportions of selected immune cell populations can provide sufficient information on the general status of the patient, and how the patient will respond to immunotherapies. Biomarkers and immunological profiles can be obtained from peripheral blood, which is an easily accessible tissue which can be used to detect circulating tumor-genetic material but also detailed information on the immunological status of the patient (Mazzaschi et al., 2020; Nabet et al., 2020). Over the years, quantification of immunological markers has been carried out in numerous studies, with the aim of associating immune cell profiles and their ratios (Cao et al., 2018). Amongst the molecules that have been studied were soluble PD-L1 and IL-8 (Sanmamed et al., 2017; Wei et al., 2018). Other markers of general health/nutritional status such as albumin and cholesterol levels have also been associated with response to treatment (Trestini et al., 2020).

We tried to validate these prognostic markers in our cohort. Although the dynamics of these populations can change quickly in response to damage, infection or stress, we observed that their change from the start of immunotherapies to the second cycle of treatment had prognostic relevance. Patients with raised neutrophil numbers had shortened survival. Many patients showed a fast clinical deterioration accompanied by a marked NLR increase. In these cases, treatment administration in the third cycle was not possible. Moreover, in the remaining patients, the NLR relationship with clinical outcome weakened when assessing the differences between baseline and third cycle of therapy. This observation enabled us to conclude that close clinical observation and frequent laboratory assessments after treatment initiation are essential steps of clinical management, and helpful in predicting treatment response and survival.

The onset of immune-related adverse events (IRAEs) to immunotherapies is associated with immune hyperactivation against healthy tissues, and may be linked to increased anti-tumor responses. Initial observations in immunotherapy clinical trials associated IRAEs with better response and longer survival

(Freeman-Keller et al., 2016). In agreement with these observations, in our cohort, there was a higher proportion of detected irAEs in patients responding to therapy compared to non-responders. However, this difference did not reach statistical significance ($p = 0.175$), possibly due to the limited number of patients. Additionally, the study presented in this PhD thesis did not have the proper inclusion/exclusion criteria applied in clinical trials to remove variability.

Recent studies have associated lipid metabolism with the activity and specialization of neutrophils (Turner et al., 2020). It is likely that physiological characteristics such as body composition related to cholesterogenesis could influence myeloid cell activity. Previous reports suggested that a worsened nutritional status is associated with a decline in OS (Lee et al., 2020). In this study, differences in baseline body composition, and markers of systemic nutritional status such as cholesterol and albumin were analyzed, but without significant association with clinical response. Serum cholesterol and albumin concentrations were similar in both groups. The effect of previous systemic therapies on the nutritional status might have influenced survival/response to treatments. We observed decreased total muscle area in patients with three or more lines of chemotherapy when compared with patients that had progressed to first-line chemotherapy, but without statistical significance (59.4 cm^2/m^2 vs 63.3 $cm^2/m^{2,}$ $p = 0.275$, Student's t test). Nevertheless, we cannot disregard the role of these markers due to the limited size of the cohort under study.

Different published studies have unsurfaced the importance of neutrophil numbers on the response to treatment. More specifically, their association with shortened OS. Neutrophils are key elements in an adequate response against infection, and use several mechanisms such as degranulation, phagocytosis and neutrophil-extracellular traps (NETs) as effector mechanisms. However, tumors can utilize them to promote progression and metastatic spreading (Masucci et al., 2020). In cancer, granulocytic MDSCs (G-MDSCs) and pathologically activated neutrophils contribute to immunosuppression and tumor progression. Very recently, Veglia et al have uncovered the differences and similarities between

different subsets of neutrophils and G-MDSCs in cancer progression (Veglia et al., 2021). In this thesis, we performed a very extensive analysis on myeloid populations in cancer, which has allowed us to compare our data with the reported studies on neutrophils and MDSCs.

In immunotherapy, it is not only important to identify biomarkers that can help us stratify patients according to probability of response. It is also important to identify biomarkers associated with severe adverse events. Hyperprogression (HP) is such an adverse event especially in immunotherapy, which is characterized by an accelerated tumor growth after treatment initiation often leading to rapid deterioration and death. Whether HP is a direct consequence of ICB or a phenomenon associated with specific characteristics in the patient, it is currently a heated matter of debate. Identification of this phenomenon is based on calculating tumor growth kinetic (TGK) parameters, which measure the variation in changes of target lesions between re-evaluations (Saada-Bouzid et al., 2017). Identification of true hyperprogressing patients is quite a challenge. It has to be taken into account that the rapid growth of small lesions may overestimate the significance of relative changes in diameter.

In our cohort, the worst prognostic group was represented by patients with a fast and profound clinical deterioration, which impaired any radiological evaluation. These patients amounted to a number of 7. The advantage of our immunological profiling is that we could evaluate immunological parameters in this particular group, even though radiological data could not be collected. In these patients, NLR was highly elevated. Three of these patients had relative proportions of G-MDSC within the $CD11b^{+}$ population above 50%. Two other patients exhibited elevated M-MDSC proportions. These results strongly point out the association of MDSCs with hyperprogressive disease, although if their elevation is a cause or consequence, it is still unclear. In our cohort, one patient was initially identified as a hyperprogressor but who turned out to present pseudoprogression. This clinical phenomenon is defined as a sudden increment of tumor size followed by a prolonged tumor regression. Pseudoprogression is associated with significant

infiltration of activated anti-tumor immune cells into the tumor, leading to increase in volume followed by tumor regression. This is a rare condition only present in a single patient in our cohort, in agreement with other studies (Kazandjian et al., 2017). This patient had elevated baseline numbers of G-MDSCs. The clinical progression of this patient suggested that pseudoprogression occurred early following the start of ICB. It could be speculated that pseudoprogression could be generally underestimated with the usual radiological schedules.

Unexpectedly, one of the variables that independently predicted an improved survival was the administration of more than two lines of chemotherapy. The time between disease diagnosis and ICB was more than twice longer in this group than in patients who received ICB after first-line chemotherapy (median 538 vs 300 days, $p = 0.002$). This result could reflect a selection of patients with a less aggressive and slower progressive disease in the group receiving more than two lines of chemotherapy. However, this difference was statistically detected in multivariate tests only when adjusting per chemokine ligand 2 (CCL2) plasma concentrations.

In our cohort, the correlation of CCL2 plasma concentration with clinical response did not reach statistical significance possibly due to our limited sample size (582 vs 347 pg/mL, Mann-Whitney U test $p = 0.182$). Interestingly, CCL2 was found increased in heavily pretreated patients, who previously received docetaxel. This protein, also known as monocyte chemoattractant protein 1 (MCP1), is a member of the CCL chemokine family. CCL2 has pro-inflammatory activities and it has been linked to MDSC and macrophage recruitment into the tumor, and T cell inhibition in the metastatic niche (Qian et al., 2011; Zhou et al., 2019). It has been shown that CCL2 activates PI3K/AKT signaling in the human lung adenocarcinoma A549 cell line, leading to docetaxel resistance (Wang et al., 2018b). This mechanism may explain its correlation with the intrinsic resistance to immunotherapy observed in some patients. Considering these results, and the results shown in this thesis, CCL2 blockade could be combined with immunotherapy in a new therapeutic strategy. It needs to be remarked that

pharmacological inhibition of its receptor is in the early stages of clinical development (Noel et al., 2020).

Docetaxel was the most frequently administered drug after progression to ICB in our study. Chemotherapy acts by inducing tumor cell death, but also by eliminating Tregs and preventing Th2 polarization. Taxanes and other chemotherapy agents at low doses have been shown to eliminate MDSCs, and cause the polarization of M2 macrophages into an M1 phenotype. For example, immunosuppressive myeloid cells are eliminated by paclitaxel and epirrubicin in gastric cancer, leading to improved prognosis (Li et al., 2018). Nevertheless, a balance has to be found in the therapeutic window between toxicity on normal tissues and the immunostimulatory effects of some types of chemotherapy.

The combination of chemotherapy with ICB is currently a reality. Although originally intended to achieve disease control by reducing tumor burden while allowing the organism to generate an adequate immune response, it is likely that treated patients are subjected to elimination of immunosuppressive populations. In the context of NSCLC treatment, a short course (2 cycles) of platinum-based chemotherapy combined with ICB (nivolumab and ipilimumab) leads to early disease control and improves OS, as assessed in the clinical trial Checkmate-9LA phase III (Paz-Ares et al., 2021). The benefit was found for both patients with squamous and non-squamous lung cancer in the subgroup analysis and it has opened the way for the introduction of more immune checkpoint blockers in this clinical setting.

The present study only included patients that had received previous regimes of chemotherapy, but during these last years immune checkpoint blockers have been incorporated into the front-line treatment of NSCLC, based on results from several clinical trials. Pembrolizumab monotherapy is the standard of care in patients presenting PD-L1 tumor expression above 50%. Five-year survival rates in an updated analysis of the KEYNOTE-024 trial were 32% in the pembrolizumab arm and 16% in the chemotherapy arm (Mariamidze and Mezquita, 2021; Reck et al., 2016).

The improvements in OS observed in the KEYNOTE-149 and KEYNOTE-407 clinical trials have also changed first line treatment regimes in both non-squamous and squamous tumors. The combination of pembrolizumab with a doublet of platinum-based chemotherapy plus pemetrexed was found adequate for the treatment of non-squamous tumors, while squamous tumors benefit from the administration of paclitaxel instead of pemetrexed (Gandhi et al., 2018; Paz-Ares et al., 2018).

PD-L1/PD-1 blockers in first line treatment regimens, either in monotherapy or in combination with other drugs, are nowadays the standard of care for advanced NSCLC. There is evidence that combination therapies can overcome primary resistance, responsible for a large proportion of patients that die early. This will result in new challenges to address. The application of next generation sequencing techniques into routine clinical practice will provide molecular details on the heterogeneity of composition of tumors that will eventually improve treatment selection. Tumor mutational burden is a clear example for NSCLC, although not applicable to all cancer types (McGrail et al., 2021a).

In this thesis, we have evaluated 42 soluble factors and immune modulators in a pretreated cohort of NSCLC patients and filtered the results to detect meaningful differences according to prognosis and treatment response. We found evidence that small variations in plasma concentrations of some of the potential biomarkers may have important functional consequences in anti-tumor immunity. Some of the evaluated plasma factors under study were undetectable, while others varied within the range of picograms per mL, with some patients exhibiting values several orders of magnitude above the mean, as previously reported for other cohorts (Chen and Flies, 2013). An interesting possibility is that the concentration of some of these factors depends on their solubility in plasma and their binding to other circulating proteins. Their presence in extracellular vesicles, or exosomes, could be of importance if they retain their functional properties ((Del Re et al., 2018).

From these factors, six of them had prognostic value in the univariate analysis. TIM-3 has co-inhibitory properties, in accordance with its elevated value in less responsive patients as a potential mechanism of intrinsic resistance to treatment. HVEM, on the contrary, is a co-stimulatory molecule that helps in T-cell priming and secretion of Th1-related cytokines, although it can also have immunosuppressive capacities through the interaction with B- and T-lymphocyte attenuator (BTLA) in Tregs (Chen and Flies, 2013; Tao et al., 2008). However, adjusting the results per other clinical variables led to the identification of only one factor with independent prognostic value, that are related to myeloid cell chemoattraction and cell adhesion (CCL2/MCP1 and). This suggests an important interplay between immune cell populations and soluble factors in the circulation and in the tumor microenvironment.

Biomarker identification is a highly complex process and it requires resources in validation and application as part of routine clinical care. We have observed differences in monocytes, neutrophils and MDSCs that could not be adequately detected by conventional techniques used in routine clinical evaluations.

It is expected that an increase in cohort size would increment the statistical power of our study, helping to refine the multivariate analysis and allowing a larger subgroup distribution. Still, we detected heterogeneity in the immunological profiles of different histologies of lung cancer that may be overlooked with the scarcity of other therapeutic options. Many clinical trials include NSCLC as part of the inclusion criteria without an upfront patient selection based on histology. Although subgroup analysis is usually performed, this might occur in landmark trials that have led to drug approvals in immunotherapy. For example, EMA label on pembrolizumab describes its indication as first line therapy in squamous and non-squamous lung carcinomas, based on results of the trials mentioned before (Gandhi et al., 2018; Paz-Ares et al., 2018). However, the difference in indication relies on the chemotherapy doublet that is combined with chemotherapy. We aimed to study whether specific lung cancer histologies differ in the immunological conditions that lead to anti-tumor responses.

In our cohort, tumors could be classified into squamous and non-squamous and in this latter group, adenocarcinomas were by far the most frequent histology. A single patient presented a sarcomatoid tumor but could not be radiologically evaluated because of early death, limiting conclusions. We have found out that some circulating factors and their prognostic impact may affect both histologies, suggesting a possible role on the immune system rather than the tumor.

Adenocarcinomas with elevated levels of fractalkine/CX3CL1 presented better evolution. Although was not statistically significant in the multivariate analysis, it could represent more cohesive and less immunosuppresive tumors that allow better antigen presentation and antitumor responses. In the case of squamous tumors, it was the increased concentration of soluble immune checkpoints that conferred a clearly deleterious prognosis despite a limited patient population. The proangiogenic factor VEGF also differed in its prognostic impact, suggesting a negative effect in tumors of epithelial origin, in contrast with non-squamous tumors. Few studies addressing the pro-oncogenic role of VEGF have compared the differences between lung cancer histologies, and in fact, this role can vary in specific adenocarcinoma subtypes such as the solid pattern (Jung et al., 2021).

Another interesting possibility is the immunological profiling in plasma of other less frequent but aggressive lung cancer types, such as SCLC, which were not included in our study. In this context, atezolizumab in combination with chemotherapy was recently approved in Europe as a first-line treatment, independently of tumor expression of PD-L1 (Horn et al., 2018).

Biomarker identification and validation in immunology is highly complex due to the variety of biological factors in play. Generally speaking, there is possibly not a single feature that can predict treatment response by itself. There are patient-specific factors and tumor-specific factors that include the composition of the tumor microenvironment, and its interactions with other cell types and with specific treatments. These factors are connected and highly dynamic over time, making biomarker identification an elusive task.

Coordination between biologists, molecular pathologists and oncologists is a necessity as part of a broad “precision immuno-oncology” policy. A series of international recommendations (REMARK, PROGRESS, TMUGS) have been proposed to improve the validation process of biomarkers, addressing variability at several levels: inter-individual, processing and analytic variability.

The incorporation of mutational information through NGS into clinical practice will improve patient selection but will possibly require the application of bioinformatic approaches to integrate data and ease the decision-making process. Molecular tumor boards can be of help in clinical practice to cover issues of accessibility, homogeneous testing and updated clinical management in a context of rapidly changing technological advances (Walk et al., 2020). The extent of these advances may even influence trial design, and data interpretation with the support of biostatisticians. The dynamic changes in the hazard ratios after ICB have put a limit to the utility of classical endpoints and statistical tests that rely on proportionality of hazards. Alternative analytical methods include the changes of risk over time such as the Royston-Parmar spline model. These methods will be of interest in immuno-oncology trial design and result interpretation in the near future (Castanon et al., 2020; Ferrara et al., 2018b).

The consideration that the immune response unchained by checkpoint blockade has not only a local effect in the tumor microenvironment, but very importantly a systemic modulation of the immune system, is an important lesson for medical oncologists that prescribe immunotherapies. This requires a coordination of many organs and systems that contribute to the overall well-being of the patient. The systemic immune states are significantly different depending on the histology of the primary tumor, the systemic treatments administered to the patient, and intrinsic patient-specific characteristics. One of the conclusions that can be drawn from this thesis and from other published studies is that the more detailed the immunological profiles are, the most accurate the prognostic and predictive correlators become.

Despite recent developments in precision oncology, the “tumor-agnostic” therapeutic strategies and the implementation of NGS techniques in the management of advanced cancer, the importance of an accurate pathological diagnosis and an appropriate clinical management of lung cancer cannot be overshadowed.

6. Conclusions

- Nutritional status measured by concentrations of cholesterol and albumin, as well as body composition assessment by computed tomography were not predictors of anti-tumoral response in our cohort.
- Patients with advanced NSCLC not responding to ICB immunotherapy after chemotherapy failure present increased neutrophil counts in peripheral blood. This phenomenon is accelerated prior to clinical deterioration and death of the patient.
- Monocyte and neutrophil concentrations, identified by an in-depth phenotyping and characterization of myeloid cells, were shown to be associated with antitumoral responses. PD-L1 expression levels on these myeloid populations can be associated with potential responses to ICB treatment.
- Plasma concentrations of circulating TIM-3, HVEM, CCL2/MCP-1, fractalkine, IFNγ, IL-17A, and VEGF prior to treatment initiation were associated with treatment activity and prognosis.
- Immune-mediated anti-tumor responses varied depending on the histopathology of the primary tumor in NSCLC. Patients with SCC presenting elevated concentrations of soluble immune checkpoints did not respond to PD-1/PD-L1 blockade immunotherapies.
- In a multivariate analysis of our cohort, the number of prior lines of treatment, an ECOG PS higher than 2, the number of metastatic lesions including those in the liver, and an increment of circulating neutrophils, soluble CCL2 and IL-17a were independent predictors of survival.

7. Bibliography

Ameratunga, M., Chenard-Poirier, M., Moreno Candilejo, I., Pedregal, M., Lui, A., Dolling, D., Aversa, C., Ingles Garces, A., Ang, J.E., Banerji, U.*, et al.* (2018). Neutrophil-lymphocyte ratio kinetics in patients with advanced solid tumours on phase I trials of PD-1/PD-L1 inhibitors. Eur J Cancer *89*, 56-63.

Anagnostou, V., Niknafs, N., Marrone, K., Bruhm, D.C., White, J.R., Naidoo, J., Hummelink, K., Monkhorst, K., Lalezari, F., Lanis, M.*, et al.* (2020). Multimodal genomic features predict outcome of immune checkpoint blockade in non-small-cell lung cancer. Nat Cancer *1*, 99-111.

Anic, G.M., Park, Y., Subar, A.F., Schap, T.E., and Reedy, J. (2016). Index-based dietary patterns and risk of lung cancer in the NIH-AARP diet and health study. Eur J Clin Nutr *70*, 123-129.

Antonia, S.J., Borghaei, H., Ramalingam, S.S., Horn, L., De Castro Carpeno, J., Pluzanski, A., Burgio, M.A., Garassino, M., Chow, L.Q.M., Gettinger, S.*, et al.* (2019). Four-year survival with nivolumab in patients with previously treated advanced non-small-cell lung cancer: a pooled analysis. Lancet Oncol *20*, 1395-1408.

Antonia, S.J., Villegas, A., Daniel, D., Vicente, D., Murakami, S., Hui, R., Yokoi, T., Chiappori, A., Lee, K.H., de Wit, M.*, et al.* (2017). Durvalumab after Chemoradiotherapy in Stage III Non-Small-Cell Lung Cancer. N Engl J Med *377*, 1919-1929.

Arasanz, H., Gato-Canas, M., Zuazo, M., Ibanez-Vea, M., Breckpot, K., Kochan, G., and Escors, D. (2017). PD1 signal transduction pathways in T cells. Oncotarget *8*, 51936-51945.

Arasanz, H., Zuazo, M., Bocanegra, A., Gato, M., Martinez-Aguillo, M., Morilla, I., Fernandez, G., Hernandez, B., Lopez, P., Alberdi, N.*, et al.* (2020). Early detection of hyperprogressive disease in non-small cell lung cancer by monitoring of systemic T cell dynamics. Cancers (Basel) *12(2)*, 344-358.

Arbour, K.C., Jordan, E., Kim, H.R., Dienstag, J., Yu, H.A., Sanchez-Vega, F., Lito, P., Berger, M., Solit, D.B., Hellmann, M.*, et al.* (2018). Effects of Co-occurring Genomic Alterations on Outcomes in Patients with KRAS-Mutant Non-Small Cell Lung Cancer. Clin Cancer Res *24*, 334-340.

Bigot, F., Castanon, E., Baldini, C., Hollebecque, A., Carmona, A., Postel-Vinay, S., Angevin, E., Armand, J.P., Ribrag, V., Aspeslagh, S.*, et al.* (2017). Prospective validation of a prognostic score for patients in immunotherapy phase I trials: The Gustave Roussy Immune Score (GRIm-Score). Eur J Cancer *84*, 212-218.

Bocanegra, A., Fernandez-Hinojal, G., Zuazo-Ibarra, M., Arasanz, H., Garcia-Granda, M.J., Hernandez, C., Ibanez, M., Hernandez-Marin, B., Martinez-Aguillo, M., Lecumberri, M.J*., et al.* (2019). PD-L1 Expression in Systemic Immune Cell Populations as a Potential Predictive Biomarker of Responses to PD-L1/PD-1 Blockade Therapy in Lung Cancer. Int J Mol Sci *20(7)*, 1631-1644.

Borghaei, H., Paz-Ares, L., Horn, L., Spigel, D.R., Steins, M., Ready, N.E., Chow, L.Q., Vokes, E.E., Felip, E., Holgado, E*., et al.* (2015). Nivolumab versus Docetaxel in Advanced Nonsquamous Non-Small-Cell Lung Cancer. N Engl J Med *373*, 1627-1639.

Botticelli, A., Cerbelli, B., Lionetto, L., Zizzari, I., Salati, M., Pisano, A., Federica, M., Simmaco, M., Nuti, M., and Marchetti, P. (2018). Can IDO activity predict primary resistance to anti-PD-1 treatment in NSCLC? Journal of translational medicine *16(1)*, 219-226.

Brahmer, J., Reckamp, K.L., Baas, P., Crino, L., Eberhardt, W.E., Poddubskaya, E., Antonia, S., Pluzanski, A., Vokes, E.E., Holgado, E*., et al.* (2015). Nivolumab versus Docetaxel in Advanced Squamous-Cell Non-Small-Cell Lung Cancer. N Engl J Med *373*, 123-135.

Cabrerizo, S., Cuadras, D., Gomez-Busto, F., Artaza-Artabe, I., Marin-Ciancas, F., and Malafarina, V. (2015). Serum albumin and health in older people: Review and meta analysis. Maturitas *81*, 17-27.

Campbell, J.D., Alexandrov, A., Kim, J., Wala, J., Berger, A.H., Pedamallu, C.S., Shukla, S.A., Guo, G., Brooks, A.N., Murray, B.A*., et al.* (2016). Distinct patterns of somatic genome alterations in lung adenocarcinomas and squamous cell carcinomas. Nature genetics *48*, 607-616.

Campbell, J.D., Yau, C., Bowlby, R., Liu, Y., Brennan, K., Fan, H., Taylor, A.M., Wang, C., Walter, V., Akbani, R*., et al.* (2018). Genomic, Pathway Network, and Immunologic Features Distinguishing Squamous Carcinomas. Cell reports *23*, 194-212 e196.

Cancer Genome Atlas Research, N. (2012). Comprehensive genomic characterization of squamous cell lung cancers. Nature *489*, 519-525.

Cao, D., Xu, H., Xu, X., Guo, T., and Ge, W. (2018). A reliable and feasible way to predict the benefits of Nivolumab in patients with non-small cell lung cancer: a pooled analysis of 14 retrospective studies. Oncoimmunology *7(11)*, e1507262.

Castanon, E., Sanchez-Arraez, A., Alvarez-Mancenido, F., Jimenez-Fonseca, P., and Carmona-Bayonas, A. (2020). Critical reappraisal of phase III trials with immune checkpoint inhibitors in non-proportional hazards settings. Eur J Cancer *136*, 159-168.

Chen, L., and Flies, D.B. (2013). Molecular mechanisms of T cell co-stimulation and co-inhibition. Nat Rev Immunol *13*, 227-242.

Chowell, D., Morris, L.G.T., Grigg, C.M., Weber, J.K., Samstein, R.M., Makarov, V., Kuo, F., Kendall, S.M., Requena, D., Riaz, N.*, et al.* (2018). Patient HLA class I genotype influences cancer response to checkpoint blockade immunotherapy. Science (New York, NY *359*, 582-587.

Conroy, M.J., and Lysaght, J. (2020). CX3CL1 Signaling in the Tumor Microenvironment. Adv Exp Med Biol *1231*, 1-12.

Cortellini, A., Verna, L., Porzio, G., Bozzetti, F., Palumbo, P., Masciocchi, C., Cannita, K., Parisi, A., Brocco, D., Tinari, N.*, et al.* (2019). Predictive value of skeletal muscle mass for immunotherapy with nivolumab in non-small cell lung cancer patients: A "hypothesis-generator" preliminary report. Thorac Cancer *10*, 347-351.

Costantini, A., Julie, C., Dumenil, C., Helias-Rodzewicz, Z., Tisserand, J., Dumoulin, J., Giraud, V., Labrune, S., Chinet, T., Emile, J.F.*, et al.* (2018). Predictive role of plasmatic biomarkers in advanced non-small cell lung cancer treated by nivolumab. Oncoimmunology *7(8)*, e1452581.

de Castro, J., Cobo, M., Isla, D., Puente, J., Reguart, N., Cabeza, B., Gayete, A., Sanchez, M., Torres, M.I., and Ferreiros, J. (2015). Recommendations for radiological diagnosis and assessment of treatment response in lung cancer: a national consensus statement by the Spanish Society of Medical Radiology and the Spanish Society of Medical Oncology. Clin Transl Oncol *17*, 11-23.

de Goeje, P.L., Bezemer, K., Heuvers, M.E., Dingemans, A.C., Groen, H.J., Smit, E.F., Hoogsteden, H.C., Hendriks, R.W., Aerts, J.G., and Hegmans, J.P. (2015). Immunoglobulin-like transcript 3 is expressed by myeloid-derived suppressor cells and correlates with survival in patients with non-small cell lung cancer. Oncoimmunology *4(7)*, e1014242.

de Koning, H.J., van der Aalst, C.M., de Jong, P.A., Scholten, E.T., Nackaerts, K., Heuvelmans, M.A., Lammers, J.J., Weenink, C., Yousaf-Khan, U., Horeweg, N.*, et al.* (2020). Reduced Lung-Cancer Mortality with Volume CT Screening in a Randomized Trial. N Engl J Med *382*, 503-513.

Del Re, M., Marconcini, R., Pasquini, G., Rofi, E., Vivaldi, C., Bloise, F., Restante, G., Arrigoni, E., Caparello, C., Bianco, M.G.*, et al.* (2018). PD-L1 mRNA expression in plasma-derived exosomes is associated with response to anti-PD-1 antibodies in melanoma and NSCLC. Br J Cancer *118*, 820-824.

Detterbeck, F.C., Boffa, D.J., Kim, A.W., and Tanoue, L.T. (2017). The Eighth Edition Lung Cancer Stage Classification. Chest *151*, 193-203.

Diem, S., Schmid, S., Krapf, M., Flatz, L., Born, D., Jochum, W., Templeton, A.J., and Fruh, M. (2017). Neutrophil-to-Lymphocyte ratio (NLR) and Platelet-to-Lymphocyte ratio (PLR) as prognostic markers in patients with non-small cell lung cancer (NSCLC) treated with nivolumab. Lung Cancer *111*, 176-181.

Diskin, B., Adam, S., Cassini, M.F., Sanchez, G., Liria, M., Aykut, B., Buttar, C., Li, E., Sundberg, B., Salas, R.D.*, et al.* (2020). PD-L1 engagement on T cells promotes self-tolerance and suppression of neighboring macrophages and effector T cells in cancer. Nat Immunol *21*, 442-454.

Dong, M.P., Enomoto, M., Thuy, L.T.T., Hai, H., Hieu, V.N., Hoang, D.V., Iida-Ueno, A., Odagiri, N., Amano-Teranishi, Y., Hagihara, A.*, et al.* (2020). Clinical significance of circulating soluble immune checkpoint proteins in sorafenib-treated patients with advanced hepatocellular carcinoma. Sci Rep *10(1)*, 3392-3402.

Duan, Q., Zhang, H., Zheng, J., and Zhang, L. (2020). Turning Cold into Hot: Firing up the Tumor Microenvironment. Trends Cancer *6*, 605-618.

Eisenhauer, E.A., Therasse, P., Bogaerts, J., Schwartz, L.H., Sargent, D., Ford, R., Dancey, J., Arbuck, S., Gwyther, S., Mooney, M.*, et al.* (2009). New response evaluation criteria in solid tumours: revised RECIST guideline (version 1.1). Eur J Cancer *45*, 228-247.

Escors, D., Gato-Canas, M., Zuazo, M., Arasanz, H., Garcia-Granda, M.J., Vera, R., and Kochan, G. (2018). The intracellular signalosome of PD-L1 in cancer cells. Signal transduction and targeted therapy *3*, 26-35.

Ferrara, R., Mezquita, L., Texier, M., Lahmar, J., Audigier-Valette, C., Tessonnier, L., Mazieres, J., Zalcman, G., Brosseau, S., Le Moulec, S.*, et al.* (2018a). Hyperprogressive Disease in Patients With Advanced Non-Small Cell Lung Cancer Treated With PD-1/PD-L1 Inhibitors or With Single-Agent Chemotherapy. JAMA oncology *4*, 1543-1552.

Ferrara, R., Pilotto, S., Caccese, M., Grizzi, G., Sperduti, I., Giannarelli, D., Milella, M., Besse, B., Tortora, G., and Bria, E. (2018b). Do immune checkpoint inhibitors need new studies methodology? J Thorac Dis *10*, S1564-S1580.

Fife, B.T., and Bluestone, J.A. (2008). Control of peripheral T-cell tolerance and autoimmunity via the CTLA-4 and PD-1 pathways. Immunological reviews *224*, 166-182.

Forschner, A., Hilke, F.J., Bonzheim, I., Gschwind, A., Demidov, G., Amaral, T., Ossowski, S., Riess, O., Schroeder, C., Martus, P.*, et al.* (2020). MDM2, MDM4 and EGFR Amplifications and Hyperprogression in Metastatic Acral and Mucosal Melanoma. Cancers (Basel) *12(3)*, 540-556.

Freeman-Keller, M., Kim, Y., Cronin, H., Richards, A., Gibney, G., and Weber, J.S. (2016). Nivolumab in Resected and Unresectable Metastatic Melanoma: Characteristics of Immune-Related Adverse Events and Association with Outcomes. Clin Cancer Res *22*, 886-894.

Fujimoto, D., Yoshioka, H., Kataoka, Y., Morimoto, T., Hata, T., Kim, Y.H., Tomii, K., Ishida, T., Hirabayashi, M., Hara, S.*, et al.* (2019). Pseudoprogression in

Previously Treated Patients with Non-Small Cell Lung Cancer Who Received Nivolumab Monotherapy. J Thorac Oncol *14*, 468-474.

Galon, J., Mlecnik, B., Bindea, G., Angell, H.K., Berger, A., Lagorce, C., Lugli, A., Zlobec, I., Hartmann, A., Bifulco, C.*, et al.* (2014). Towards the introduction of the 'Immunoscore' in the classification of malignant tumours. J Pathol *232*, 199-209.

Gandara, D.R., Riess, J.W., and Lara, P.N., Jr. (2018). In Search of an Oncogene Driver for Squamous Lung Cancer. JAMA oncology *4*, 1197-1198.

Gandhi, L., Rodriguez-Abreu, D., Gadgeel, S., Esteban, E., Felip, E., De Angelis, F., Domine, M., Clingan, P., Hochmair, M.J., Powell, S.F.*, et al.* (2018). Pembrolizumab plus Chemotherapy in Metastatic Non-Small-Cell Lung Cancer. N Engl J Med *378*, 2078-2092.

Gato-Canas, M., Zuazo, M., Arasanz, H., Ibanez-Vea, M., Lorenzo, L., Fernandez-Hinojal, G., Vera, R., Smerdou, C., Martisova, E., Arozarena, I.*, et al.* (2017). PDL1 Signals through Conserved Sequence Motifs to Overcome Interferon-Mediated Cytotoxicity. Cell reports *20*, 1818-1829.

Gettinger, S.N., Horn, L., Gandhi, L., Spigel, D.R., Antonia, S.J., Rizvi, N.A., Powderly, J.D., Heist, R.S., Carvajal, R.D., Jackman, D.M.*, et al.* (2015). Overall Survival and Long-Term Safety of Nivolumab (Anti-Programmed Death 1 Antibody, BMS-936558, ONO-4538) in Patients With Previously Treated Advanced Non-Small-Cell Lung Cancer. J Clin Oncol *33*, 2004-2012.

Gu, D., Ao, X., Yang, Y., Chen, Z., and Xu, X. (2018). Soluble immune checkpoints in cancer: production, function and biological significance. J Immunother Cancer *6*, 132-146.

Gu, X.B., Tian, T., Tian, X.J., and Zhang, X.J. (2015). Prognostic significance of neutrophil-to-lymphocyte ratio in non-small cell lung cancer: a meta-analysis. Sci Rep *5*, 12493-12502.

Gubin, M.M., Esaulova, E., Ward, J.P., Malkova, O.N., Runci, D., Wong, P., Noguchi, T., Arthur, C.D., Meng, W., Alspach, E.*, et al.* (2018). High-Dimensional Analysis Delineates Myeloid and Lymphoid Compartment Remodeling during Successful Immune-Checkpoint Cancer Therapy. Cell *175*, 1014-1030 e1019.

Hanahan, D., and Weinberg, R.A. (2011). Hallmarks of cancer: the next generation. Cell *144*, 646-674.

Herbst, R.S., Baas, P., Kim, D.W., Felip, E., Perez-Gracia, J.L., Han, J.Y., Molina, J., Kim, J.H., Arvis, C.D., Ahn, M.J.*, et al.* (2016). Pembrolizumab versus docetaxel for previously treated, PD-L1-positive, advanced non-small-cell lung cancer (KEYNOTE-010): a randomised controlled trial. Lancet *387*, 1540-1550.

Hofmarcher, T., Lindgren, P., Wilking, N., and Jonsson, B. (2020). The cost of cancer in Europe 2018. Eur J Cancer *129*, 41-49.

Horn, L., Mansfield, A.S., Szczesna, A., Havel, L., Krzakowski, M., Hochmair, M.J., Huemer, F., Losonczy, G., Johnson, M.L., Nishio, M.*, et al.* (2018). First-Line Atezolizumab plus Chemotherapy in Extensive-Stage Small-Cell Lung Cancer. N Engl J Med *379*, 2220-2229.

Howard, R., Kanetsky, P.A., and Egan, K.M. (2019). Exploring the prognostic value of the neutrophil-to-lymphocyte ratio in cancer. Sci Rep *9(1)*, 19673-19683.

Hui, E., Cheung, J., Zhu, J., Su, X., Taylor, M.J., Wallweber, H.A., Sasmal, D.K., Huang, J., Kim, J.M., Mellman, I.*, et al.* (2017). T cell costimulatory receptor CD28 is a primary target for PD-1-mediated inhibition. Science (New York, NY *355*, 1428-1433.

Ibañez-Vea, M., Zuazo, M., Gato, M., Arasanz, H., Fernandez-Hinojal, G., Escors, D., and Kochan, G. (2018). Myeloid-Derived Suppressor Cells in the Tumor Microenvironment: Current Knowledge and Future Perspectives. Arch Immunol Ther Exp (Warsz) *66*, 113-123.

Iseki, K., Yamazato, M., Tozawa, M., and Takishita, S. (2002). Hypocholesterolemia is a significant predictor of death in a cohort of chronic hemodialysis patients. Kidney international *61*, 1887-1893.

Jin, J., Yang, L., Liu, D., and Li, W. (2020). Association of the neutrophil to lymphocyte ratio and clinical outcomes in patients with lung cancer receiving immunotherapy: a meta-analysis. BMJ Open *10*, e035031.

Jung, W.Y., Min, K.W., and Oh, Y.H. (2021). Increased VEGF-A in solid type of lung adenocarcinoma reduces the patients' survival. Sci Rep *11(1)*, 1321-1330.

Kagamu, H., Kitano, S., Yamaguchi, O., Yoshimura, K., Horimoto, K., Kitazawa, M., Fukui, K., Shiono, A., Mouri, A., Nishihara, F.*, et al.* (2020). CD4(+) T-cell Immunity in the Peripheral Blood Correlates with Response to Anti-PD-1 Therapy. Cancer immunology research *8*, 334-344.

Kamphorst, A.O., Pillai, R.N., Yang, S., Nasti, T.H., Akondy, R.S., Wieland, A., Sica, G.L., Yu, K., Koenig, L., Patel, N.T.*, et al.* (2017a). Proliferation of PD-1+ CD8 T cells in peripheral blood after PD-1-targeted therapy in lung cancer patients. Proc Natl Acad Sci U S A *114*, 4993-4998.

Kamphorst, A.O., Wieland, A., Nasti, T., Yang, S., Zhang, R., Barber, D.L., Konieczny, B.T., Daugherty, C.Z., Koenig, L., Yu, K.*, et al.* (2017b). Rescue of exhausted CD8 T cells by PD-1-targeted therapies is CD28-dependent. Science (New York, NY *355(6332)*, 1423-1427.

Kang, D.H., Park, C.K., Chung, C., Oh, I.J., Kim, Y.C., Park, D., Kim, J., Kwon, G.C., Kwon, I., Sun, P.*, et al.* (2020). Baseline Serum Interleukin-6 Levels Predict

the Response of Patients with Advanced Non-small Cell Lung Cancer to PD-1/PD-L1 Inhibitors. Immune network *20(3)*, e27-e38.

Karwacz, K., Bricogne, C., MacDonald, D., Arce, F., Bennett, C.L., Collins, M., and Escors, D. (2011). PD-L1 co-stimulation contributes to ligand-induced T cell receptor down-modulation on CD8+ T cells. EMBO Mol Med *3*, 581-592.

Kazandjian, D., Keegan, P., Suzman, D.L., Pazdur, R., and Blumenthal, G.M. (2017). Characterization of outcomes in patients with metastatic non-small cell lung cancer treated with programmed cell death protein 1 inhibitors past RECIST version 1.1-defined disease progression in clinical trials. Semin Oncol *44(1)*, 3-7.

Keller, U. (2019). Nutritional Laboratory Markers in Malnutrition. J Clin Med *8(6)*, 775-786.

Kim, J.Y., Lee, K.H., Kang, J., Borcoman, E., Saada-Bouzid, E., Kronbichler, A., Hong, S.H., de Rezende, L.F.M., Ogino, S., Keum, N.*, et al.* (2019). Hyperprogressive Disease during Anti-PD-1 (PDCD1) / PD-L1 (CD274) Therapy: A Systematic Review and Meta-Analysis. Cancers (Basel) *11(11)*, 1699-1710.

Kos, M., Hocazade, C., Kos, F.T., Uncu, D., Karakas, E., Dogan, M., Uncu, H.G., Yildirim, N., and Zengin, N. (2016). Prognostic role of pretreatment platelet/lymphocyte ratio in patients with non-small cell lung cancer. Wien Klin Wochenschr *128*, 635-640.

Le, D.T., Uram, J.N., Wang, H., Bartlett, B.R., Kemberling, H., Eyring, A.D., Skora, A.D., Luber, B.S., Azad, N.S., Laheru, D.*, et al.* (2015). PD-1 Blockade in Tumors with Mismatch-Repair Deficiency. N Engl J Med *372*, 2509-2520.

Le Pechoux, C., Pourel, N., Barlesi, F., Faivre-Finn, C., Lerouge, D., Zalcman, G., Antoni, D., Lamezec, B., Nestle, U., Boisselier, P.*, et al.* (2020). An international randomized trial, comparing post-operative conformal radiotherapy (PORT) to no PORT, in patients with completely resected non-small cell lung cancer (NSCLC) and mediastinal N2 involvement: Primary end-point analysis of LungART (IFCT-0503, UK NCRI, SAKK) NCT00410683. Annals of Oncology *31*, S1178-S1178.

Leach, D.R., Krummel, M.F., and Allison, J.P. (1996). Enhancement of antitumor immunity by CTLA-4 blockade. Science (New York, NY *271*, 1734-1736.

Lee, C.S., Devoe, C.E., Zhu, X., Fishbein, J.S., and Seetharamu, N. (2020). Pretreatment nutritional status and response to checkpoint inhibitors in lung cancer. Lung cancer management *9(2)*, LMT31.

Legoupil, C., Debieuvre, D., Marabelle, A., Michiels, S., Kapso, R., Besse, B., and Bonastre, J. (2020). A microsimulation model to assess the economic impact of immunotherapy in non-small cell lung cancer. ERJ Open Res *6(2)*, 00174-02019.

Li, N., Han, D., Sun, J., Li, Y., Zhang, J., Zhang, Y., Liu, M., Peng, R., Wang, H., Zhang, Z.*, et al.* (2018). Subtypes of MDSCs in mechanisms and prognosis of gastric cancer and are inhibited by epirubicin and paclitaxel. Discov Med *25*, 99-112.

Lin, G.N., Peng, J.W., Xiao, J.J., Liu, D.Y., and Xia, Z.J. (2014). Prognostic impact of circulating monocytes and lymphocyte-to-monocyte ratio on previously untreated metastatic non-small cell lung cancer patients receiving platinum-based doublet. Medical oncology (Northwood, London, England) *31(7)*, 70-76.

Liu, J., Li, S., Zhang, S., Liu, Y., Ma, L., Zhu, J., Xin, Y., Wang, Y., Yang, C., and Cheng, Y. (2019). Systemic immune-inflammation index, neutrophil-to-lymphocyte ratio, platelet-to-lymphocyte ratio can predict clinical outcomes in patients with metastatic non-small-cell lung cancer treated with nivolumab. J Clin Lab Anal *33*, e22964.

Lo Russo, G., Moro, M., Sommariva, M., Cancila, V., Boeri, M., Centonze, G., Ferro, S., Ganzinelli, M., Gasparini, P., Huber, V.*, et al.* (2019). Antibody-Fc/FcR Interaction on Macrophages as a Mechanism for Hyperprogressive Disease in Non-small Cell Lung Cancer Subsequent to PD-1/PD-L1 Blockade. Clin Cancer Res *25*, 989-999.

Mariamidze, E., and Mezquita, L. (2021). ESMO20 YO for YO: highlights on metastatic NSCLC-Keynote 024 update. ESMO Open *6(1)*, 100022.

Martins, F., Sofiya, L., Sykiotis, G.P., Lamine, F., Maillard, M., Fraga, M., Shabafrouz, K., Ribi, C., Cairoli, A., Guex-Crosier, Y.*, et al.* (2019). Adverse effects of immune-checkpoint inhibitors: epidemiology, management and surveillance. Nat Rev Clin Oncol *16*, 563-580.

Masucci, M.T., Minopoli, M., Del Vecchio, S., and Carriero, M.V. (2020). The Emerging Role of Neutrophil Extracellular Traps (NETs) in Tumor Progression and Metastasis. Front Immunol *11*, 1749.

Mazieres, J., Rittmeyer, A., Gadgeel, S., Hida, T., Gandara, D.R., Cortinovis, D.L., Barlesi, F., Yu, W., Matheny, C., Ballinger, M.*, et al.* (2021). Atezolizumab Versus Docetaxel in Pretreated Patients With NSCLC: Final Results From the Randomized Phase 2 POPLAR and Phase 3 OAK Clinical Trials. J Thorac Oncol *16(1)*, 140-150.

Mazzaschi, G., Minari, R., Zecca, A., Cavazzoni, A., Ferri, V., Mori, C., Squadrilli, A., Bordi, P., Buti, S., Bersanelli, M.*, et al.* (2020). Soluble PD-L1 and Circulating CD8+PD-1+ and NK Cells Enclose a Prognostic and Predictive Immune Effector Score in Immunotherapy Treated NSCLC patients. Lung Cancer *148*, 1-11.

McGrail, D.J., Pilie, P.G., Rashid, N.U., Voorwerk, L., Slagter, M., Kok, M., Jonasch, E., Khasraw, M., Heimberger, A.B., Lim, B.*, et al.* (2021a). High tumor mutation burden fails to predict immune checkpoint blockade response across all cancer types. Ann Oncol *32*, 661-672.

McGrail, D.J., Pilie, P.G., Rashid, N.U., Voorwerk, L., Slagter, M., Kok, M., Jonasch, E., Khasraw, M., Heimberger, A.B., *et al.* (2021b). High tumor mutation burden fails to predict immune checkpoint blockade response across all cancer types. Ann Oncol *32(5)*, 661-672.

McGranahan, N., Furness, A.J., Rosenthal, R., Ramskov, S., Lyngaa, R., Saini, S.K., Jamal-Hanjani, M., Wilson, G.A., Birkbak, N.J., Hiley, C.T., *et al.* (2016). Clonal neoantigens elicit T cell immunoreactivity and sensitivity to immune checkpoint blockade. Science (New York, NY *351(6280)*, 1463-1469.

Mezquita, L., Auclin, E., Ferrara, R., Charrier, M., Remon, J., Planchard, D., Ponce, S., Ares, L.P., Leroy, L., Audigier-Valette, C., *et al.* (2018). Association of the Lung Immune Prognostic Index With Immune Checkpoint Inhibitor Outcomes in Patients With Advanced Non-Small Cell Lung Cancer. JAMA oncology *4(3)*, 351-357.

Nabet, B.Y., Esfahani, M.S., Moding, E.J., Hamilton, E.G., Chabon, J.J., Rizvi, H., Steen, C.B., Chaudhuri, A.A., Liu, C.L., Hui, A.B., *et al.* (2020). Noninvasive Early Identification of Therapeutic Benefit from Immune Checkpoint Inhibition. Cell *183*, 363-376 e313.

Nakamura, Y., Watanabe, R., Katagiri, M., Saida, Y., Katada, N., Watanabe, M., Okamoto, Y., Asai, K., Enomoto, T., Kiribayashi, T., *et al.* (2016). Neutrophil/lymphocyte ratio has a prognostic value for patients with terminal cancer. World J Surg Oncol *14*, 148-153.

Negrao, M.V., Lam, V.K., Reuben, A., Rubin, M.L., Landry, L.L., Roarty, E.B., Rinsurongkawong, W., Lewis, J., Roth, J.A., Swisher, S.G., *et al.* (2019). PD-L1 Expression, Tumor Mutational Burden, and Cancer Gene Mutations Are Stronger Predictors of Benefit from Immune Checkpoint Blockade than HLA Class I Genotype in Non-Small Cell Lung Cancer. J Thorac Oncol *14*, 1021-1031.

Nesline, M.K., Knight, T., Colman, S., and Patel, K. (2020). Economic Burden of Checkpoint Inhibitor Immunotherapy for the Treatment of Non-Small Cell Lung Cancer in US Clinical Practice. Clin Ther *42*, 1682-1698 e1687.

Noel, M., O'Reilly, E.M., Wolpin, B.M., Ryan, D.P., Bullock, A.J., Britten, C.D., Linehan, D.C., Belt, B.A., Gamelin, E.C., Ganguly, B., *et al.* (2020). Phase 1b study of a small molecule antagonist of human chemokine (C-C motif) receptor 2 (PF-04136309) in combination with nab-paclitaxel/gemcitabine in first-line treatment of metastatic pancreatic ductal adenocarcinoma. Investigational new drugs *38*, 800-811.

Paz-Ares, L., Ciuleanu, T.E., Cobo, M., Schenker, M., Zurawski, B., Menezes, J., Richardet, E., Bennouna, J., Felip, E., Juan-Vidal, O., *et al.* (2021). First-line nivolumab plus ipilimumab combined with two cycles of chemotherapy in patients with non-small-cell lung cancer (CheckMate 9LA): an international, randomised, open-label, phase 3 trial. Lancet Oncol *22*, 198-211.

Paz-Ares, L., Luft, A., Vicente, D., Tafreshi, A., Gumus, M., Mazieres, J., Hermes, B., Cay Senler, F., Csoszi, T., Fulop, A.*, et al.* (2018). Pembrolizumab plus Chemotherapy for Squamous Non-Small-Cell Lung Cancer. N Engl J Med *379*, 2040-2051.

Peng, B., Wang, Y.H., Liu, Y.M., and Ma, L.X. (2015). Prognostic significance of the neutrophil to lymphocyte ratio in patients with non-small cell lung cancer: a systemic review and meta-analysis. Int J Clin Exp Med *8*, 3098-3106.

Pignon, J.P., Tribodet, H., Scagliotti, G.V., Douillard, J.Y., Shepherd, F.A., Stephens, R.J., Dunant, A., Torri, V., Rosell, R., Seymour, L.*, et al.* (2008). Lung adjuvant cisplatin evaluation: a pooled analysis by the LACE Collaborative Group. J Clin Oncol *26(21)*, 3552-3559.

Pinato, D.J., Howlett, S., Ottaviani, D., Urus, H., Patel, A., Mineo, T., Brock, C., Power, D., Hatcher, O., Falconer, A.*, et al.* (2019). Association of Prior Antibiotic Treatment With Survival and Response to Immune Checkpoint Inhibitor Therapy in Patients With Cancer. JAMA oncology *5*, 1774-1778.

Planchard, D., Popat, S., Kerr, K., Novello, S., Smit, E.F., Faivre-Finn, C., Mok, T.S., Reck, M., Van Schil, P.E., Hellmann, M.D.*, et al.* (2018). Metastatic non-small cell lung cancer: ESMO Clinical Practice Guidelines for diagnosis, treatment and follow-up. Ann Oncol *29*, iv192-iv237.

Qian, B.Z., Li, J., Zhang, H., Kitamura, T., Zhang, J., Campion, L.R., Kaiser, E.A., Snyder, L.A., and Pollard, J.W. (2011). CCL2 recruits inflammatory monocytes to facilitate breast-tumour metastasis. Nature *475*, 222-225.

Reck, M., Rodriguez-Abreu, D., Robinson, A.G., Hui, R., Csoszi, T., Fulop, A., Gottfried, M., Peled, N., Tafreshi, A., Cuffe, S.*, et al.* (2016). Pembrolizumab versus Chemotherapy for PD-L1-Positive Non-Small-Cell Lung Cancer. N Engl J Med *375*, 1823-1833.

Ringel, A.E., Drijvers, J.M., Baker, G.J., Catozzi, A., Garcia-Canaveras, J.C., Gassaway, B.M., Miller, B.C., Juneja, V.R., Nguyen, T.H., Joshi, S.*, et al.* (2020). Obesity Shapes Metabolism in the Tumor Microenvironment to Suppress Anti-Tumor Immunity. Cell *183*, 1848-1866 e1826.

Rittmeyer, A., Barlesi, F., Waterkamp, D., Park, K., Ciardiello, F., von Pawel, J., Gadgeel, S.M., Hida, T., Kowalski, D.M., Dols, M.C.*, et al.* (2017). Atezolizumab versus docetaxel in patients with previously treated non-small-cell lung cancer (OAK): a phase 3, open-label, multicentre randomised controlled trial. Lancet *389*, 255-265.

Rizvi, N.A., Mazieres, J., Planchard, D., Stinchcombe, T.E., Dy, G.K., Antonia, S.J., Horn, L., Lena, H., Minenza, E., Mennecier, B.*, et al.* (2015). Activity and safety of nivolumab, an anti-PD-1 immune checkpoint inhibitor, for patients with advanced, refractory squamous non-small-cell lung cancer (CheckMate 063): a phase 2, single-arm trial. Lancet Oncol *16*, 257-265.

Ronchetti, S., Ricci, E., Migliorati, G., Gentili, M., and Riccardi, C. (2018). How Glucocorticoids Affect the Neutrophil Life. Int J Mol Sci *19(12)*, 4090-4102.

Routy, B., Le Chatelier, E., Derosa, L., Duong, C.P.M., Alou, M.T., Daillere, R., Fluckiger, A., Messaoudene, M., Rauber, C., Roberti, M.P.*, et al.* (2018). Gut microbiome influences efficacy of PD-1-based immunotherapy against epithelial tumors. Science (New York, NY *359*, 91-97.

Saada-Bouzid, E., Defaucheux, C., Karabajakian, A., Coloma, V.P., Servois, V., Paoletti, X., Even, C., Fayette, J., Guigay, J., Loirat, D.*, et al.* (2017). Hyperprogression during anti-PD-1/PD-L1 therapy in patients with recurrent and/or metastatic head and neck squamous cell carcinoma. Ann Oncol *28*, 1605-1611.

Sanchez-Salcedo, P., de-Torres, J.P., Martinez-Urbistondo, D., Gonzalez-Gutierrez, J., Berto, J., Campo, A., Alcaide, A.B., and Zulueta, J.J. (2016). The neutrophil to lymphocyte and platelet to lymphocyte ratios as biomarkers for lung cancer development. Lung Cancer *97*, 28-34.

Sanmamed, M.F., Perez-Gracia, J.L., Schalper, K.A., Fusco, J.P., Gonzalez, A., Rodriguez-Ruiz, M.E., Onate, C., Perez, G., Alfaro, C., Martin-Algarra, S.*, et al.* (2017). Changes in serum interleukin-8 (IL-8) levels reflect and predict response to anti-PD-1 treatment in melanoma and non-small-cell lung cancer patients. Ann Oncol *28*, 1988-1995.

Seymour, L., Bogaerts, J., Perrone, A., Ford, R., Schwartz, L.H., Mandrekar, S., Lin, N.U., Litiere, S., Dancey, J., Chen, A.*, et al.* (2017). iRECIST: guidelines for response criteria for use in trials testing immunotherapeutics. Lancet Oncol *18*, e143-e152.

Shoji, F., Matsubara, T., Kozuma, Y., Haratake, N., Akamine, T., Takamori, S., Katsura, M., Toyokawa, G., Okamoto, T., and Maehara, Y. (2017). Relationship Between Preoperative Sarcopenia Status and Immuno-nutritional Parameters in Patients with Early-stage Non-small Cell Lung Cancer. Anticancer Res *37*, 6997-7003.

Simonaggio, A., Elaidi, R., Fournier, L., Fabre, E., Ferrari, V., Borchiellini, D., Thouvenin, J., Barthelemy, P., Thibault, C., Tartour, E.*, et al.* (2020). Variation in neutrophil to lymphocyte ratio (NLR) as predictor of outcomes in metastatic renal cell carcinoma (mRCC) and non-small cell lung cancer (mNSCLC) patients treated with nivolumab. Cancer Immunol Immunother *69*, 2513-2522.

Skoulidis, F., Goldberg, M.E., Greenawalt, D.M., Hellmann, M.D., Awad, M.M., Gainor, J.F., Schrock, A.B., Hartmaier, R.J., Trabucco, S.E., Gay, L.*, et al.* (2018). STK11/LKB1 Mutations and PD-1 Inhibitor Resistance in KRAS-Mutant Lung Adenocarcinoma. Cancer Discov *8*, 822-835.

Skoulidis, F., Li, B.T., Dy, G.K., Price, T.J., Falchook, G.S., Wolf, J., Italiano, A., Schuler, M., Borghaei, H., Barlesi, F.*, et al.* (2021). Sotorasib for Lung Cancers with KRAS p.G12C Mutation. N Engl J Med *384*, 2371-2381.

Spitzer, M.H., Carmi, Y., Reticker-Flynn, N.E., Kwek, S.S., Madhireddy, D., Martins, M.M., Gherardini, P.F., Prestwood, T.R., Chabon, J., Bendall, S.C.*, et al.* (2017). Systemic Immunity Is Required for Effective Cancer Immunotherapy. Cell *168*, 487-502 e415.

Sung, H., Ferlay, J., Siegel, R.L., Laversanne, M., Soerjomataram, I., Jemal, A., and Bray, F. (2021). Global Cancer Statistics 2020: GLOBOCAN Estimates of Incidence and Mortality Worldwide for 36 Cancers in 185 Countries. CA: a cancer journal for clinicians *71*, 209-249.

Sylman, J.L., Boyce, H.B., Mitrugno, A., Tormoen, G.W., Thomas, I.C., Wagner, T.H., Lee, J.S., Leppert, J.T., McCarty, O.J.T., and Mallick, P. (2018). A Temporal Examination of Platelet Counts as a Predictor of Prognosis in Lung, Prostate, and Colon Cancer Patients. Sci Rep *8*, 6564.

Tao, R., Wang, L., Murphy, K.M., Fraser, C.C., and Hancock, W.W. (2008). Regulatory T cell expression of herpesvirus entry mediator suppresses the function of B and T lymphocyte attenuator-positive effector T cells. J Immunol *180*, 6649-6655.

Teachey, D.T., Lacey, S.F., Shaw, P.A., Melenhorst, J.J., Maude, S.L., Frey, N., Pequignot, E., Gonzalez, V.E., Chen, F., Finklestein, J.*, et al.* (2016). Identification of Predictive Biomarkers for Cytokine Release Syndrome after Chimeric Antigen Receptor T-cell Therapy for Acute Lymphoblastic Leukemia. Cancer Discov *6*, 664-679.

Teijeira, A., Garasa, S., Ochoa, M.C., Villalba, M., Olivera, I., Cirella, A., Eguren-Santamaria, I., Berraondo, P., Schalper, K.A., de Andrea, C.E.*, et al.* (2021). IL8, Neutrophils, and NETs in a Collusion against Cancer Immunity and Immunotherapy. Clin Cancer Res *27*, 2383-2393.

Templeton, A.J., McNamara, M.G., Seruga, B., Vera-Badillo, F.E., Aneja, P., Ocana, A., Leibowitz-Amit, R., Sonpavde, G., Knox, J.J., Tran, B.*, et al.* (2014). Prognostic role of neutrophil-to-lymphocyte ratio in solid tumors: a systematic review and meta-analysis. J Natl Cancer Inst *106(6)*, dju124.

Teng, M.W., Ngiow, S.F., Ribas, A., and Smyth, M.J. (2015). Classifying Cancers Based on T-cell Infiltration and PD-L1. Cancer Res *75*, 2139-2145.

Travis, W.D., Brambilla, E., Nicholson, A.G., Yatabe, Y., Austin, J.H.M., Beasley, M.B., Chirieac, L.R., Dacic, S., Duhig, E., Flieder, D.B.*, et al.* (2015). The 2015 World Health Organization Classification of Lung Tumors: Impact of Genetic, Clinical and Radiologic Advances Since the 2004 Classification. J Thorac Oncol *10*, 1243-1260.

Trestini, I., Sperduti, I., Sposito, M., Kadrija, D., Drudi, A., Avancini, A., Tregnago, D., Carbognin, L., Bovo, C., Santo, A.*, et al.* (2020). Evaluation of nutritional status in non-small-cell lung cancer: screening, assessment and correlation with treatment outcome. ESMO Open *5(3)*, 2020-000689.

Turner, T.C., Sok, M.C.P., Hymel, L.A., Pittman, F.S., York, W.Y., Mac, Q.D., Vyshnya, S., Lim, H.S., Kwong, G.A., Qiu, P.*, et al.* (2020). Harnessing lipid signaling pathways to target specialized pro-angiogenic neutrophil subsets for regenerative immunotherapy. Sci Adv *6(44)*, eaba7702.

Veglia, F., Hashimoto, A., Dweep, H., Sanseviero, E., De Leo, A., Tcyganov, E., Kossenkov, A., Mulligan, C., Nam, B., Masters, G.*, et al.* (2021). Analysis of classical neutrophils and polymorphonuclear myeloid-derived suppressor cells in cancer patients and tumor-bearing mice. The Journal of experimental medicine *218(4)*, :e20201803.

Veglia, F., Perego, M., and Gabrilovich, D. (2018). Myeloid-derived suppressor cells coming of age. Nat Immunol *19*, 108-119.

Walk, E.E., Yohe, S.L., Beckman, A., Schade, A., Zutter, M.M., Pfeifer, J., Berry, A.B., and College of American Pathologists Personalized Health Care, C. (2020). The Cancer Immunotherapy Biomarker Testing Landscape. Arch Pathol Lab Med *144*, 706-724.

Wang, J., Liu, Q., Yuan, S., Xie, W., Liu, Y., Xiang, Y., Wu, N., Wu, L., Ma, X., Cai, T.*, et al.* (2017). Genetic predisposition to lung cancer: comprehensive literature integration, meta-analysis, and multiple evidence assessment of candidate-gene association studies. Sci Rep *7(1)*, 8371-8384.

Wang, P.F., Song, S.Y., Wang, T.J., Ji, W.J., Li, S.W., Liu, N., and Yan, C.X. (2018a). Prognostic role of pretreatment circulating MDSCs in patients with solid malignancies: A meta-analysis of 40 studies. Oncoimmunology *7*, e1494113.

Wang, T., Zhan, Q., Peng, X., Qiu, Z., and Zhao, T. (2018b). CCL2 influences the sensitivity of lung cancer A549 cells to docetaxel. Oncology letters *16*, 1267-1274.

Wang, X., Yang, X., Zhang, C., Wang, Y., Cheng, T., Duan, L., Tong, Z., Tan, S., Zhang, H., Saw, P.E.*, et al.* (2020). Tumor cell-intrinsic PD-1 receptor is a tumor suppressor and mediates resistance to PD-1 blockade therapy. Proc Natl Acad Sci U S A *117*, 6640-6650.

Wei, W., Xu, B., Wang, Y., Wu, C., Jiang, J., and Wu, C. (2018). Prognostic significance of circulating soluble programmed death ligand-1 in patients with solid tumors: A meta-analysis. Medicine (Baltimore) *97*, e9617.

Wolf, Y., Anderson, A.C., and Kuchroo, V.K. (2020). TIM3 comes of age as an inhibitory receptor. Nat Rev Immunol *20*, 173-185.

Xiong, D., Wang, Y., Singavi, A.K., Mackinnon, A.C., George, B., and You, M. (2018). Immunogenomic Landscape Contributes to Hyperprogressive Disease after Anti-PD-1 Immunotherapy for Cancer. iScience *9*, 258-277.

Yang, H.B., Xing, M., Ma, L.N., Feng, L.X., and Yu, Z. (2016). Prognostic significance of neutrophil-lymphocyteratio/platelet-lymphocyteratioin lung cancers: a meta-analysis. Oncotarget *7*, 76769-76778.

Yin, Y., Wang, J., Wang, X., Gu, L., Pei, H., Kuai, S., Zhang, Y., and Shang, Z. (2015). Prognostic value of the neutrophil to lymphocyte ratio in lung cancer: A meta-analysis. Clinics (Sao Paulo) *70*, 524-530.

Yoshimura, T. (2018). The chemokine MCP-1 (CCL2) in the host interaction with cancer: a foe or ally? Cellular & molecular immunology *15*, 335-345.

Zhao, J., Huang, W., Wu, Y., Luo, Y., Wu, B., Cheng, J., Chen, J., Liu, D., and Li, C. (2020). Prognostic role of pretreatment blood lymphocyte count in patients with solid tumors: a systematic review and meta-analysis. Cancer Cell Int *20*, 15-29.

Zhao, Q.T., Yang, Y., Xu, S., Zhang, X.P., Wang, H.E., Zhang, H., Wang, Z.K., Yuan, Z., and Duan, G.C. (2015). Prognostic role of neutrophil to lymphocyte ratio in lung cancers: a meta-analysis including 7,054 patients. Onco Targets Ther *8*, 2731-2738.

Zhou, L., Jiang, Y., Liu, X., Li, L., Yang, X., Dong, C., Liu, X., Lin, Y., Li, Y., Yu, J.*, et al.* (2019). Promotion of tumor-associated macrophages infiltration by elevated neddylation pathway via NF-kappaB-CCL2 signaling in lung cancer. Oncogene *38*, 5792-5804.

Zuazo, M., Arasanz, H., Bocanegra, A., Chocarro, L., Vera, R., Escors, D., Kagamu, H., and Kochan, G. (2020). Systemic CD4 immunity: A powerful clinical biomarker for PD-L1/PD-1 immunotherapy. EMBO Mol Med *12(9)*, e12706.

Zuazo, M., Arasanz, H., Fernandez-Hinojal, G., Garcia-Granda, M.J., Gato, M., Bocanegra, A., Martinez, M., Hernandez, B., Teijeira, L., Morilla, I.*, et al.* (2019). Functional systemic CD4 immunity is required for clinical responses to PD-L1/PD-1 blockade therapy. EMBO Mol Med *11*, e10293.

Zwickl, H., Hackner, K., Kofeler, H., Krzizek, E.C., Muqaku, B., Pils, D., Scharnagl, H., Solheim, T.S., Zwickl-Traxler, E., and Pecherstorfer, M. (2020). Reduced LDL-Cholesterol and Reduced Total Cholesterol as Potential Indicators of Early Cancer in Male Treatment-Naive Cancer Patients With Pre-cachexia and Cachexia. Frontiers in oncology *10*, 1262-1271.

Figures and Tables

Supplementary Material

Published Articles

2018

Myeloid-Derived Suppressor Cells in the Tumor Microenvironment: Current Knowledge and Future Perspectives.
Ibáñez-Vea M, Zuazo M, Gato M, Arasanz H, **Fernández-Hinojal G**, Escors D, Kochan G. Arch Immunol Ther Exp (Warsz). 2018 Apr;66(2):113-123. doi: 10.1007/s00005-017-0492-4. Epub 2017 Oct 14.

2019

Functional systemic CD4 immunity is required for clinical responses to PD-L1/PD-1 blockade therapy.
Zuazo M, Arasanz H, **Fernández-Hinojal G**, García-Granda MJ, Gato M, Bocanegra A, Martínez M, Hernández B, Teijeira L, Morilla I, Lecumberri MJ, Fernández de Lascoiti A, Vera R, Kochan G, Escors D. EMBO Mol Med. 2019 Jul;11(7):e10293. doi: 10.15252/emmm.201910293.

PD-L1 Expression in Systemic Immune Cell Populations as a Potential Predictive Biomarker of Responses to PD-L1/PD-1 Blockade Therapy in Lung Cancer.
Bocanegra A[†], **Fernandez-Hinojal G**[†], Zuazo-Ibarra M[†], Arasanz H[†], Garcia-Granda MJ, Hernandez C, Ibañez M, Hernandez-Marin B, Martinez-Aguillo M, Lecumberri MJ, Fernandez de Lascoiti A, Teijeira L, Morilla I, Vera R, Escors D, Kochan G. Int J Mol Sci. 2019 Apr 2;20(7):1631. doi: 10.3390/ijms20071631

[†] *These authors contributed equally*

2020

Systemic Blood Immune Cell Populations as Biomarkers for the Outcome of Immune Checkpoint Inhibitor Therapies.
Hernandez C, Arasanz H, Chocarro L, Bocanegra A, Zuazo M, **Fernandez-Hinojal G**, Blanco E, Vera R, Escors D, Kochan G. Int J Mol Sci. 2020 Mar 31;21(7):2411

PD-L1 in Systemic Immunity: Unraveling Its Contribution to PD-1/PD-L1 Blockade Immunotherapy.
Bocanegra A, Blanco E, **Fernandez-Hinojal G**, Arasanz H, Chocarro L, Zuazo M, Morente P, Vera R, Escors D, Kochan G. Int J Mol Sci. 2020 Aug 18;21(16):5918. doi: 10.3390/ijms21165918.

Early Detection of Hyperprogressive Disease in Non-Small Cell Lung Cancer by Monitoring of Systemic T Cell Dynamics.
Arasanz H, Zuazo M, Bocanegra A, Gato M, Martínez-Aguillo M, Morilla I, **Fernández G**, Hernández B, López P, Alberdi N, Hernández C, Chocarro L, Teijeira L, Vera R, Kochan G, Escors D. Cancers (Basel). 2020 Feb 4;12(2):344. doi: 10.3390/cancers12020344.

2021

Understanding LAG-3 Signaling.
Chocarro L, Blanco E, Zuazo M, Arasanz H, Bocanegra A, Fernández-Rubio L, Morente P, **Fernández-Hinojal G**, Echaide M, Garnica M, Ramos P, Vera R, Kochan G, Escors D. Int J Mol Sci. 2021 May 17;22(10):5282. doi: 10.3390/ijms22105282.

Scientific Communications

Comunicación oral: Evolución dinámica y valor pronóstico de la relación Neutrófilo:Linfocito en cáncer escamoso pulmonar en tratamiento con inmunoterapia
Gonzalo Fernández Hinojal, Hugo Arasanz Esteban, Ana Bocanegra Gondán, Ester Blanco Palmeiro, Luisa Chocarro de Erauso, Grazyna Kochan, David Escors
CONGRESO ANUAL DE ESTUDIANTES DE DOCTORADO – UMH 02/02/2021

Poster: Elevación acelerada del Ratio Neutrófilo-Linfocito (NLR) en carcinomas no microcíticos de pulmón avanzados en progresión a inmunoterapia.
Gonzalo Fernández Hinojal, Hugo Arasanz Esteban; Maite Martínez Aguillo; Idoia Morilla Ruiz; Lucía Teijeira Sánchez; Ana Bocanegra Gondan; Miren Zuazo Ibarra; Luisa Chocarro de Erauso; Carlos Hernández; Ester Blanco Palmeiro; Edurne Muruzábal Huarte; Natalia Castro Unanua; Arturo Lecumberri Aznárez; Sandra Laguna Roman; David Escors Murugarren; Grazyna Kochan; Ruth Vera Garcia.
SEOM2020 VIRTUAL. 19/10/2020

Comunicación oral: Subpoblaciones inmunes medidas por citometría de flujo a partir de sangre periférica condicionan la respuesta a inmunoterapia en CNMP en 1º línea.
Arasanz H; Zuazo M; Bocanegra A; Chocarro L; Morilla I; Martinez-Aguillo M; Blanco E; **Fernandez-Hinojal G**; Teijeira L; Hernandez C; Vera R; Kochan G; Escors D.
SEOM2020 VIRTUAL. 19/10/2020

Poster: Engineering and expression of constitutive activators of the PD-1 and LAG-3 signaling pathways
Chocarro L; Garcia Granda MJ; Zuazo M; Arasanz H; Bocanegra A; Blanco E; Hernandez Saez C; **Fernández Hinojal G**; Vera R; Kochan G; Escors D.
ESMO Virtual Congress 2020. 17/09/2020

Poster: Dinámica de la relación neutrófilos-linfocitos en la respuesta al tratamiento con inmunoterapia del cáncer no microcítico pulmonar avanzado
Nombre del congreso: Congreso SEOM2019. 22/10/2019
Gonzalo Fernandez Hinojal; Hugo Arasanz Esteban; Idoia Morilla Ruiz; Maite Martinez Aguillo; Lucia Teijeira Sanchez; Arturo Lecumberri Aznarez; Natalia Castro Unanua; Edurne Belen Muruzabal Huarte; Leyre Perez Ricarte; Ruth Vera Garcia.

Poster: Functional systemic CD4 Immunity is required for clinical responses to PD-1/PD-L1 Blockade Therapy
Miren Zuazo; Hugo Arasanz; Maria Jesus Garcia Granda; Ana Isabel Bocanegra; **Gonzalo Fernandez Hinojal**; Maria Gato Cañas; Maite Martinez Aguillo; Berta Hernandez Marin; Lucia Teijeira; Idoia Morilla Ruiz; Ruth Vera; Grazyna Kochan; David Escors.
ESMO Congress 2019. 27/09/2019